Deployment strategy for mobile batteries to alleviate low-voltage grid congestion

Rick Vijverberg

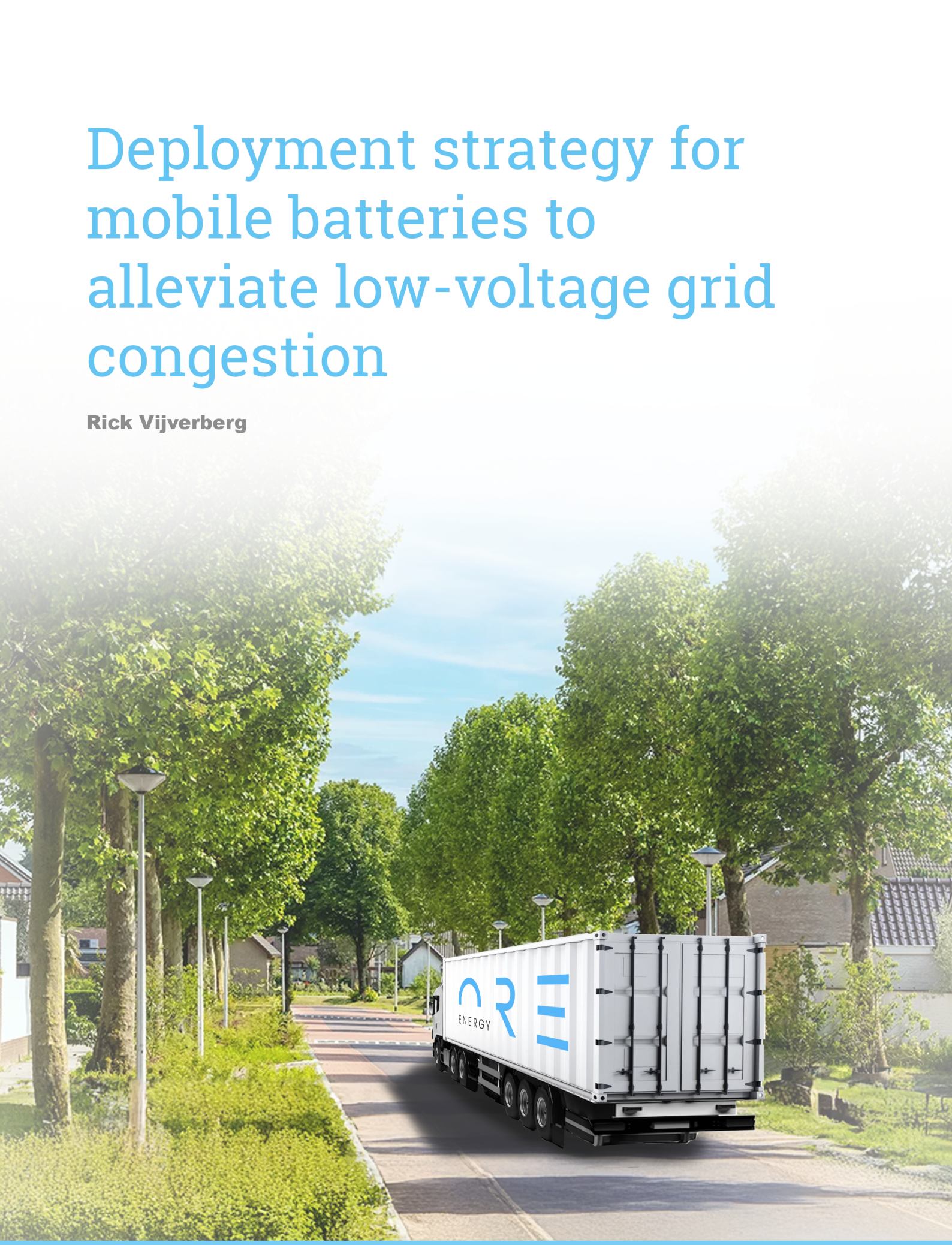

TU Delft

Deployment strategy for mobile batteries to alleviate low-voltage grid congestion

by

Rick Vijverberg

to obtain the degree of Master of Science
in Complex System Engineering and Management
at the Delft University of Technology,
to be defended publicly on July 11, 2025 at 10.30 AM.

Student number:	6098908	
Project duration:	February, 2025 – July, 2025	
Thesis committee:	Dr. ir. P. Heijnen,	TU Delft, chair and supervisor
	Dr. ir. Ö. Okur,	TU Delft, supervisor
	Dr. ir. N. Li,	Ore Energy, advisor

An electronic version of this thesis is available at `http://repository.tudelft.nl/`.

TU Delft

Preface

With my thesis, I hope to have contributed to the existing body of knowledge on the potential of mobile batteries. Additionally, I aim to have provided some practical insight by comparing the short-duration Lithium-ion battery with the long-duration Iron Air battery.

Over the past few years, the necessities for the electrification of society have captured my strong interest. In particular, energy storage systems have drawn my attention, as I believe they are crucial to the future energy system. I hope to further expand the knowledge I have acquired during my studies and continue working in the energy sector in my professional career.

This thesis would not have been possible without the continuous support of many people and parties. At first, I want to thank Ore Energy for providing me the opportunity to cooperate with an innovative and promising company. I firmly believe in the company's potential to become a leading European player in the long-duration battery sector. From all kind and interesting people at Ore Energy, I want to express my gratitude particularly to Na Li, for the many meetings and nice discussions concerning my project, Ore Energy and the energy sector in general. Furthermore, I want to thank my supervisors Özge Okur and Petra Heijnen for their help and advice whenever I needed it. In would like to extent my thanks to Petra Heijnen, who played a central role in supervising my project. It was a real pleasure working with you, and your support was crucial to my progress. Your positive attitude and eye for perfection gave me continuous motivation throughout the process. Furthermore, I want to thank Anton Ishchenko for introducing me to the low-voltage grid simulation tool 'GAIA'. Your support whenever I had questions greatly helped me to understand and work with GAIA more effectively. Then, I would also like to thank Wouter and Stan, for the great time during our theses and earlier assignment at Ore Energy. Last but not least, I want thank my family and friends for supporting me throughout my academic career. And finally, to Chiara, who has been there for me unconditionally.

Rick Vijverberg

Delft, June, 2025

Executive summary

The energy transition in the Netherlands has resulted in a rapid increase in electricity demand and decentralised energy generation. Electrification across sectors—combined with the rising share of intermittent renewable sources such as solar and wind—has placed growing pressure on the electricity distribution network. Low-voltage (LV) grids are particularly affected, as they were not originally designed to handle high peak loads or bidirectional power flows. Traditional mitigation methods, such as grid expansion through cable reinforcement and transformer upgrades, are costly and time-consuming. As a result, there is a pressing need for flexible, alternative solutions that can be deployed in a timely and efficient manner.

This thesis investigates the deployment of mobile batteries as a promising short-term measure to alleviate congestion in LV-grids and reduce pressure on grid expansion. Unlike stationary batteries, mobile batteries offer operational flexibility by being relocatable based on grid demand. Previous work has been focusing on optimization models for short-duration mobile batteries, but lacks acknowledgement of long-duration mobile batteries, and real-world considerations.

To address this knowledge gap, the aim of the research is to develop and assess a deployment strategy for mobile batteries, focusing on two parts: the charging profile and the optimal battery location. The designed deployment strategy is indifferent for battery technologies in order to make it widely applicable. In addition, practical considerations, such as spatial limitations and nuisance are discussed to make the deployment strategy practically feasible. Furthermore, the research aims to perform a cost comparison between the Lithium-ion battery (short-duration) and the Iron Air battery (long-duration).

This research uses a case study of a Dutch neighbourhood experiencing significant LV-grid congestion. The charging profile is designed to minimize this congestion, based on the expected load in the LV-grid, network losses and cable capacities. The expected load is derived from the Gaussian Mixture Model (GMM), which is a predictive model containing electricity demand and supply forecasted by Dutch DSOs. These data are provided by Phase to Phase, a company that develops features to help planning, designing and managing electricity networks.

In addition, the optimal battery location was found by deploying the battery, including the charging profile, at potentially suitable locations. The locations were assessed on minimization of congestion. Before this could be done, potentially suitable locations were determined based on network centrality, congested cables in the LV-grid, and cable capacities.

The findings demonstrate that the designed deployment strategy for mobile batteries can reduce 84.6% to 99.8% of system congestion, depending on the season and day of the week. In addition, maximum congestion can be reduced by 69.9% to 88.1%, bringing it within an acceptable European Standard. This demonstrates that mobile batteries are effective in alleviating congestion and supporting compliance with regulatory norms.

Furthermore, the results show that relocations of both the Iron Air battery and Lithium-ion battery are required to continue alleviating congestion according to the proposed deployment strategy. These battery relocations mostly occur during the winter months, as stationary batteries cannot balance their SoC after the required amount energy is discharged to alleviate congestion. Of the two battery technologies, the Iron Air battery requires fewer relocations than the Lithium-ion battery due to its larger energy capacity, leading to lower transportation costs. In addition, the significantly lower energy capital costs of the Iron Air battery lead to reduced fixed costs. Consequently, the Iron Air battery was found to be more cost effective.

Although the Iron Air battery is more cost-effective, trade-offs must be made based on real-world factors, particularly in terms of space requirements. The Iron Air battery's larger required installed energy capacity to alleviate congestion leads to more space occupation, which might be a limiting factor in densely populated areas. The significance of this trade-off is neighbourhood-dependent and must be evaluated on a case-by-case basis.

Future research could focus on validating the deployment strategy in LV-grids that are representative of those in the Netherlands. Such validation will allow for more general conclusions and enable wider battery deployment. Another possibility is to expand the cost comparison between the Lithium-ion battery and the Iron Air battery. By incorporating all associated costs—beyond those that differ between technologies—this expanded analysis allows for comparison with alternative solutions for LV-grid congestion.

In conclusion, this thesis demonstrates that mobile batteries are a technically viable and practically feasible solution to alleviate LV-grid congestion. They offer a flexible and quickly deployable alternative to alleviate congestion, reducing pressure on grid expansion. To this end, mobile batteries can serve as an instrument to bridge the short-term limitations and long-term needs for congestion alleviation in LV-grids.

Acknowledgements

While preparing this work, I used Overleaf's LanguageTool to correct grammatical mistakes. In addition, I used ChatGPT to help write Python code. After using these tools, I reviewed and edited the content as needed, and I take full responsibility for the content of my thesis.

Contents

Nomenclature

Abbreviations

Abbreviation	Definition
DSO	Distribution System Operator
DoD	Depth of Discharge
EV	Electric Vehicle
GMM	Gaussian Mixture Model
HP	Heat Pump
HV	High-voltage
LV	Low-voltage
MCS	Monte Carlo Simulations
PV	Photovoltaic solar
TSO	Transmission System Operator
SoC	State of Charge

Symbols

Symbol	Definition	unit
BL	Base load	kW
C_{instal}	Total instalment costs	$\frac{€}{kWh}$
C_{Dtr}	Truck depreciation costs	$\frac{€}{km}$
C_{fuel}	Fuel costs	€
C_{rel}	Total relocation costs	€
C_{tr}	Truck costs	€
C_{wage}	Wage costs	€
C_{woe}	Wage operational employee	$\frac{€}{relocation}$
C_{wtr}	Wage truck driver	€
cap	Battery energy capacity	kWh
$CAPEX_{an}$	Annual CAPEX	€
$CAPEX_{an,IA}$	Annual CAPEX Iron Air battery	€
$CAPEX_{an,Li}$	Annual CAPEX Lithium-ion battery	€
D	Battery duration	hours
$E[BL]$	Expected base load	kW
$E[ElEq]$	Expected load for electrical equipment	kW
$E[Load]$	Expected total load	kW
$ElEq$	Load for electrical equipment	kW
LF	Lifetime	years
n_{bat}	Number of batteries required at the charging location	#
n_{rel}	Number of required relocations per month	$\frac{\#}{month}$
P_{bat}	Battery power	kW
P_{fuel}	Fuel price	$\frac{€}{L}$
P_{max}	Installed capacity	kW
Pr	Charging profile	kW or ratio
tr	Trend for electrical equipment	n.a.
w	Weight	n.a.

Symbol	Definition	unit
$\bar{d}$	Average distance from charging location to LV-grid and back	km
ΔE_d	Daily mismatch between charged and discharged energy	kWh
η_{charge}	Charging efficiency	ratio
$\eta_{discharge}$	Discharging efficiency	ratio
η_{Tr}	Truck efficiency (fuel-based)	$\frac{L}{km}$
$\bar{t}_{bs}$	Average time to switch batteries	hour
$\bar{v}$	Average truck speed	$\frac{km}{h}$
$\cos\phi$	Power factor: ratio of active to apparent power	–
μ	Average value	% (electrical equipment), kW (base load)
$\mathcal{N}_g$	Gaussian distribution of group g	n.a.
$\mathcal{N}_j$	Gaussian distribution of electrical equipment j	n.a.
$_{(D_i)}$	Depends on demand at node i	n.a.

List of Figures

List of Tables

1

Introduction

1.1. Problem introduction

Electricity grid congestion is a significant and growing problem in the Netherlands [1]. This problem is amplified by the rising integration of renewable energy sources, such as wind and solar power. The intermittent nature of these sources leads to unpredictable energy peaks that frequently exceed the capacity of existing electricity grid [2]. Additionally, the electrification of society, including heating and transportation, increases demand intermittency. To this end, the mismatch between energy supply and demand increases [3], [4]. Although system operators are working to expand the electricity infrastructure to accommodate these changes, experts expect congestion to remain a pressing issue until at least 2035 [5], [6].

While congestion challenges are present throughout the grid, the low-voltage (LV) grids, used for final delivery to residential and small commercial users, are especially vulnerable. For instance, LV-grids were not originally designed to handle bidirectional energy flows from installed photovoltaic (PV) panels on rooftops [7]. In addition, heavy electrical equipment, such as electrical vehicle (EV) chargers, introduce demand intermittency on LV-grid level [7]. As a consequence of the supply and demand intermittency, LV-grids are increasingly difficult to operate. As highlighted by Kiedanski, Kofman, Maille *et al.* [8], the increasing decentralization of energy production requires urgent adaptation of LV-grids, which are currently ill-equipped to manage such dynamics without system-wide upgrades or demand-side management.

A traditional approach to mitigate grid congestion is grid expansion, that can be done by replacing cables, upgrading transformers, and building new substations. These long-term investments aim to permanently increase the grid's capacity and resilience. However, this strategy contains several limitations. Grid expansion is costly and time consuming [9]. A key cause of the time intensity is the complexity of grid expansion projects [10]. For example, the limited availability of underground space, particularly in densely populated areas, poses a significant challenge.

In light of this challenge, quick and easy to deploy solutions are required. One promising solution is the deployment of mobile batteries. These batteries are typically transported by trucks to specific locations based on need. Mobile batteries offer a flexible and modular response to local congestion by storing excess energy during peak generation and discharging it during peak demand [9]. This capability helps to balance electricity grids without requiring expansion. Moreover, mobile batteries can support seasonal demands, which would otherwise require significant grid reinforcement for only a short period within the year.

The strategic deployment of mobile batteries can serve as short-term solutions, as they might provide a scalable and cost-effective tool for distribution system operators (DSOs) to manage congestion while longer-term infrastructure investments are realized. Thus, mobile batteries are not only a technical solution to LV grid congestion, but also a policy instrument to bridge the gap from long-term ambitions to short-term need.

The aim of this research is to develop a deployment strategy for mobile batteries to alleviate LV-grid congestion. The proposed method will support short-term deployment of mobile batteries for grid

balancing purposes, while accounting for real-world complexity to ensure practical feasibility.

1.2. Key concepts

This chapter will dive into the key concepts used throughout this report. First, the most important differences between LV-grids and HV-grids will be outlined. Second, the meaning and causalities of congestion will be explained. Third, grid congestion mitigation strategies will be discussed.

1.2.1. Low-voltage vs. High-voltage grids

The difference between low voltage (LV)-grids and high voltage (HV)-grids considers multiple aspects, such as the responsible party and the characteristics of the grid. A LV-grid is part of the distribution grid which functions as an interface between electricity generators and consumers [11]. In an electrical distribution grid, substations reduce high voltage (>25kV) to medium voltage (MV) (1kV><25kV). The MV electricity is transmitted through cables to local MV-substations in which the voltage is further reduced to LV (<1kV), making it usable for small consumers. Thus, the LV-grid is the last stage of the distribution grid.

The party responsible for a safe and reliable distribution grid is called a distribution system operator (DSO) [12]. In the Netherlands, there are multiple DSOs, such as Alliander, Enexis, and Stedin, operating in their own jurisdiction. These jurisdictions are separated by city boundaries and do not have technical constraints [13], meaning that a cable from one city to another may be the responsibility of two DSOs.

Figure 1.1a shows the typical network topology of the medium voltage (MV)-grid and LV-grid. By closely analyzing the figure, it can be observed that the LV grid has a tree structure. This means that all nodes are connected by exactly one path [14]. This indicates that, in LV-grids, congestion will be the highest close to the MV-substation, assuming that all cables have the same capacity. This can be explained by imagining that most electricity needs to flow through the cable neighbouring the source and sink of the network, which is the MV-substation. This leads to the highest chance of congestion.

On the other hand, the transmission system operator (TSO) is responsible for a safe and reliable HV-grid. In the Netherlands, there is only one TSO, Tennet. The HV-grid is considered the backbone of the electricity system [15], transporting energy from production sites to big energy consumers and distribution grids. it can be compared with the highway of electricity. Figure 1.1b shows the network topology of the grid with the highest voltage (220kV & 380kV) in the Netherlands.

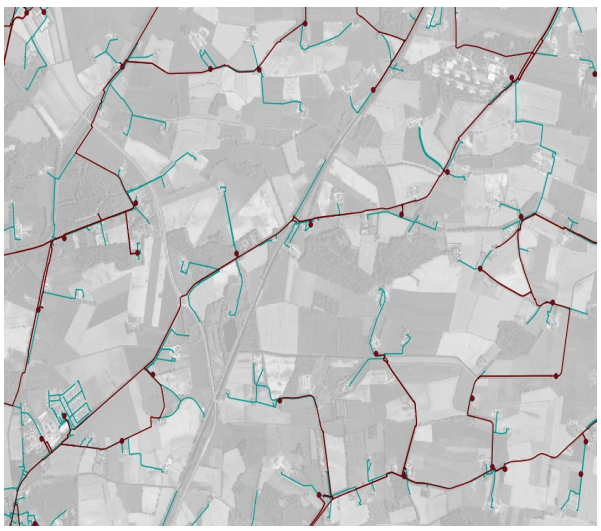

(a) MV-grid in brown and LV-grid in blue; source: [16]

(b) The cables shown are a subset of the Dutch HV-grid. This subset includes only the highest voltage cables in the Netherlands (220kV in green and 380kV in red); source: [17]

Figure 1.1: Grid topology of different voltage networks.

1.2.2. Grid congestion

Congestion occurs when the maximum capacity of the grid is exceeded [18]. Exceeding the maximum capacity of the grid can be caused by both energy generation and energy consumption. Congestion could result in equipment overheating and voltage drops, but does not limit the flow of electricity.

In electrical grids in the Netherlands, congestion is increasing, as the demand for electricity transportation increases faster than the capacity of the grid can be expanded [19]. In LV-grids, the rapid rise of installed photovoltaic (PV) panels and large energy demanding equipment, such as electrical vehicles (EV), and heat pumps (HP) contribute significantly to this problem [20].

PV panels generate electricity when the sun shines. Therefore, high energy production peaks arise around noon, when insolation is the highest. In addition, in the Netherlands, the sun power and duration are longer in summer than in winter. This results in both daily and seasonal fluctuations in energy generation. Electricity flow through LV-grids is influenced by PV generation. Subsequently, congestion could be expected to fluctuate accordingly.

Furthermore, EV charging also has daily patterns. In residential neighbourhoods, the peak demand is between 16.00 and 21.00 when people return home from work [21], [22]. Therefore, high installed capacity for EV chargers can cause congestion, as EVs are usually charged around the same time [23]. In contrast to PV generation, charging patterns for EV are less seasonal dependent. Therefore, strong daily patterns, but almost no seasonal patterns are present. Subsequently, the congestion patterns are expected to fluctuate accordingly.

Heat pumps may also contribute to grid congestion, depending on the neighbourhood. In some areas, distribution system operators (DSOs) are preparing for the rollout of heat networks, while in others, they are planning for the adoption of heat pumps [24]. Heat pumps also have daily and seasonal demand patterns. In the Netherlands, heat pumps demand more energy in winter than in summer. In addition, heat pumps require more energy in the morning and beginning of the evening than in the afternoon and night. Subsequently, the congestion patterns are expected to fluctuate accordingly.

Besides, there should be made a distinction between system congestion and maximum congestion. In this research, system congestion is defined as the sum of congestion in the network. This can be calculated by adding the congestion [in kW] of all congested cables together. The system congestion can be calculated for one time step or a time span. In addition, maximum congestion is defined as the congestion [in kW] at one moment in time. This can be found to take the maximum congestion of the congested cables in the network. The maximum congestion might vary for different moments in time and time spans. It is important to consider maximum congestion, as high congestion peaks might damage the infrastructure. Higher maximum congestion for the same system congestion may imply that less cables are congested but with higher congestion levels. High congestion can eventually lead to failure of the cables, which in turn can lead to cascading failure in the network [25].

1.2.3. Grid congestion mitigation strategies

Grid expansion

The expansion of the grid is one of the possibilities to prevent future congestion. By expanding the grid, the grid can accommodate a higher flow of electricity, allowing more intermittent energy sources. However, grid expansion is both cost and time consuming. The expansion of the grid required for the energy transition is expected to cost €200 billion in the Netherlands alone [26]. In addition, the expansion of the electricity grid currently progressing fast enough, as the need for additional grid capacity increases faster than the grid can be expanded [27].

Furthermore, grid expansion is particularly effective when load is constant over time, as the grid will be used more efficiently with constant load. When the grid is expanded to enable the transportation of high energy peaks, a large share of the grid capacity will not be used during many hours. Figure 1.2a and Figure 1.2 show how this works. In both figures, the grid is capable of transmitting electricity. However, in Figure 1.2a, the grid is utilized less efficient than in Figure 1.2, as higher energy peaks arise. This variability in energy peaks can have both diurnal and seasonal patterns.

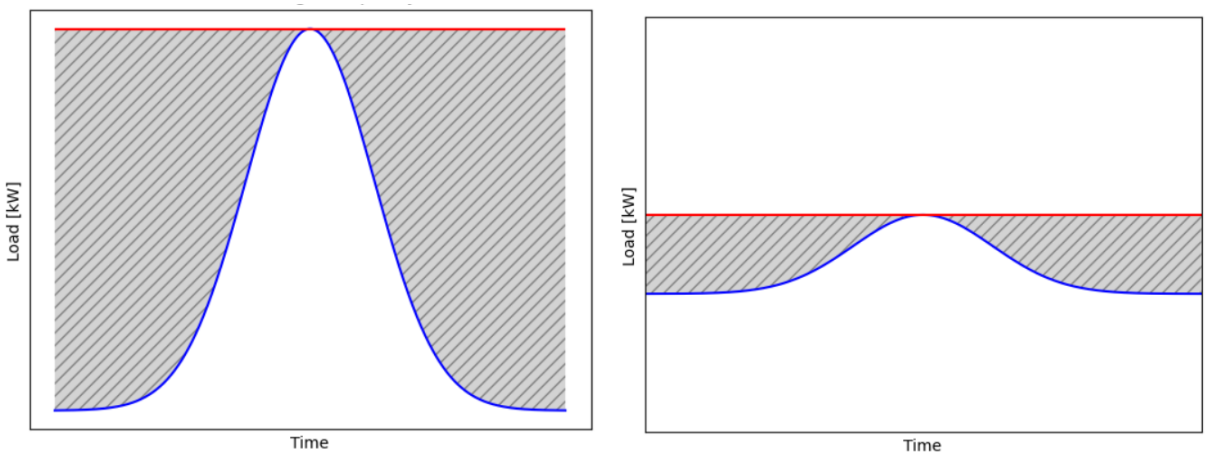

(a) High energy peaks **(b)** Low energy peaks

Figure 1.2: Available grid capacity under different scenarios.

Renewable generation curtailment

One solution to using the electricity grid more efficiently is curtailment. Curtailment refers to the reduction or temporary shutdown of renewable energy production, such as solar or wind farms [28]. Curtailment might be necessary when, under optimal wind or solar conditions, the energy generated exceeds the capacity of the grid connection.

To enhance grid efficiency, renewable energy production facilities are often overdimensioned. Overdimensioned production facilities indicate that the maximum output power of the facility is larger than the grid connection. This is done to use a larger percentage of the grid. The downside of curtailment is that potential energy is lost.

Batteries

Another approach to improve grid efficiency and prevent congestion is the use of batteries [23]. Batteries enable energy storage and come in various forms, including electrochemical (e.g. lithium-ion), chemical (e.g. hydrogen), and mechanical (e.g. flywheels) [29]. The focus in this research will be on grid-scale electrochemical batteries, which convert electrical energy to chemical energy for energy storage and chemical energy to electrical energy for energy supply.

In the following sections, additional battery distinctions will be made. Both stationary versus mobile batteries and short-duration versus long-duration batteries will be discussed.

Stationary vs. mobile batteries

A stationary battery is defined as a battery deployed at a fixed location. The battery might be used at this location for varying objectives, such as congestion management or ancillary services. In contrast, mobile batteries can be deployed at multiple locations. This can provide advantages over stationary batteries, as grid congestion might prevent stationary batteries from charging or discharging. It is also possible to deploy a mobile battery at locations with temporal variations in peak supply and demand, achieving a more efficient and flexible energy system [30].

Grid-scale batteries have a modular structure and are easy to transport due to their container shape [9]. However, transportation is costly, which limits the size of mobile batteries in order to remain economically viable. In addition, mobile batteries require more resources than stationary batteries, including trucks and manpower for transportation, as well as additional grid connections to enable operation at multiple locations.

Short-duration vs. long-duration batteries

In general, a battery can be schematically visualized as shown in Figure 1.3. The figure shows two main components: the battery energy capacity (in kWh) and the battery energy power (in kW). Throughout the remainder of this report, these components will be referred to as capacity and power, respectively.

The difference between short-duration and long-duration batteries lies in the ratio between the power capacity (in kW) and the energy capacity (in kWh), often referred to as the power-to-energy ratio.

Long-duration batteries typically have a lower power-to-energy ratio, meaning that the battery power is relatively low compared to the capacity. This allows the battery to discharge over many hours. In the figure, a long-duration battery would have a narrow output. In contrast, short-duration batteries typically have a high power-to-energy ratio, meaning that they have short a relatively short discharge time, but can provide high power. In the figure, short-duration batteries would have a wide output.

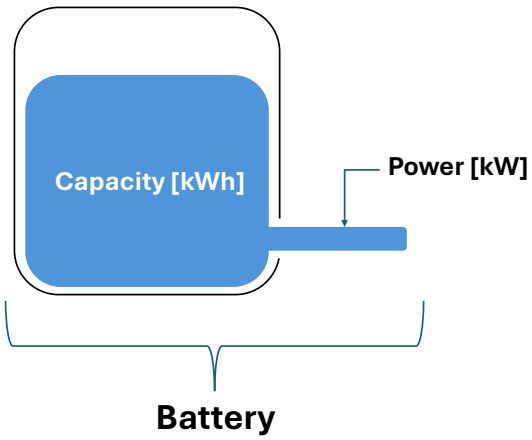

Figure 1.3: Battery energy capacity and power.

An application for long-duration batteries is the energy supply of industry during multiple days of low renewable energy production under a high share of installed renewable energy sources. This is a suitable application, as the battery is capable of supplying energy for multiple days when energy generation is low. In contrast, a short-duration battery is suitable for applications that require high power for short periods of time. Examples are electric vehicles that need high power to accelerate, or powerbanks to charge phones.

The discharge duration of a battery can be calculated using Formula 1.1.

$$D = \frac{cap}{P_{bat}} \tag{1.1}$$

, where D is the battery duration in hours, cap is the battery energy capacity in kWh, and P_{bat} is the battery power in kW.

1.3. Stakeholders

The stakeholders of this research are the people or parties involved in the deployment of batteries in LV-grids. This section will outline the stakeholder values with respect to battery deployment to alleviate LV-grid congestion. The stakeholders' values will be considered throughout this research. These values might be overlapping for some stakeholders, but will be discussed in the section where the value is most relevant. The most important stakeholders are the DSO, the neighbourhood residents, and the municipality. In addition, a separate section discusses battery ownership for congestion alleviation purposes, as this is a complex on-going discussion.

1.3.1. DSO/TSO

DSOs are responsible for maintaining a stable and secure electricity distribution network [31]. As DSOs are responsible for managing the LV-grid, they have a direct interest in mitigating congestion and stabilizing the LV-grid. In this context, DSOs are concerned with both system congestion and maximum congestion. Recall that system congestion indicates the summed congestion in the LV-grid at one moment in time or over a time span, and the maximum congestion indicates the maximum load exceeding the capacity of a cable in the Lv-grid. While system congestion affects long-term planning and operational efficiency,

maximum congestion can cause immediate reliability issues, such as voltage deviations or even outages. Addressing both forms of congestion is critical to maintaining grid stability. Detailed explanation is provided in Section 2.3.1.

To address both system congestion and maximum congestion, DSOs need to utilize balancing measures. Battery deployment for congestion alleviation is one such measure, offering a flexible asset to support grid stability. At the same time, DSOs also prioritize operational efficiency. In some cases, battery systems may not be as cost-effective or efficient as traditional grid expansion [32]. However, with congestion levels rising and grid expansion being time-consuming and resource-intensive, batteries might offer an easy and quick to deploy solution. This is particularly the case in areas with a high penetration of distributed energy resources such as PV, where local flexibility is critical.

1.3.2. Residents

The residents of the neighbourhood are also the energy consumers and producers in the LV-grid. Residents value affordable and reliable energy [33]. While battery deployment to alleviate grid congestion may not have immediately noticeable effects for consumers, it contributes indirectly by helping to prevent grid expansion or damage. This will reduce costs. However, a more likely stronger value is the liveability of the neighbourhood. According to a test developed by the Ministry of the Interior and Kingdom Relations, aesthetics and nuisance are important metrics to measure the liveability of a neighbourhood [34].

Batteries can raise concerns about aesthetics, as they can be container size. In addition, cooling system of batteries might generate noise. Therefore, battery deployment should consider the battery type and location to mitigate these effects.

1.3.3. Municipality

The municipality represents public interest and supports local sustainability. For instance, the municipality of Amsterdam provides subsidies for complex sustainable projects that contribute to sustainable energy and energy savings [35]. In addition, the municipality of Rotterdam provides smart energy system subsidies for entrepreneurs that want to conduct feasibility studies or start a pilot for sustainable innovation regarding the energy transition [36]. Therefore, in general, municipalities will support deployment of batteries to decarbonization the local energy system.

However, the municipality is also responsible for the zoning plan [37]. Therefore, the battery deployment should also comply with the prospect of the environment of the municipality.

1.3.4. Battery owner and renewable energy facilities

Congestion alleviation is the responsibility of grid operators. However, these parties are not allowed to own batteries [38]. Therefore, an incentive should exists for people or organizations to own a battery and provide congestion management.

Companies, such as energy providers, or residents might not be suitable to own the battery for congestion alleviation purposes, as the objective will be profitability instead of grid balancing. These two objectives might interact sometimes, but also might be contradictory. The organization of this is at the moment of writing still under discussion. The most important considerations are the financial and contractual agreements between the system operator and battery owner [32]. This would require policy intervention, such a new market or subsidies. From the perspective of the battery owner, a remuneration should be available that is higher than any other battery deployment strategy.

Another possibility for DSOs might be to tender battery projects to provide flexibility [39]. These tenders should contain information on battery power, capacity, and the duration of possible flexibility service. In addition, agreements should be made beforehand to give the DSO the power to operate the battery for congestion alleviation purposes. Tendering could be done to attract companies to invest in batteries. It might be possible to tender specially for municipalities, as utility ownership is one of the most effective levers to co-create with municipalities [40]. In addition, tendering especially for neighbourhood residents might improve social acceptance. The disadvantage of this approach is that tenders are time consuming, undermining the need of quick deployment.

An other possibility is to tender specifically for renewable energy facilities. This will be interesting when mobile batteries are deployed, as the renewable energy facilities could charge the battery at their own facility, and potentially also reduce curtailment. This would enhance the efficiency of battery use, as the battery would be deployed for two purposes at once: congestion alleviation in the LV-grid, and

curtailment prevention.

There is a long-running discussion about the ownership of batteries for grid balancing purposes, and no clear solution has been introduced yet. Further analysis of battery ownership is outside the scope of this research. Therefore, it is assumed that the DSO will operate the battery to alleviate congestion.

1.3.5. Key stakeholder values

In summary, the key values of the stakeholders relevant for battery deployment in LV-grids are shown in Table 1.1.

Table 1.1: Key values of stakeholders of battery deployment in LV-grids. *: Although land use can be quantified, the metric will be evaluated as qualitative metric, as the importance of land use is neighbourhood dependent. Therefore, land use cannot solely be compared based on land occupation, as one neighbourhood will allow for more land occupation than the other, leading to different assessment.

Stakeholder	Key value(s)	Evaluation metric	Evaluation metric type
DSO	Reliability	System congestion Maximum congestion	Quantitative Quantitative
Residents	Affordability Liveability	Electricity costs Nuisance Aesthetics	Quantitative Qualitative Qualitative
Municipality	Spatial integrity	Land use	Qualitative*
Battery owner	Efficiency	Continuous battery use	Qualitative

1.4. Literature review

This chapter will dive into the state of knowledge on mobile batteries in LV-grids. The aim of the analysis is to gain insight in the lacking knowledge on mobile batteries in LV-grids. To this end, a knowledge gap will be defined, and research questions will be established. The chapter ends with the interdisciplinary relevance to answer the research question, and the relevance to the CoSEM program.

1.4.1. Comparison Stationary and mobile batteries

The past few years, there has been growing interest in research on mobile batteries. The growing interest arises due to additional benefits of mobile batteries compared to their stationary equivalents, such as enhanced flexibility and reliability [41]. This section will outline existing literature on alleviating congestion with stationary and mobile batteries. In addition, literature on the comparison of stationary and mobile batteries will be examined.

Research has been conducted on stationary batteries for several years. However, new research keeps emerging as new scenarios, such as high penetration of EVs, arise. In addition, research for stationary batteries is expanding, in which it is compared to alternative solutions, such as grid expansion or mobile batteries, under various scenarios. For instance, Martínez, Mateo, Gómez *et al.* [42] analysed the technical and economic viability of stationary batteries, owned by the DSO, as alternative for grid expansion. The paper concludes upon the comparison between stationary batteries, grid expansion, and mobile batteries. The conclusion is that stationary batteries are expensive compared to grid expansion and that stationary batteries only have preference during a few peak hours. It is found that stationary batteries are cost-effective compared to grid expansion when the DSO expects a low demand growth rate. However, the research explored the potential of mobile batteries, and argues that it could be interesting to redeploy stationary batteries to improve cost-effectiveness. Nevertheless, it expects that mobile batteries will be too expensive compared with grid expansion due to high transportation costs.

Research on mobile batteries has attracted rising interest in the past few years. Existing literature focus on deploying mobile batteries for different purposes, such as congestion management or maximizing revenue. For instance, Saboori and Jadid [43] performed a case study on reducing operational costs of mobile batteries by proposing a new method to for optimal battery scheduling. It uses a 33-bus system in which six locations were chosen as potential battery deployment locations. The system is optimized for costs and power losses, and it was found that the battery is transferred between two locations. The charging location is at the closest location of the substation which is the energy source, and discharging

location tends to be in the centre of load. It was found that using a mobile battery, total energy losses could be reduced with 15.2%, compared to a scenario without battery deployment.

In addition, literature examines EV participation in balancing activities and energy markets. EVs are basically mobile batteries and their participation in energy markets is already examined for a longer period of time in literature. According to [44], distributed energy sources, such as EVs, can provide ancillary services to the system operator. Ancillary services are services provided by storage operators and have the goal to ensure reliable power supply [45]. These services can be tendered by system operators, as system operators in the Netherlands may not own batteries themselves. Hu, You, Lind *et al.* [44] describes a theoretical framework in which fleet operators represent EV owners and cooperate with DSOs to alleviate congestion.

Furthermore, in the last few years, multiple studies have compared stationary batteries and mobile batteries for different objectives in different environments. For instance, Ahmed, Sindi, Azzouz *et al.* [30] analysed the deployment of mobile batteries in a 69-bus system for which the battery operation was optimized for costs, energy losses, voltage deviations, and expected energy not supplied. A reduction of 4.5%, 51.6%, 53.0%, and 45.5% for the optimization parameters compared to the system without battery deployment, respectively. In addition, compared to stationary batteries, mobile batteries improved 29.4%, 1.2%, 4.0%, and 25.3% for the optimization parameters, respectively.

In summary, both stationary and mobile batteries have been studied for alleviating grid congestion. Stationary batteries are well-established in literature and often evaluated against grid expansion strategies. In contrast, mobile batteries are a more recent topic of study and are primarily explored for their flexibility and operational advantages. Several studies have compared mobile and stationary configurations in various performance metrics, often finding that mobile batteries outperform stationary batteries.

1.4.2. Battery duration

Next to the distinction between stationary and mobile batteries, a distinction between battery duration can be made. Recall from Chapter 1.2 that the duration of a battery implies the time a battery is capable of supplying or withdrawing electricity at full power. This section will outline existing research for short-duration and long-duration batteries used to alleviate congestion.

Research has been addressing the importance of long-duration energy storage. According to Aspitarte and Woodside [46], Chu, Baik and Benson [47] and Mantegna, Ricks, Manocha *et al.* [48], long-duration batteries are expected to play a crucial role in the future energy system. Chu, Baik and Benson [47] researches the role of long-duration batteries in a system with limited transmission. The study found that 1 MW of long-duration batteries have the same system value as 14-19 MW installed solar or wind with short-duration batteries. The research concludes that long-duration batteries will lower the costs of decarbonizing the energy system, particularly when energy capital costs are low (< 10$/kWh).

In addition, Dowling, Rinaldi, Ruggles *et al.* [49] analysed, by means of a macro-scale energy model, a 100% renewable scenario with deployment of wind and solar energy, and long-duration and short-duration batteries. The study found that the total system costs reduce with the deployment of long-duration batteries compared to a scenario without long-duration batteries. It also discusses the higher sensitivity of the costs of long-duration batteries compared to short-duration batteries, indicating that long-duration batteries are important to reduce system costs.

Furthermore, existing literature focuses primarily on short-duration batteries for mobile applications. For instance, Qiao, Mi, Shen *et al.* [50] uses a 2.5 hour duration mobile battery to test a proposed operation strategy for mobile batteries. In addition, Wang, Ma, Wei *et al.* [51] uses a three hour duration battery to explore market trading strategies. Also, Moraski, Popovich and Phadke [52] explores the potential of mobile batteries to provide a reliability solution for low-frequency, high-impact events, such as extreme weather, with a four hour duration battery. Furthermore, He, Michalek, Kar *et al.* [53] investigates the potential of a spatio-temporal decision model to determine the optimal operation and transportation schedules for a one-hour duration mobile battery, aiming to maximize its business model value.

A few papers that were analysed during this research include batteries technologies allowing for long-duration storage in mobile batteries. Ghadi, Mishra, Azizivahed *et al.* [54] models the deployment of mobile compressed air energy storage (CAES). CAES uses a compressor to store air under high pressure. The pressurized air can be released after storage through a turbine and converted to electricity [55]. The longevity of CAES improves its reliability and makes it suitable for long-duration energy storage. However, a large storage capacity is required to enable a long discharge time. Large storage capacities

could be provided by caverns, for instance. However, Ghadi, Mishra, Azizivahed *et al.* [54] uses a tank to transport the stored energy, limiting the storage capacity. As no large capacities are considered in the research, CAES is deployed as short-duration energy storage. Specifically, a duration of one hour is used, whilst the technology itself allows for long-duration energy storage.

Another potential long-duration energy storage technology in mobile configuration was discussed by Alva, Lin and Fang [56]. Alva, Lin and Fang [56] discusses two prototypes of mobile heat storage. One of the prototypes is the storage of heat in a zeolite/water mixture (zeolite is a mineral) in a transportable tank. The mixture is heated at one location and cooled at another location to charge and discharge the battery, respectively. Mobile thermal storage can be used when pipelines are not economically feasible. Furthermore, the storage tank capacity is similar to that of Lithium-ion. However, the technology is primarily suited for heat transport rather than for electricity transmission, as losses from the conversion from power to heat to power will reduce its efficiency significantly. Besides, the technology has a total cycle time of about 35 hours, indicating an average charge and discharge time of 17.5 hours. This is relatively short for long-duration batteries.

In summary, while both short-duration and long-duration batteries have been studied, research on their application differs. Short-duration batteries are commonly explored for mobile use, whereas long-duration storage has primarily been examined in stationary settings. The potential of long-duration batteries in mobile applications remains largely underexplored, with only limited and preliminary research addressing this configuration.

1.4.3. Time span

Another important factor for researching mobile batteries is the time span used for simulation. This might be interesting, as too short time spans might fail to capture seasonal variations. In addition, big time steps may result in the failure to capture diurnal variations.

Research conducted by Qiao, Mi, Shen *et al.* [50] studied the deployment of one mobile battery in combination with dynamic network reconfiguration in a 33-bus system. The study found beneficial results, such as enhancement of voltage quality and the promotion of renewable energy. The simulation was done for one day with time steps of 15 minutes. During this day, the mobile battery had ten different locations. The study also addressed a considerable difference in convergence time per solver, but finds that an accurate result can be found within 6 minutes.

In addition, Saboori [9] simulated the deployment of one, two, and three mobile batteries for emergency purposes. To do this, batteries are charged at disconnected areas that produce a surplus of energy and discharged at disconnected areas with energy shortage. The time span for the simulation was one day with hourly time steps. During this day, the mobile battery is the scenario of one deployed battery had six different locations. Simulating emergencies and restoring load over the course of one day is more reasonable than simulating balancing operations for the same time span, as battery deployment for emergency purposes typically involves a shorter time span than balancing purposes.

Furthermore, research conducted by Qu, Chen, Peng *et al.* [57] studied the deployment of one mobile battery between three micro-grids. The study finds that deployment of a mobile battery smoothens the load curve and improves the grid connection volumes of wind and solar. Here, the grid connection volumes refers to the amount of used wind and solar energy. The simulation was performed for one day with hourly time steps. During this day, the battery was transferred seventeen times. The developed method is capable of handling generation uncertainty to allow calculation for multiple days. However, the results are only provided for one day, limiting the assessment of the method's performance over longer periods with varying demand and generation patterns.

In summary, existing literature test proposed strategies for one day, leading to improvements for assessed objectives. However, the optimization models result in required battery transfers of ten, six and seventeen times within this day. Although this is the optimal outcome, these are extreme frequencies of required battery transfers. As a result, limited resources, such as personnel, might prevent the real world use of the developed methods.

1.5. Knowledge gap

The results of the literature review discussed in the previous sections outlined existing literature on (mobile) battery deployment. The analysis leads to the following remarks.

The existing literature on mobile batteries predominantly overlooks differences between battery technologies, focusing instead on short-duration batteries. Therefore, no insight is provided on long-duration mobile batteries.

In addition, existing literature provides methods to test mobile battery deployment strategies. These methods are validated for short time horizons (i.e. one day), failing to address long-term and seasonal implications.

However the remarks above are important and will be taken in consideration in this research, the key knowledge gap is identified as: existing literature focuses on technical models and numerical analysis for mobile battery deployment. Therefore, the literature lacks practical considerations in the deployment of mobile batteries. This include practical consideration as the number of feasible battery transfers per day and inclusion of stakeholder values.

1.6. Research questions

The identified knowledge gap led to the following main research question.

How can mobile batteries be deployed to alleviate low-voltage grid congestion, based on a case study comparing short- and long-duration batteries?

The main research question aims to find a method for the deployment of mobile batteries to alleviate congestion in a LV-grid. The deployment strategy will be indifferent for battery technologies to make the strategy widely applicable. In addition, battery-specific real-world factors will be included to enhance the feasibility of the deployment strategy. Furthermore, a quantitative comparison between short- and long-duration batteries will be conducted to obtain the most suitable technology for congestion alleviation in LV-grids.

To answer the main research question, the following sub-questions have been formulated. The first two sub-questions are indifferent for any battery technology, while the last three are specific to the battery technology. The first two sub-question are aimed at the deployment strategy of a battery to alleviate LV-grid congestion. The third sub-question aims at the required relocations of the battery to minimize congestion. The fourth sub-question aims at the comparison between short-duration and long-duration batteries. The fifth sub-question aims to outline practical considerations that should be made, when deploying a battery for congestion alleviation purposes and to choose between battery technologies. The contribution of every sub-question towards the main research question is shown below every sub-question.

1. How can the optimal charging profile for mobile batteries be designed to address low-voltage grid congestion while reflecting the specific characteristics of an low-voltage grid?

   This sub-question captures the first part of the deployment strategy: the battery charging profile. Specifically, the sub-question aims to develop a method to create a charging profile to alleviate congestion in the LV-grid. The charging profile can consist of both positive and negative values, indicating charging and discharging, respectively. The method will be designed to be applicable for all battery technologies in all LV-grids.

2. What is the optimal location to deploy mobile batteries to alleviate congestion in a low-voltage grid?

   This sub-question addresses the second aspect of the deployment strategy: the battery location. Specifically, the sub-question aims to identify the location enabling the battery to minimize LV-grid congestion. This will be studied by simulating the battery at various locations and analysing how congestion reduction is affected by its position. A sensitivity analysis will be conducted to assess the effect of a non-optimal battery location on congestion alleviation, as real-world constraints might limit battery deployment at the optimal location.

3. What trends in required battery relocations arise when following the designed deployment strategy to minimize congestion in low-voltage grids?

   This sub-question aims to identify trends in required battery relocations to minimize congestion in LV-grids. These relocations might be necessary to respect the batteries' SoC while continuing to

execute the deployment strategy designed in sub-questions one and two.

4. How do short-duration and long-duration mobile batteries compare in terms of cost effectiveness for alleviating congestion in low-voltage grids?

   This sub-question aims to find the cheapest battery technology to alleviate LV-grid congestion. This will be done by using the validated deployment strategy for mobile batteries in the first three sub-questions, which provide the battery indifferent charging profile and location, and the battery specific required relocations. The costs specific for both battery technologies will be used to determine the differences in overall costs.

5. Which real-world factors must be considered to support effective deployment of mobile batteries?

   This sub-question aims to capture essential practical considerations for the deployment of mobile batteries. Its objective is to complement the deployment strategy by incorporating real-world factors specific to LV-grids and neighbourhoods, ensuring the feasibility of battery deployment. The practical considerations will be outlined alongside the sensitivity analysis of battery location (sub-question two) to draw conclusions about the likelihood of successful battery deployment in neighbourhoods. These practical considerations will be addressed in the discussion.

1.7. Relevance of the research

Answering the research question will be relevant from multiple perspectives. This section will elaborate on the academic and societal relevance of this research. In addition, the relevance with respect to the Complex System Engineering and Management (CoSEM) program will be discussed.

1.7.1. Academic relevance

By answering the research question, this study will contribute to the existing body of knowledge on mobile batteries and their potential to alleviate grid congestion. It does so by proposing and validating a deployment strategy, with the aim of bridging theoretical insights with practical feasibility. This will address real-world considerations that are often overlooked in existing literature.

In addition, these practical insights may reveal implementation challenges that must be addressed before real-world deployment becomes feasible, thereby providing valuable input for future research.

1.7.2. Societal relevance

By answering the research question, this study will provide insights into the possibility of alleviating congestion with mobile batteries. The insights could change energy infrastructure investment decisions with the goal of alleviating congestion. In turn, congestion alleviation will contribute to the possibility to achieve net zero emissions by 2050, as it allows the integration of intermittent renewable energy sources.

In addition, by addressing the research questions and alleviating grid congestion, this study contributes to a more reliable electricity grid. A more reliable grid facilitates the integration of intermittent renewable energy sources, thereby supporting climate change mitigation. Moreover, reducing congestion enables new grid connections for both households and businesses, fostering further electrification and economic development.

1.7.3. CoSEM

This research aligns with the Complex Systems Engineering and Management (CoSEM) program due to its multidisciplinary nature. It integrates technical aspects of battery technologies, network analysis, stakeholder perspectives, economic considerations, and regulatory frameworks. In addition, the insights generated through this research will contribute valuable information to support policy-making.

1.8. Reading guide

This report is structured as follows. Chapter 2 will outline the modelling and analysis approach to answer the research questions. Chapter 3 will present the design choices made to find the answers on the research questions. In addition, the chapter provides input data, and examines a congestion analysis with the purpose of making design choices. Chapter 4 presents the results. Chapter 5 will discuss the relevance, applicability, and feasibility of the results. Additionally, the limitations of the research will be discussed. Chapter 6 will conclude on the findings, provide recommendations, and propose future research.

2

Research Approach

This chapter will dive into the research approach to answer the research questions. The chapter will start with an overview of the research approach by pointing out the most important components of the research and providing a corresponding visualization. Then, the model used for the research is discussed according to the guidelines provided by Nikolic, Lukszo, Chappin *et al.* [58]. Thereafter, the approach for congestion analysis is provided. Then, the approach for the deployment strategy is explained. At last, the approach for the cost comparison between short-duration and long-duration batteries is discussed.

2.1. Overview research approach

The aim of this research is to test a proposed deployment strategy for short- and long-duration mobile batteries to alleviate congestion in an LV-grid. The research will study the charging profile and battery location that are capable of alleviating congestion, whether mobile batteries have an advantage over stationary batteries to alleviate congestion, and if short- or long-duration batteries are more cost effective.

To do this, a modelling approach will be used in which an LV-grid will be simulated with and without battery deployment. Simulation will be performed in GAIA, which is an application built especially to simulate LV-grids. GAIA is provided by Phase to Phase, a company that develops features to help planning, designing and managing electricity networks [59]. GAIA uses a probabilistic model that uses Gaussians (or normal distributions) to predict demand and generation in the grid. Then, GAIA uses Monte Carlo Simulations (MSC) to sample from the Gaussians to determine the load. The load data can be exported to Excel and further be analysed using Python.

To evaluate the results, quantitative and qualitative evaluation metrics derived from the stakeholder analysis discussed in Section 1.3 will be used. Quantitative evaluation metrics, which are system congestion, maximum congestion, and costs, will be used to assess the battery deployment strategy and the comparison between short- and long-duration battery technologies. This will provide an overview of how well the deployment strategy alleviates congestion and what the corresponding costs are. In addition, the quantitative evaluation metrics are the real-world factors important for the stakeholders. These are nuisance, aesthetics, and use of space. These will provide important constraints on the environment in which the battery will be operating.

The graphical overview in Figure 2.1 visualizes the research approach. The figure shows that there are two main components of the research approach: modelling and analysis. The modelling part will obtain the charging profile and the optimal battery location. In addition, the modelling part will model the LV-grid with and without battery deployment to be able to compare the system congestion and maximum congestion for both scenarios. Then, the analysis will use the battery technologies-specific values toe determine the number of required battery relocations and the costs.

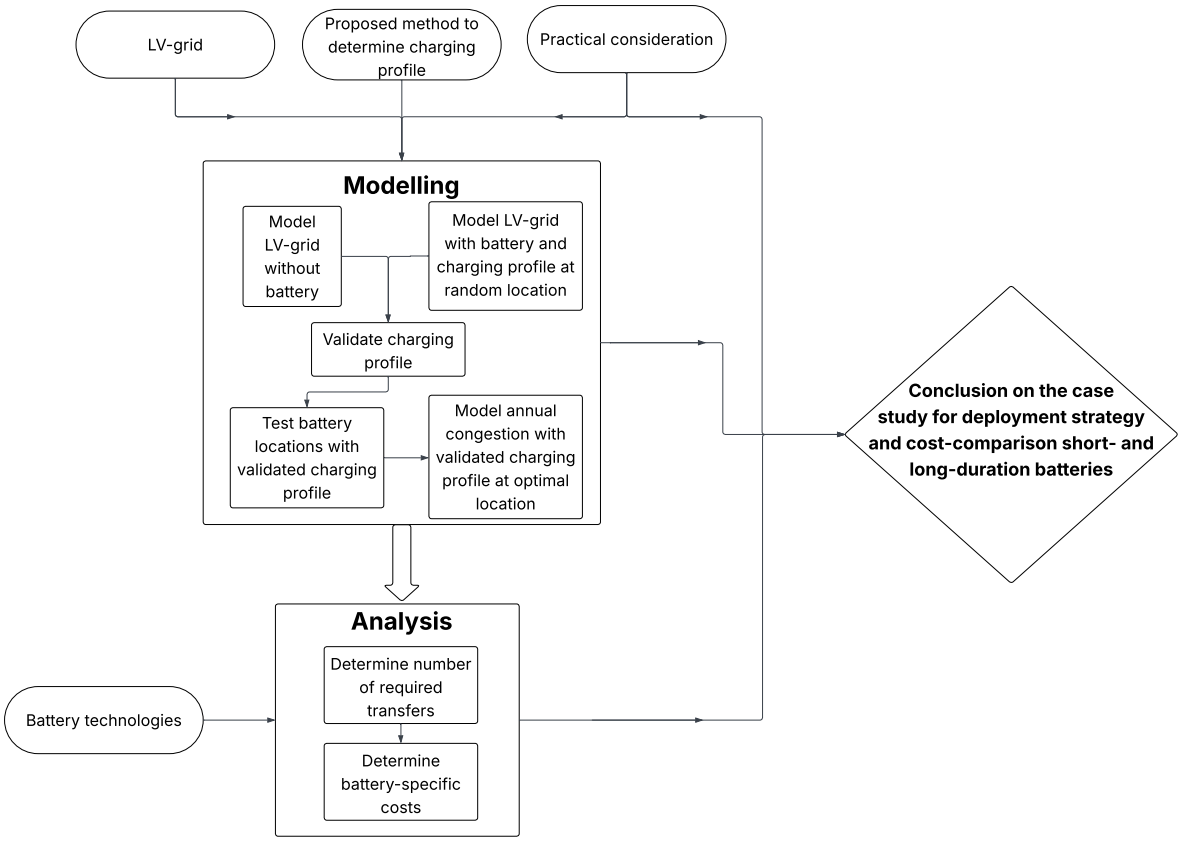

Figure 2.1: Visualized research approach, including input parameters.

2.2. Modelling for policy support

This section will provide the modelling approach. The section will include the modelling objective, the model description, the limitations of the model, the required input data, and the model output.

2.2.1. Modelling objective

The model aims to obtain the load data of the LV-grid in multiple system configurations. It is designed to simulate and analyse the performance of the LV-grid under different battery deployment scenarios. Specifically, the model should provide results on the load data of the LV-grid in three cases: (1) without battery deployment, (2) with battery deployment following a proposed charging profile at an estimated well performing location (as the optimal location is not known yet), and (3) with battery deployment at various deployment locations with the validated charging profile. This allow for the comparison of system congestion and maximum between in the scenario with and without battery deployment. The objective is to generate insights into how mobile battery systems can be strategically deployed to alleviate congestion, both for short-duration and long-duration battery technologies. The results will inform the development of policy recommendations on optimal deployment strategies.

2.2.2. Model description

LV-grid modelling

The future load in the LV-grid cannot be known exactly in advance. Historical exact data can be used to find the most suitable mobile battery deployment strategy. However, this will not represent reality, as future load cannot be known. Therefore, a stochastic model should be used that predicts future load. Using predicted load will be slightly of the exact load, providing an environment close to reality. In reality, load predictions should be made which will also not be exact. Depending on the type of congestion management, these predictions are made seconds to days in advance [60].

GAIA is able to accommodate at least two models. The first is the Strand-Axelsson (SA) model. SA models are strongly connected to base load (background electricity usage due to equipment, such as refrigerators

and Wi-Fi routers) and less to additional energy peaks [61]. The additional and increasing energy peaks in LV-grids are mainly due to increased installed capacity of electrical equipment, such as PV panels, EV chargers and HPs.

Figure 2.2a shows the probability of load in 1950 when the SA model was used. The SA model used in GAIA accounted for average load value and deviation. In addition, no time dependent weights were included, meaning that no diurnal and seasonal fluctuations were taken into account. Figure 2.2b shows the measured load probability in 2013. From the figures can be obtained that the SA model cannot capture the load probability of these days accurately, as the SA in GAIA used a single normal distribution. Moreover, seasonal fluctuation became increasingly important due to wide deployment of solar PV.

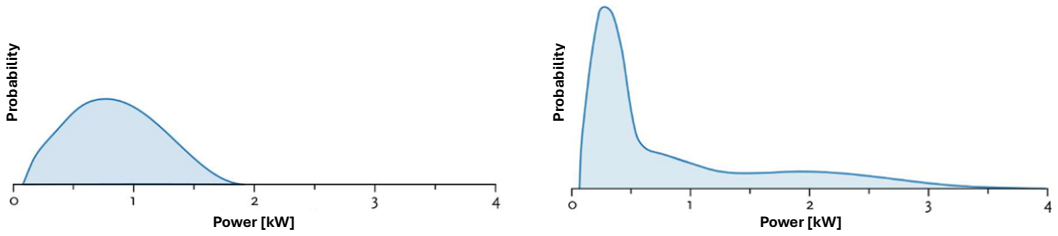

(a) Load probability in 1950. **(b)** Load probability in 2013.

Figure 2.2: Load probabilities from 1950 and 2013 to demonstrate that Gaussian Mixture Model is currently a more suitable model than Strand-Axelsson model for predicting household electricity load; Source: [61]

The mismatch between the SA model and reality led to the implementation of the second model, the Gaussian mixture model (GMM). The GMM is able to capture multiple normal distributions and includes diurnal and seasonal variations that are essential for reliable load simulation nowadays. Therefore, it is chosen to continue with the GMM.

GMM is a clustering algorithm using a probabilistic approach in which data points can be a mixture of multiple clusters [62]. This is an important distinction from other clustering algorithms, such as K-means, in which every data point belongs to one cluster. As the data points in GMM are assigned a soft clustering approach, each data point has a probability to be part of a cluster. For instance, when four Gaussians determine the base load of an household, each Gaussian has its own probability of being active.

To be more specific, GAIA accommodates Gaussian Mixture models (GMMs) to simulate the load for the households. This load is estimated for both base demand and electrical equipment, such as EV charging points, PV generation, and HP demand. For base demand, the GMM uses four Gaussians for which the average value (in kW), the standard deviation and the probability that a Gaussian will be active are stored in a dataset for all distinct Guassians. For electrical equipment, GAIA uses one Gaussian for which the peak value [in %], the standard deviation and the probability are stored in the dataset. The probabilities, or weight of the sum of the Gaussians can be smaller or larger than one, but these will be normalized internally in GAIA.

Then, the value should be divided by the power factor ($\cos\phi$), indicating how efficiently the electrical power is used. Specifically, it tells the ratio between the active power [in kW] and apparent power [in kVA]. The data obtained from the Phase to Phase download portal indicates that the power factor is equal to 0.98. Equation 2.1 shows how GAIA determines the base load at node i at a given time:

$$\mathrm{BL}_{i,t} = \frac{\sum_{g=1}^{4} \left(\mathcal{N}_g^{(D_i)}(\mu) \cdot w_{g,t}^{(D_i)} \right)}{\cos\phi} \tag{2.1}$$

, where $BL_{i,t}$ is the base load of node i at time t (which is the multiplied parameter of month m, day type (workday or weekend) d at quarter (15 minute time step) q), $\mathcal{N}_g$ is the normal distribution for Gaussian g, μ_g is the mean (in kW) of the Gaussian g, $w_{g,t}$ is the weight of Gaussian g at time t, and the superscript D_i

indicates that the Gaussians are dependent on the annual demand D of node i. To obtain the annual base load profile of node i, the node time series should be created by iterating the equation for all time steps.

The load of electrical equipment is simulated differently from the base load. Here, only one Gaussian is used for which the mean is measured in %, indicating the average percentage of the maximum power of the equipment **if** the equipment is used. In addition, the Gaussian is also independent of the node, as it can be imagined that PV generation per installed capacity does (almost) not differ within a neighbourhood. Furthermore, the Gaussian also has a standard deviation and weights assigned just as for the base load. The power factor (recall: $\cos\phi$) differs for the type of electrical equipment. For both PV and EV, the power factor is 1. For HP, the power factor is 0.95. Equation 2.2 shows how GAIA determines the load for electrical equipment at node i at a given time:

$$ElEq_{j,i,t} = \frac{\mathcal{N}_j(\mu) \cdot w_t}{\cos\phi_j} \cdot \frac{P_{\max,j,i}}{100} \tag{2.2}$$

, where $ElEqt_{j,i}$ is the load (positive for demand and negative for supply (PV generation)) of electrical equipment j in kW for node i, $\mathcal{N}$ is the normal distribution for the Gaussian with mean μ in %, $w_{d,q}$ is the weight of the Gaussian at day type d (workday or weekend) at quarter (15 minute time step) q, w_m is the weight of the Gaussian at month m, $P_{max,j,i}$ is the installed capacity in kW of electrical equipment j of node i.

Then, MCS (recall: Monte Carlo Simulations) is used to sample from the probability distributions. To do this, MCS runs simulations repeatedly, generating pseudo-random variables based on the distribution. The sampled values are pseudo-random, as an algorithm (Mersenne-Twister) is initialized with a combination of predefined values in order to obtain the same values in every MCS. By this means, the same calculation in GAIA will provide the same results for every run. This allows for a fair comparison between different system configurations.

In GAIA, 200 samples are taken with MCS. The maximum load value used is the 95th percentile value of the Monte Carlo samples sorted for each variable. GAIA takes the 95th percentile value of the sorted array, meaning that 95% of the values are lower than the value accounted for. By taking the 95th percentile value, GAIA attempts to exclude rare situations with extreme values. Nevertheless, statistically, the 95th percentile value will still provide a higher load than statistically expected, and will represent a high load scenario. However, this is considered a viable approach for congestion analysis, as the focus is on probable yet realistic high load scenarios.

Battery modelling

In GAIA, batteries can be manually added to every node in the LV-grid. This enables simulation of the LV-grid with a deployed battery at the location of choice. However, there is a difference in modelling the LV-grid itself and the batteries. In contrast to the predictive model to determine the load in the grid, batteries are modelled deterministically. This means that the charging profile of the batteries consists of a sequence of discrete load flows. The deterministic charging profile has a value for every time step between zero and one. This value is multiplied by the maximum battery power to obtain the actual charging or discharging power. Combining the maximum battery power and the charging profile results in a time series of battery input and output power.

Furthermore, the SoC is transferred from one time step to the next to respect battery capacity. To do this, the charging and discharging efficiency of the battery technology is taken into account.

2.2.3. Limitations

The GMM uses Gaussians to capture the probability of load. The Gaussians are based on synthetic load profiles predicted by the DSOs. These are estimates and will deviate from the actual load values, as synthetically created probability distributions will not capture real-world load dynamics perfectly accurate. In addition, the created Gaussians have values for time steps of 15 minutes. This indicates that load is equal for a continuous 15 minutes. In reality, load is dynamic and does not exists at one moment in time. The Gaussians are also independently for workdays in the same month and weekend days in the same month. This results in 24 various Gaussian combinations. As a result, there will be no smooth connection between months. However, the staggered data from month to month is not expected to influence the results and the main message of the research significantly, as the trend in congestion and costs is considered more important than the exact values. In addition, it should be considered that the

data for 2030 will be used, so load profiles might have been changed before 2030. Also, modifications in the LV-grid might arise before 2030. This is however, extremely hard to predict.

Furthermore, MCS uses random sampling from the Gaussian distributions to obtain 200 values. These samples do not cover the entire distribution, which could influence the results. This is especially the case for the 95th percentile value, which may deviate from the true 95th percentile of the distribution. While 200 values is not an extremely large sample size, it is expected to represent the distribution sufficiently, as orthogonal sampling is applied. This approach ensures that an equal distance is maintained between intervals in the sample space, and that a random value is selected from each subset. As a result, the samples are more evenly distributed across the entire range of the distribution.

2.2.4. Input data

LV-grid

The first data required is the LV-grid. In GAIA, it is possible to create a network yourself. However, this is time consuming and requires assumptions, such as installed capacities for electrical equipment for every household in the neighbourhood in 2030. It is also possible to obtain an LV-grid from the Phase to Phase download portal. Next to provding the LV-grid simulation application: GAIA, Phase to Phase also gathers data from multiple DSOs. The download portal of Phase to Phase can be accessed with a license. In the download portal, there are 49 anonymized LV-grids available from varying DSO jurisdictions, with varying topologies, and varying characteristics. Specifically, the LV-grids vary for the type of houses, such as terraced houses or houses in rural area. Also, the LV-grids vary on density of houses, energy label, and more. The different types of LV-grids are shown in Appendix A. The LV-grids will be assessed based on hard and soft criteria indicating the suitability of the LV-grids to deploy (mobile) batteries to alleviate congestion.

Time span

The chosen LV-grid can be loaded into GAIA, including the grid topology and grid characteristics, such as cable capacities and installed capacities of electrical equipment per household. These data is available for both 2020 and 2030 and consist of the same Gaussians, but different installed capacities. This means that there are no differences in the normal distributions of demand (i.e. base load, EV, and HP) and supply (i.e. PV), but the installed capacities vary for the different years. In general, installed capacities of PV, EVs, and HPs will increase in the LV-grid in 2030 compared to 2020.

Data for 2030 were chosen, as the electricity grid should be prepared for future scenarios rather than analysed for solutions for the past. In addition, mobile batteries should be deployable in the short term in order to alleviate congestion and reduce pressure on grid expansion. Therefore, forecasted data for beyond 2030 would be less relevant. In addition, by using yearly data, the selected time span will capture both diurnal and seasonal variations in LV-grid congestion. These variations may arise from behavioural patterns related to electricity demand or fluctuations in PV generation due to changing insolation.

The available data consist of GMM values for one workday and one weekend day for each month of the year. This implies that the dataset assumes all weekdays in a given month have load profiles, and the same holds for all weekend days within that month. To conduct a year-long analysis, the data will be interpolated, resulting in a time series in which all workdays in the same month share identical values, as do all weekend days. The limitation of the data and the interpolation of the data is that finer variations within weeks or months are not considered. A benefit is that it allows for the simulation of one year. If all days had to be modelled separately, the computational time would exceed a feasible range.

Furthermore, a time step of 15 minutes is used, as this is the smallest possible time step to simulate in GAIA. This will result in the most accurate results.

Load data

The data required for the GMM are the load distributions, which contains the mean value when the base load or electrical equipment is active, the standard deviation, and the probability that the Gaussian will be active. These data distributions are presented in an Excel file that can be downloaded in the download portal of Phase to Phase. The Gaussians are assumed to be indifferent for the LV-grids, as the LV-grids are all located in the Netherlands and are expected to have the same demand profiles and PV generation. Figure 2.3 shows the Gaussians for the base load, PV, EV, and HP for one household connection on March 21st at 5 PM. The percentages in the legend on top of the figure show the probability for the electrical equipment is on. In addition, the figure shows the probability over the power, for which the latter can be positive (demand) or negative (supply). The probability is normalized in GAIA.

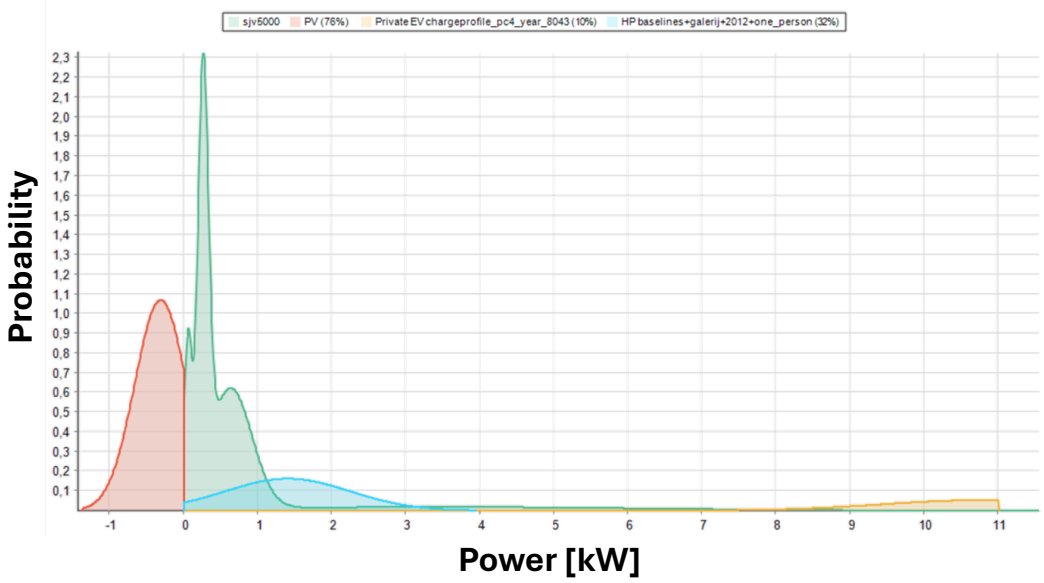

Figure 2.3: Load probabilities for base load and electrical equipment for a household connection in an LV-grid at March 21st at 5 PM. This is an visualization of the input parameters of demand and supply in the GMM for one grid connection at one moment in time.

Furthermore, the Excel file contains the additional information required to perform the load analysis in the network. This includes the dimensions and resistances of the cables, and the nominal voltage of the transformer that transforms low-voltage to medium-voltage. Additional specifications can be added to the Excel file, such as a new battery technology, including its efficiency.

Using the data of Phase to Phase allows analysis of an LV-grid with corresponding data that is also used by Dutch DSOs [59]. Therefore, the data is considered reliable.

Battery data

In contrast to the load data, the input parameters of the battery will be determined during this research. The charging profile is part of the deployment strategy and will be determined based on a proposed method. In addition, the required power of the battery will also be determined during this research. The battery power is chosen to be equal to the maximum power required to alleviate congestion. This means that, theoretically, battery power cannot be the limiting factor to solve congestion. As a result of this approach, the power of both battery technologies is equal. The power will be multiplied with battery technology-specific duration to determine the battery capacities. The duration of the Iron Air battery will be fixed, as only one Iron Air duration is currently developed. In contrast, Lithium-ion batteries are available in many different sizes and durations [63]. Therefore, the optimal battery duration will be determined to enhance efficient use. This will be done by fitting the duration to congestion patterns in the LV-grid. This can be done by using the Fourier Transforms. It must be mentioned that using the Fourier Transform might not result in the optimal location and has its limitations. Those will be discussed after the Fourier Transform is explained.

The Fourier transform converts a signal from the time domain to the frequency domain [64]. By applying the Fourier transform to congestion in the LV-grid, it becomes clear how often a frequency occurs in that signal and what the amplitude of that frequency was. For instance, if much congestion arises every 24 hours due to PV generation, the Fourier transform will show a peak at the corresponding frequency. The more significant the pattern, the higher the peak at that frequency will be. By this means, the Fourier transform can reveal congestion patterns.

It is important to note that the fitting duration is not equal to the frequency, but to half the frequency. This is illustrated in Figure 2.4. The figure shows a perfect signal that peaks every 12 hours. This will be revealed by the Fourier by a peak in the plot at frequency 0.0833 (as $\frac{1}{12} = 0.0833$). The figure shows congestion in one direction for six hours followed by 6 hours of no congestion (positive and negative for

congestion and no congestion, respectively). The period of congestion is 6 hours, which is the suitable battery duration.

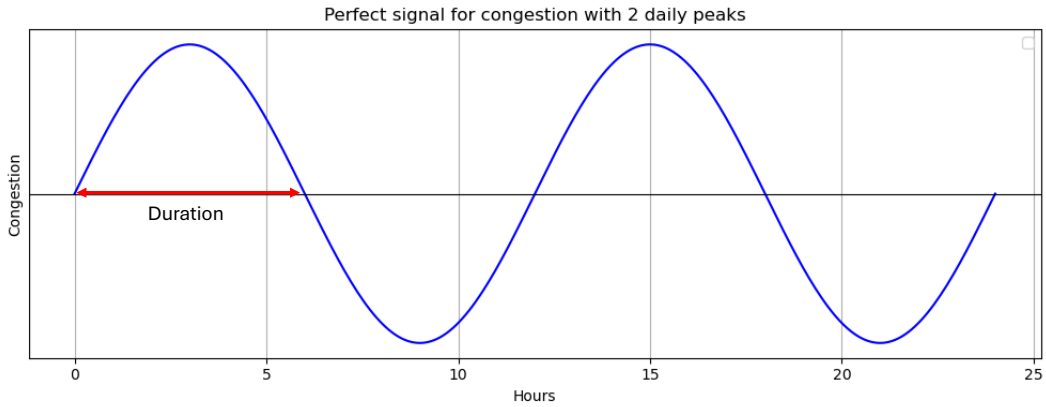

Figure 2.4: The figure shows a perfect signal of the main peaks found with the Fourier transform. From this figure can be obtained that the duration of the battery should ideally be half of the time before a congestion peak reoccurs. This allows for both charging and discharging during one cycle.

Using the Fourier Transform for determining battery duration has its limitations. For instance, congestion will not be a perfect signal. Congestion might arise every 12 hours for only one hour, indicating that a duration of six hours might be too long. Too high duration will lead to overdimensioned capacity (see Equation 1.1 and too high costs. However, this approach attempts to determine a potentially suitable battery duration by assuming the perfect signal instead of picking a duration randomly. Therefore, it is expected that this approach adds value to the research.

Furthermore, the applicability of this approach will be similar for all LV-grids in the Netherlands. Using the same normal distributions for base load and electrical equipment will result in the peaks, after applying the Fourier Transform, occurring at the same moments in time. However, the amplitude of these peaks depends on the installed capacities, as these proportionally influence the electricity flow. The topology of the LV-grid, in turn, determines whether congestion occurs.

2.2.5. Output

GAIA accommodates the simulation of the chosen LV-grids with the input data. After grid load simulation, it is possible to export the results into an xlsx file to Excel. This xlsx file contains the simulation data, including the current [in A] for each cable in the LV-grid for each time step. The current in the cables is important because it indicates the level of congestion. An part of the GAIA generated xlsx file is shown in Appendix B in Figure B.1 to provide an example. To obtain the level of congestion, the xlsx file is used as input in the congestion analysis.

2.3. Congestion analysis

Before the data are analysed, the data will be scraped, as GAIA exports a large dataset including unnecessary information. The first data which will be removed are the data of the nodes that are not used for the analysis. The LV-grids that can be uploaded into GAIA provides one or multiple MV-stations with multiple LV-grids connected. For this research, one LV-grids is studied rather than all the LV-grids connected to the MV-station(s). It is chosen to study one LV-grid rather than multiple, as a LV-grid is a tree network connected to the MV-station. This indicates that the LV-grids are operating independently of each other. Studying multiple LV-grids at the same time will therefore not add value, and makes the problem unnecessary complex. However, this does not mean that studying multiple LV grids separately does not add value to the research; on the contrary, it can provide significant value as the research will become more generic. The choice for the LV-grid will be further explained in Section 3.1. Nevertheless, to scrape the data, a Python code was created, as many runs will be required to obtain all results. The Python codes will use another xlsx file that contains the cables and nodes which should remain in the data set. The Python script can be found in Appendix E Section E.3.

In addition, the scraped data will further be modified to allow for congestion analysis. The results that will be used for analysis are the data of the current [in A] in the cables. The current indicates the load through the cable at a specific moment in time and can be compared to the nominal current (I_{nom}) to learn if the cable is congested. For instance, if the I_{nom} of a cable is 185A and the flow through the cable is 200A, there is congestion. The exported xlsx file from GAIA contains the percentages that represent the ratio between the current and I_{nom}. The percentages above 100% represent congestion. However, during this research, asymmetries were found between the maximum load [in %] and the maximum load [in A]. This observation led to the consideration of changing the way GAIA determines the maximum load [in %] in a cable. The method GAIA uses currently to determine the maximum load and how it potentially should be calculating the maximum load are explained below.

Each cable consists of three conductors (three phases) for power transmission to the destination, a neutral conductor to complete the electrical circuit, and a ground (earth) conductor for safety. Currently, MCS takes 200 samples from the Gaussian distributions for each cable component for each time step. This results in a sample set of five columns (for each cable component) and 200 rows (for each sample). Each cell represents a sample [in A] of one of the 200 samples taken for one component. Currently, GAIA converts the maximum value [in A] of each of the 200 rows to percentages, to obtain the maximum load [in %] in the cable for that row. Then, the maximum load [in %] for all 200 rows is sorted in ascending order. GAIA obtains the 95th percentile value by picking the 190th value (representing 95% of 200 rows) and assigning this value as the maximum load [in %] in that cable for that time step. However, it is argued that the samples [in A] per cable component should be sorted first. Then, the maximum load [in A] of the values in the 190th row should be converted to the maximum load [in %]. This should be the maximum load assigned to that cable for that time step. It is argued that the last approach would make more sense, as the maximum load depends on the individual components. Revising the approach would lead to significant changes in the results in GAIA. In general, it would decrease the level of congestion. Reflection on this method is ongoing at the time of writing.

In this research, congestion is calculated based on the 95th percentile value of the currents. This means that the congestion is calculated according to the potentially implemented method in GAIA, that considers the maximum load [in A]. Therefore, the maximum load [in %] which has asymmetries with the current is neglected. Choosing this approach causes a lower level of measured congestion. However, it is expected to be more realistic according to the reason described in the previous paragraph.

2.3.1. Congestion evaluation

The objective of this research is to alleviate congestion. From the stakeholder analysis in Section 1.3 became clear that there can be made a distinction between system congestion and maximum congestion. This section will explain how these can be measured by means of an example.

System congestion is the total congestion occurring in the LV-grid. System congestion can be measured at one moment in time or over a time span, by accumulating the congestion in all cables for all time steps. To find the system congestion at time t, the congestion in all cables at time t should be added together. This will provide information on the total congestion in the system for one moment in time. The research will provide results for the system congestion of multiple time steps, consisting of the summed system congestion of those time steps.

On the other hand, maximum congestion refers to the highest level of congestion occurring in the network. It can be measured at a single time step or over a time span by identifying the maximum congestion observed in any cable during that period. The maximum congestion indicates the level of congestion in the most congested cable of the grid. This provides additional information to system congestion, as high maximum congestion may indicate the risks associated to the congestion. For instance, the higher the maximum congestion, the larger the risks for network degradation.

The example shown in Figure 2.5 will illustrate the calculation of system and maximum congestion. The figure shows a simple LV-grid consisting of four nodes. In addition, the figure shows cables and their congestion (flow of electricity in kW above maximum capacity) at one moment in time. As explained in this section, system congestion is the summed congestion in the grid. As a result, the system congestion in for the example is 15kW (8 + 5 + 2). In addition, the maximum congestion is occurs in cable 1 and equals 8. Note, that for two time steps, the system congestion of both time steps are added, and the maximum of the maximum congestion in both time steps is taken to obtain the maximum congestion. For multiple time steps, the same logic applies.

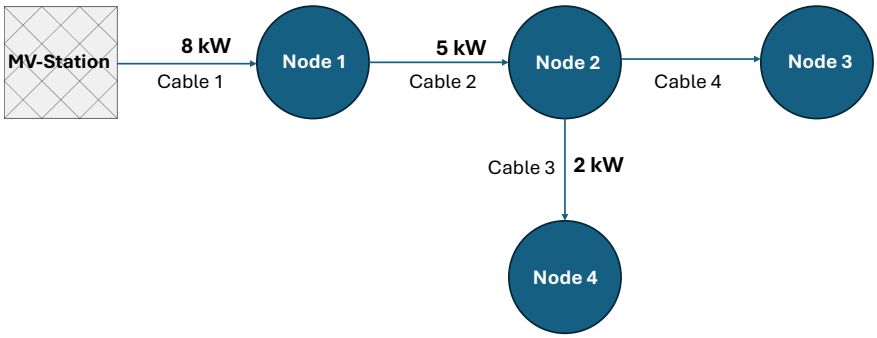

Figure 2.5: Example system congestion and maximum congestion at time t.

2.4. Deployment strategy

The deployment strategy consists of two parts: the charging profile and the optimal location. The approach to obtain the parts of the deployment strategy are discussed in the following sections.

2.4.1. Charging profile

The charging profile is the battery profile for charging and discharging. This profile should be optimized with the goal of minimizing congestion. In GAIA, it is not possible to optimize the charging profile. In addition, charging profiles will not be perfect in reality, as predictive models will estimate the optimal charging profile based on the expected load. These models will probably be close to the actual values but will not be exact. Therefore, the GMM (recall that this is the Gaussian Mixture Model that consists of predictive load distributions), is used to simulate reality as accurately as possible. Furthermore, the method to determine the charging profile constructed should be generic for all battery types. This allows for possible deployment for all battery types, as well as fair comparison between the tested battery types, Lithium-ion and Iron Air. Not including battery constraints in the method provides a fair comparison, as the results will show the suitability of a particular battery type.

The method for determining the charging profile will be developed to alleviate congestion. Therefore, the charging profile will charge and discharge when congestion occurs. This indicates that the method itself does not consider the long-term perspective for the SoC. More specifically, the battery might be fully charged or discharged at a moment in time due to the lack of leveling the SoC during idle time. To prevent this, a theoretic approach will be used to model the SoC and use the idle time. This approach will be explained in Section 2.5.

Furthermore, the charging profile will be derived from the Gaussian distributions to reflect realistic operating conditions. This is the case as Gaussians are probability distributions, mirroring real-world predictive models on expected load. As a result, the actual simulated load might deviate from the expected load, since it cannot be known what the exact load will be.

In addition, the maximum battery power will be determined based on the required power to alleviate congestion. This will, theoretically, allow the battery to resolve congestion. The battery capacity will be adjusted according to the required power and the battery-specific duration. To this end, the proposed approach to determine the charging profile will be indifferent to battery technology, making it applicable to all storage technologies. The precise method is further explained in Section 2.4.1, as it is part of the deployment strategy.

The proposed method to determine the charging profile is called real-time planning. This section will explain and validate the method.

2.4.2. Real time planning

The real time planning approach is chosen to determine the charging profile. The optimal charging profile will be determined based on the total load (oversupply or demand) of the LV-grid at time t, and the capacity of the cable connecting the MV-station to the LV-grid (called main cable from now on). The charging profile will be a time series of values to steer the battery to supplying or withdrawing electricity from the LV-grid that will exceed the capacity of the main cable.

Real time planning consists of three steps: (1) determining the load, (2) determining the power losses and add them to the load, (3) considering the cable capacities.

Determining the load

Step 1 of the real time planning method is to determine the load. GAIA uses GMM to determine the load, as discussed in Section 2.2.2. Recall that this means that Gaussians, with a corresponding average value, standard deviation and probability, are used. To obtain the charging profile of the battery, the time series of the exact load of each node is required, as the battery is modelled deterministically. To obtain these, Equation 2.1 is simplified by eliminating the standard deviation of the Gaussians. This results in the mean multiplied with the time dependent weights. By eliminating the standard deviation, it is assumed that the mean will be the actual value. This is not always the case, as the other values within the reach of the standard deviation also have a certain probability, and are determined using Monte Carlo Simulations. Although the mean value might not be the exact value, it has the highest probability to be the actual value. Equation 2.3 shows the simplified formula used to determine the expected base load at each node.

$$E[BL_{i,t}] = \frac{\sum_{g=1}^{4} \left(\mu_g \cdot w_{g,t}\right)}{\cos \phi} \tag{2.3}$$

, where $E[BL_{i,t}]$ is the expected base load of node i at time t (which is the combined parameter of month m, type of day (workday or weekend) d, and quarter (15 minute time step) q), μ_g is the mean (in kW) of Gaussian g, and $w_{g,t}$ is the weight of Gaussian g at time t.

To obtain the expected value for the electrical equipment load, the normal distribution is eliminated in the same way as for the base load. Equation 2.4 shows the simplified formula to determine the expected electrical equipment load at each node:

$$E[ElEq_{j,i,t}] = \frac{\mu_j \cdot w_t \cdot tr_{j,t}}{\cos \phi_j} \cdot \frac{P_{max,j,i}}{100} \tag{2.4}$$

, where $E[ElEq_{j,i,t}]$ is the expected load (positive for demand and negative for supply (PV generation) of the electrical equipment j (in kW) for node i at time t, μ_j is the mean (in %) of the Gaussian of electrical equipment j, w_t is the weight of the Gaussian at time t, and $tr_{PV,t}$ is the time-dependent trend that increases or decreases the average of the Gaussian when PV is used. $tr_{j,t}$ is only applicable for PV, as the maximum PV generation has daily and seasonal patterns. For EV and HP, no fluctuation in maximum possible demand is available. Furthermore, $P_{max,j,i}$ is the maximum power (in kW) of the electrical equipment j of node i.

Combining the base load and the load of electrical equipment results in the total load of a node. Equation 2.5 shows the formula to calculate the expected total node demand of node i:

$$E[Load_{i,t}] = E[BL_{i,t}] + \sum_{j=1}^{3} \left(E[ElEqt_{j,i,t}]\right) \tag{2.5}$$

, where $E[Load_{i,t}]$ is the expected load of node i at time t, $E[BL_{i,t}]$ is the expected base load of node i at time t, and $\sum_{j=1}^{3} \left(E[ElEq_{j,i,t}]\right)$ is the sum of the expected load of electrical equipment j (i.e. PV, EV, and HP) for node i at time t.

Power losses

Step 2 of the real-time planning method is the determination of the power losses. Power losses are important because they increase the required electricity input in the grid to meet demand. The most significant power losses are resistive losses. To determine these losses, the resistance of the load of each node to the source or sink (MV-station or battery) should be calculated.

To calculate the power loss due to cable resistance for time t, the load of each node and its transport distance to the source or sink should be considered. To do this, a model should be built to estimate the source and sink of the location. Estimating the source and sink of the load is necessary to determine the distance covered by the load, which is proportional to the resistance. However, building such a model is beyond the scope of this research. It is also infeasible to calculate the resistances of the load of every node and its destination manually, especially with the changing location for the location validation in mind. Therefore, it is chosen to simplify the network. The simplified network is shown in Figure 2.6. The figure shows seven groups of nodes that are the combination of the nodes in that particular branch. The combined expected load for a group of nodes is calculated according to Equation 2.6:

$$E[\text{Load}_{K,t}] = \sum_{i \in K} E[\text{Load}_{i,t}] \tag{2.6}$$

, where $E[Load_{K,t}]$ is the expected load of node group K at time t, and $\sum_{i \in K} E[\text{Load}_{i,t}]$ is the sum of the load for all nodes i in K at time t.

The expected load of a group of nodes is assumed to be allocated at exactly half of the range of nodes. For instance, if the load is supplied from the MV-station to the orange group, the distance to the orange group is the distance from the MV-station to the first orange node subtracted from the distance from the MV-station to the last orange node, divided by two, and added to the distance from the MV-station to the first orange node.

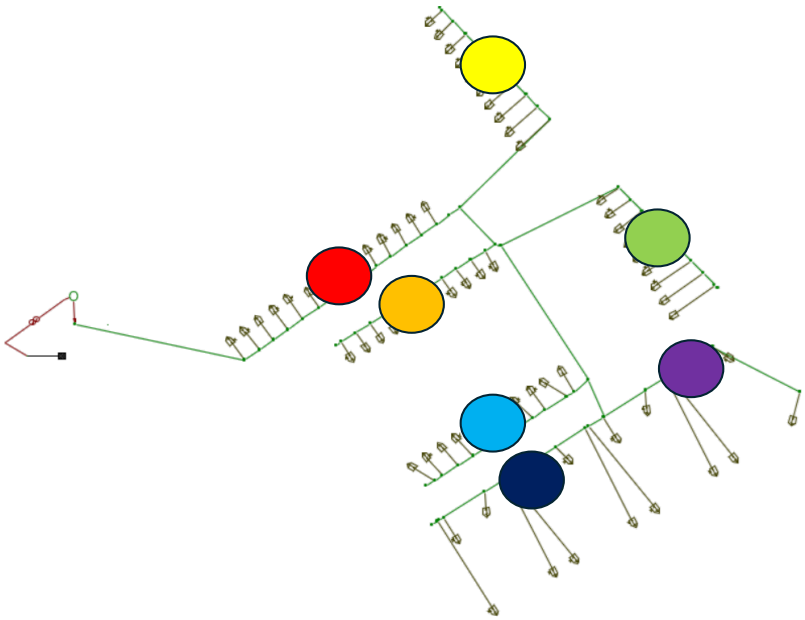

Figure 2.6: Simplified LV-grid with grouped nodes.

Calculating the resistance with a distance to halfway in the group might not lead to the exact resistance, as it might be the case that the load is the highest at the end of the branch, for instance. In that case, the resistance would be higher than accounted for. Therefore, this assumption might lead to small errors in the power losses. On the other hand, grouping the nodes can also represent reality more accurately. This is the case when some nodes of the group supply energy and others have demand. In reality, the

electricity will flow from the supplyer directly to the user. Therefore, no significant losses will be present. By grouping the nodes, the same is the case, as the the load of the nodes is summed, leading to loads cancelling each other out when there are suppliers and users. Therefore, no power flows towards the MV-station and battery, leading to no power losses for the directly used electricity. The power loss calculation errors implied by the proposed method are expected to be negligible.

As a result of the simplification, it is not necessary to calculate the power loss for each load separately, but rather for the combined load of each group. Equation 2.7 is used to calculate the power loss of each node group:

$$P_{Loss,K,t} = 3 \cdot I_{K,t}^2 \cdot R_{K,t} \tag{2.7}$$

, where $P_{Loss,K,t}$ is the power loss of K at time t in [W], I is the current through the cable to K at time t [in A], and $R_{K,t}$ is the resistance of the cable to group K at time t [in Ω]. These are multiplied by three, as the cable is a three-phase system. Resistance $R_{K,t}$ can be calculated according to equation 2.8:

$$R_{K,t} = \frac{\rho \cdot l_{K,t} \cdot 2}{A} \tag{2.8}$$

, where ρ is the resistivity of the cable material [in $\Omega \cdot m$], A is the cross-sectional area of the cable [in m^2], $l_{k,t}$ is the cable length for group K [in m] at time t, and the equation is multiplied by two as the resistance must be calculated for the round-trip path of the current for a power system. The length of the cable changes depending on the source and sink of the electricity (i.e. MV-station or battery location). In turn, the source and sink of the flow depends on the size of the electricity flow. For instance, if no congestion is present, the battery will be idle and all electricity flows from and towards the MV-station. In this situation, the distance of the load to the MV-station should be considered to calculate the resistance. In another scenario, when there is congestion, the battery will (dis)charge a share of the electricity, requiring to also take the distance from the load to the battery into account. It is proposed to calculate the flow distance by averaging the distance of the node group to the MV-station and the LV-grid. By averaging the distance, it is assumed that half of the load is using the MV-station as source and sink, and half of the load is using the battery as source and sink. If averaging the distance is a reliable approach depends on the amount of congestion in the LV-grid. The approach for this LV-grid will be validated in Section 4.1.2. Besides, various battery locations and their corresponding distances to the node groups can be found in Table C.1 in Appendix C.

Furthermore, the direction of the flow of electricity matters in considering the charging profile. In the scenario when the battery is discharging to alleviate congestion, the losses should be added to the load, as the power losses will have decreased flow of electricity when it reaches the nodes. In other words, the battery should discharge more than demand is at the nodes, as supplied load will be smaller when it arrives at the demand site. On the contrary, when the battery charges to alleviate congestion, it should charge less than the size of oversupply, as a part of the oversupply will be lost. Although, power losses should be considered differently for opposite flow of electricity, the losses can be added to the load for both directions. This is the case, as the flow changes from positive to negative when the its direction changes. During oversupply, the flow is negative, meaning that the losses can be added to the equation to reduce the amount of energy which should be charged by the battery. To this end, losses can be added to the equation for congestion in both directions.

Capacity main cable

Step 3 of the real time planning method is to consider the capacity of the cables. To alleviate all congestion, the battery should charge the surplus generated electricity in the LV-grid. The surplus of electricity can be defined as the PV-generated electricity that will exceed the capacity of the cables. Using the same reasoning, the battery should discharge the electricity demand in the LV-grid that exceed the capacity of the cables. This means that the battery has idle time (time the battery does nothing) when the cables should be able to transfer the electricity from and towards to LV-grid.

Recall that the highest congestion will occur in the main cable (the cable directly connected to the MV-grid connection), assuming that all cables have the same capacity. In the LV-grid used in this research, not all cables have the same capacity. However, the highest congestion still occurs in the main cable throughout the year. This means that when the main cable is able to transfer the electricity, no congestion will be

present in the LV-grid. Therefore, the battery charging profile should consider the maximum capacity of the main cable. The maximum capacity should be subtracted from the load and the power losses, to obtain the charging profile.

The approach is illustrated in Figure 2.7. The figure shows the expected load with the blue curve. Positive load means that there is demand, and negative load means there is supply (PV generation) in the LV-grid. The red shaded area is the load expected to be transferred by the main cable, that has a capacity of 42.5 kW (185A * 230V). Load exceeding the main cable's capacity should be charged or discharged by the battery, as the load will cause congestion otherwise. From the figure can be obtained that the battery has idle time, at moments that the load does not exceed the main cable's capacity.

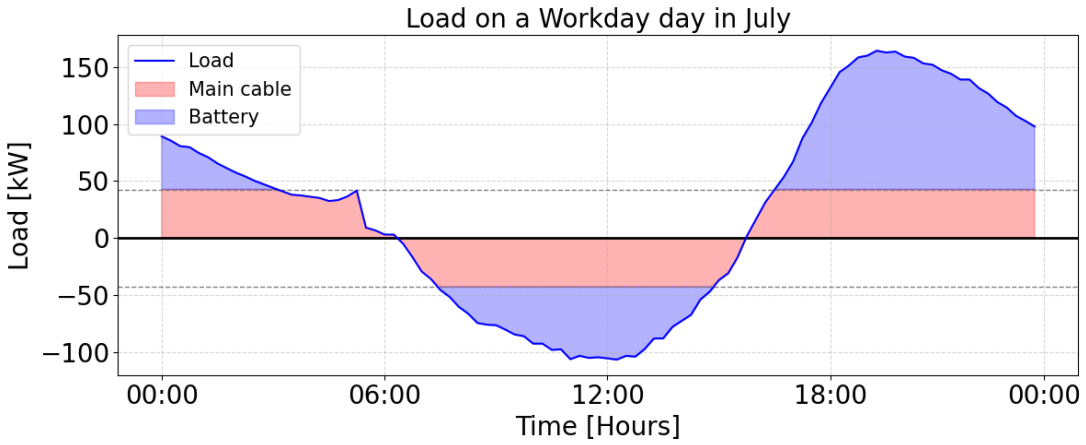

Figure 2.7: Load on a workday in July in the LV-grid to illustrate the subtraction of the main cable's capacity to determine the charging profile.

Charging profile

The real time planning approach that is proposed in the sections above estimates the electricity [in kW] that needs to be charged or discharged to alleviate all congestion for each time step. Equation 2.9 shows the charging profile [in kW] required to alleviate congestion:

$$Pr_t = \sum_{K=1}^{7} E[Load_{K,t} + P_{loss,K,t}] - C_{\max} \tag{2.9}$$

, where Pr_t is the required charging profile [in kW] to alleviate congestion at time t, $\sum_{K=1}^{7} E[Load_{K,t} + P_{loss,K,t}]$ is the sum of the load [in kW] of all node groups K at time t added to the sum of power loss of the power loss [in kW] of all node groups K at time t, and C_{max} is the maximum capacity [in kW] of the main cable. Note that, the Pr_t is zero for $C_{max} < \sum_{K=1}^{7} E[Load_{K,t} + P_{loss,K,t}] < C_{max}$.

Then, the required battery power [in kW] to alleviate congestion can be determined by finding the maximum value from the time series of the charging profile [in kW]. Using the maximum required battery power provides the possibility to alleviate all congestion. If the battery would be smaller, congestion cannot be alleviated when congestion is larger than the battery power. In addition, the battery power can be used to calculate the charging profile that can be implemented in GAIA. These should be values between zero and one, with zeros during idle time, and ones during maximum power. The time series of the charging profile [in ratio] can be determined following Equation 2.9.

$$Pr_t = \frac{\sum_{k=1}^{7} E[Load_{k,t} + P_{loss,k,t}] - C_{\max}}{P_{bat}} \tag{2.10}$$

, where Pr_t is the required charging profile [in ratio] to alleviate congestion at time is t, and P_{bat} is the battery power [in kW].

2.4.3. Optimal location

To determine the optimal battery location, the battery will be deployed with the validated charging profile at potentially suitable locations. The location where the battery is able to minimize congestion is the most suitable location. Although optimization models might suggest locating the battery along a branch, in reality, batteries are typically installed at nodes, such as substations or customer connection points. Consequently, the only locations considered are at nodes since locating the battery the middle of a cable is not practically feasible. Furthermore, just as for the charging profile, the optimal battery location will be indifferent for battery technology.

To determine the most suitable battery location, the potentially suitable locations must be determined first. This is done based on three criteria:

1. **Centrality:**
   The deployment of a battery in the LV-grid will lead to an additional electricity source and sink in the network. To optimally allocate the battery, the electricity flow in the network should be minimized to this additional source and sink. If the battery is deployed at an end of the tree, electricity must be transported throughout the entire network, which could lead to additional congestion. Therefore, it is important to allocate the battery in a central location. The most central location in the network can be found by using the closeness centrality. The closeness centrality is a network metric indicating the importance of a node based on the distance to the other nodes in the network [14]. The closeness centrality is calculated as follows:

$$C_{\text{clo}}(i) = \frac{|N| - 1}{\sum_{j \in N,\, j \neq i} \text{dist}(i, j)}, \tag{2.11}$$

   , where $C_{clo}(i)$ is the closeness centrality for node i, N is the number of nodes on the grid, and dist(i,j) is the distance between node i and node j.

2. **Congested cables**
   This criteria will be explained with the example shown in Figure 2.8. The figure shown the MV-station, three nodes, a battery and three cables connecting the MV-station and nodes. Let's assume that all three cables are congested. With the battery location at node 2, congestion cannot be resolved in cable 3, as both source and sink (MV-station and battery) are located at one side of the cable. In other words, electricity flow towards and from node 3 will remain the same.

   Now, let's assume that that the battery is located at node 3. In this case, the battery will be able to alleviate congestion in cable 3. However, the battery might be less able to alleviate congestion in cable 1 and cable 2, as electricity should also flow throug cable 3. This means that when high amount of electricity should be charged or discharged to alleviate congestion in cable 1 and cable 2, additional congestion might arise in cable 3 due to the battery. As a result, an optimum will be somewhere around the end of the congested area.

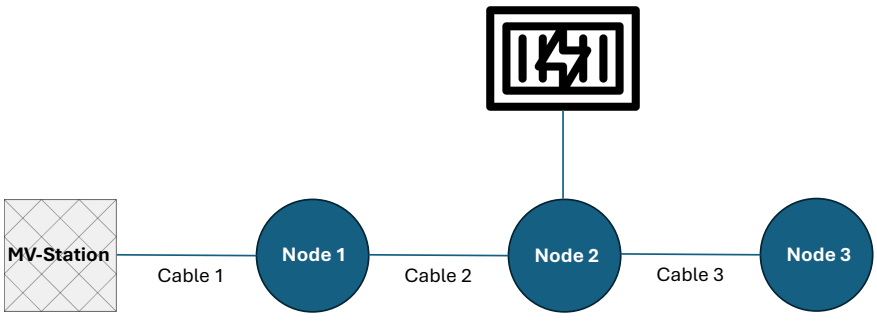

Figure 2.8: Example of simplified LV-grid to setup potentially suitable battery locations for analysis.

3. **Cable capacity**
   The last criteria is cable capacity. When potentially suitable battery locations are determined, cable capacities are important. This is because battery charging and discharging can introduce additional power flows, potentially causing congestion. If a battery is placed at a node connected by low-capacity cables, the risk of inducing further congestion increases. Therefore, it is preferable to locate the battery at a node connected to cables with higher capacity, reducing the likelihood of worsening congestion.

2.5. Battery relocation approach

This section will outline the approach to determine the number of battery relocation. This approach follows from the charging profile, as the number of required relocations is highly dependent to the amount of energy charged and discharged. The charging profile is time dependent and might require the battery to discharge more than it requires the battery to charge. When the battery discharges more energy than it charges, the battery will be empty at a certain moment and will not be able to alleviate congestion according to the charging profile. To deal with this issue, the approach explained in Section 2.5.1 is used.

2.5.1. Balancing SoC

The approach will be explained by using the examples shown Figure 2.9 and Figure 2.10. The figures show a green shaded are when the maximum capacity of the cable connecting the MV-station and the LV-grid is congested due to high demand. Therefore, the battery should discharge the energy in the green shaded area, as explained in Section 2.4.2. By applying the same logic, the battery should charge the energy shown in the orange shaded area. In Figure 2.9, the required amount of charged and discharged energy is almost equal. Nevertheless, a little more discharging is required. To even the amount charged and discharged, it is assumed that the red shaded energy can be used.

To explain the assumption, there will be elaborated on the example shown in Figure 2.9. The energy shown in the red shaded area can be charged, as the cable connecting the MV-station with the LV-grid is capable of transferring that amount of energy without exceeding its capacity. The available capacity can be used to charge the battery to compensate for the difference between charged and discharged energy imposed by the charging profile. The load (shown in blue) and maximum capacity (shown in the red dotted lines) of the main cable will be considered to not cause additional congestion. Note that the direction of electricity flow will change when the load becomes positive due to additional charging. In addition, from the figure can be obtained that no battery relocations are necessary as enough additional energy can be charged (red area) to even the required amount of energy charged (orange area) and the required amount of energy discharged (green area).

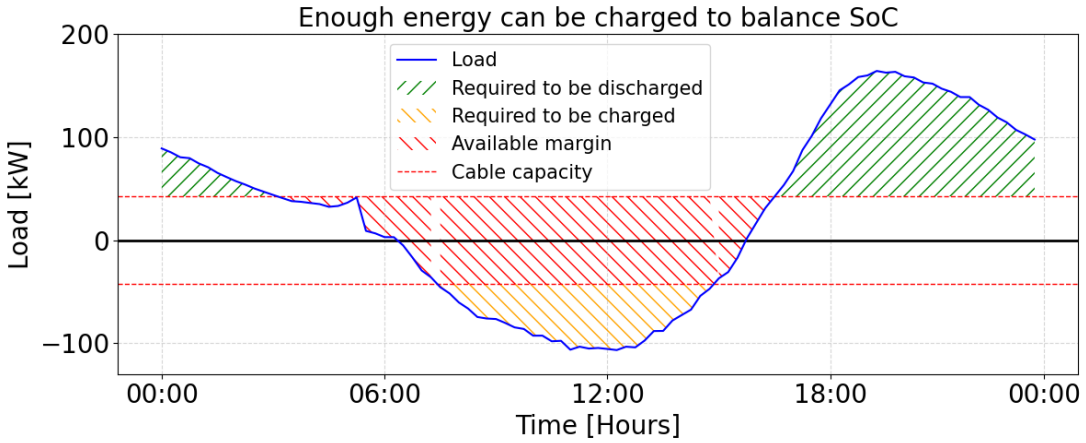

Figure 2.9: Example to illustrate if battery relocation is required: Enough energy can be charged.

For the example shown in Figure 2.10, the battery is only required to discharge, as congestion only arises due to high demand (positive load is larger than maximum capacity). Therefore, the battery should charge during idle time the equal amount of energy to balance the charged and discharged amount of energy. The amount of energy that can be charged is shown in the red shaded area. This area is smaller

than the green area, indicating that the battery cannot charge enough to continue discharging to alleviate congestion. Therefore, battery relocation is required. The calculation for the number of relocations is discussed in the following paragraphs.

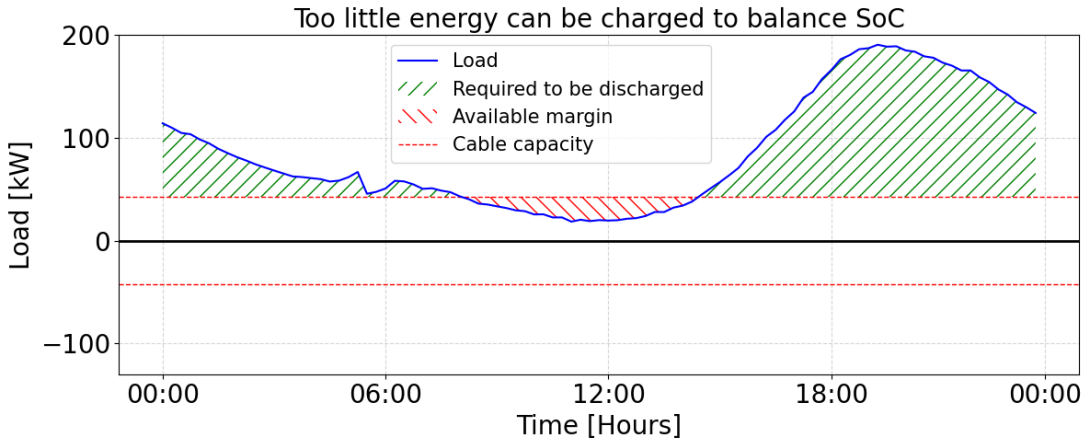

Figure 2.10: Example to illustrate if battery relocation is required: Too little energy can be charged.

The approach used is not implemented in the charging profile itself, but is rather used as a way to calculate the possibility to balance the charged and discharged energy, so that it can continue alleviating congestion.

The SoC is calculated by considering the charging and discharging efficiency of the battery technology. To this end, if the battery is charging, the SoC will increase with the available capacity multiplied with the charging efficiency. This means that low charging efficiency requires more available capacity to level daily charged and discharged energy, as it will reduce the amount of storable energy. In contrast, when the battery is discharging, the SoC decreases with the available capacity divided by the discharging efficiency. Low discharge efficiency will cause a faster reduction of the SoC for the same discharged energy than a high discharge efficiency.

2.5.2. Required number of battery relocations

When the battery is not able to balance its SoC, relocations are required. In reality, the battery will be switched on the basis of predictions on when the battery will be empty. In this research, the battery will be switched when the SoC reaches 5%, as minimum SoC is typically achievable by Lithium-ion batteries [65]. Discharging the battery further may cause damage. The difference between this research and reality is that, in reality, it is necessary to predict when the battery will reach the 5% SoC, whereas in this research, the battery is assumed to be switched exactly at 5%. In addition, in reality, planning constraints might require to switch the batteries before 5% of of the SoC is reached. This uncertainty however, will not be dealt with any further.

To calculate the number of relocations for one month, Equation 2.12 can be used.

$$n_{rel} = \frac{\sum_{d=1}^{N} |\Delta E_d|}{cap \cdot 0.95} \tag{2.12}$$

, where n_{rel} is the number of required relocations per month, N is the number of days is that month, $|\Delta E_d|$ is the absolute value of the daily mismatch between charged and discharged energy in kWh, cap is the battery capacity in kWh, and 0.95 is the depth of discharge (DoD).

2.5.3. Required number of batteries

For the battery relocation approach, a distinction should be made between one required battery and multiple required batteries to alleviate congestion. This difference can arise when the battery capacity (derived from the required battery power determined together with the charging profile and the battery technology-specific duration) and the maximum capacity per battery container require more than one battery.

In the scenario of one required battery to alleviate congestion in the LV-grid, two batteries are required in total: one discharging in the LV-grid, and one charging at a charging location. When the battery in the LV-grid is empty and can no longer alleviate congestion, the battery will be switched with the full battery which could be charged in the mean time at the charging location. This approach holds when the charging and discharging duration of the battery technology are the same, and will not always hold in case of varying charging and discharging durations.

Let's assume there are two identical batteries with a capacity of 100 kWh and a discharge duration of half of the charge duration. This means that the charging power is half of the discharging power (recall Equation 1.1). In a scenario where the battery in the LV-grid should discharge more than half of its power, so the charging profile is above 0.5 on average, the battery will be empty earlier than the battery at the charging location will be full. In this case, three batteries are required: one discharging in the LV-grid and two charging at the charging location.

This works the same for charging and discharging efficiency. When the charging efficiency is half of the discharging efficiency, the battery will store half of the electricity flowing into the battery at the charging location, compared with the loss of stored energy that flows out of the battery at the discharge location in the LV-grid. So, for the same charging and discharging duration, and consequently the same charging and discharging power, the battery at the charging location will not be full before the battery in the LV-grid is empty when the charging profile is above 0.5 on average. So, three batteries are required: one discharging in the LV-grid and two charging at the charging location.

In scenarios where multiple batteries are needed to alleviate congestion in the LV-grid, the batteries will be switched one at a time between the LV-grid and the charging location. This approach ensures that the LV-grid is never left without battery support. The number of batteries required depends, just as for one required battery, on the charging profile, (dis)charge duration, and (dis)charge efficiency. To explain the required number of batteries, the following example is constructed.

Let's assume that 4 batteries are required at the discharging location in the LV-grid, and that the battery's charging and discharging power and the charging and discharging efficiency are equal. This means that when the charging profile is 0.5 on average, additional batteries are required to be charging at full power at the charging location. This will lead to exactly the same charged and discharged over the considered period. In the case of a discharge duration of half the charge duration, the four batteries will be empty earlier than the two batteries are full. In addition, when the charging efficiency is half of the discharging efficiency the four batteries will be empty earlier than the two batteries are full.

To calculate the number of batteries required in the LV-grid, the required energy capacity must be divided by the maximum capacity of one 20ft container. The maximum capacity per container is battery technology-specific and will be discussed in Section 3.5.1. The value found must be rounded to the nearest larger integer, as no half batteries exist.

In addition, to calculate the number of batteries required at the charging location when the battery could not discharge enough to balance daily charged and discharge amount of energy, Equation 2.13 can be used. The equation calculates the required number of batteries at the day of the year that the mismatch is the largest. By this means, there will be enough batteries at all times.

$$n_{bat} = \frac{max(\Delta E_d)}{P_{bat} \cdot 24 \cdot \eta_{discharge}} \tag{2.13}$$

, where n_{bat} is the number of batteries required at the charging location, ($max(\Delta E_d)$ is the maximum daily mismatch between charged and discharged energy over the year in kWh, P_{bat} is the battery power in kW, 24 is the number of hours per day that the battery can charge, and $\eta_{discharge}$ is the discharge efficiency of the battery. Note that the charge and discharge efficiencies are included in ΔE_d. Also, note that when the battery is not able to charge enough to balance daily charged and discharged energy, max must be min, and $\eta_{discharge}$ must be η_{charge}.

2.6. Costs analysis

The power of both the short- and long-duration batteries will be set equal to ensure that all congestion can be alleviated using both technologies. The duration associated with each battery technology will determine its energy capacity, which in turn influences the total cost.

This section outlines the approach used to calculate the costs of the battery technologies required to solve all congestion. Since the level of congestion will be the same after deployment of either technology, the comparison will be based on costs. More specifically, this section describes the approach to calculate the CAPEX, transportation costs, and grid connection costs. As the choice of battery technology will be based on the analysis in Section 3.4, the input parameters specific for the battery technology will be presented after the technologies have been selected.

2.6.1. CAPEX

As discussed in Section 1.2.3, batteries have two main components: the storage tank and the inverter. The costs of these components can be divided into the power capital cost and the energy capital costs for the inverter and storage tank, respectively [66]. The total battery costs can be calculated by adding the components as follows:

$$CAPEX = C_{instal} \cdot cap \tag{2.14}$$

, where the CAPEX is in €, C_{instal} the total instalment costs in $\frac{€}{kWh}$, and cap in kWh.

To calculate the annual CAPEX, the total battery costs should be divided by the battery's lifetime. To do this, it is possible to use the lifetime in years or in the number of life cycles. If the lifetime in years is used, it is assumed that battery degradation is linear over time, and that battery activity does not matter. This is not the case in reality. However, the number of life cycles for the Iron Air battery is not known. Therefore, the lifetime in years is used. This assumption is expected to have limited impact on the results of this research, as the charging profile will be equal for both battery types. The annual CAPEX of the battery can be calculated as follows:

$$CAPEX_{an} = \frac{C_{instal} \cdot cap}{LT} \tag{2.15}$$

, where $CAPEX_an$ is in €, C_{instal} the total instalment costs in $\frac{€}{kWh}$, and cap in kWh, and LT is lifetime in years.

2.6.2. Relocation costs

The variable costs considered in this analysis are relocation costs. These costs are assumed to be the same for both battery technologies, as it is assumed that identical transport resources are used in both cases. Transportation costs consist of wage expenses, depreciation costs of the truck, and fuel consumption.

The relocation costs used in this research are estimates of the actual costs. However, these costs should be carefully considered, as they can significantly influence the results. One battery technology may require more frequent relocations than the other, which affects overall cost-effectiveness. Therefore, the sensitivity of the costs result will be considered in Section 4. By this means, the variations in relocation costs can be used to compare the battery technologies' cost effectiveness. This will be done once the number of battery relocations has been determined.

Besides, it is not practically feasible to transport the required battery capacities due to fixed container sizes and other physical constraints. As a result, relocation costs do not scale linearly with capacity but instead increase in a stepped manner. For example, if a battery container has a maximum capacity of 5 MWh and 6 MWh is required to alleviate congestion, two relocations will be necessary. This is because at least two containers are needed and it is assumed that one truck can transport one container at a time. Therefore, the maximum capacity per 20ft container will be fixed once the specific battery technologies have been identified.

The relocation costs consist of three parts: costs of the truck, fuel costs, and wages. The truck costs are calculated according to Equation 2.16.

$$C_{tr} = C_{Dtr} \cdot \bar{d} \tag{2.16}$$

, where C_{tr} is the truck costs in €, C_{Dtr} are the depreciation cost in $\frac{€}{km}$, and $\bar{d}$ is the average distance from charging location to LV-grid and back in km.

The fuel costs are calculated according to Equation 2.17.

$$C_{fuel} = \eta_{Tr} \cdot P_{fuel} \cdot \bar{d} \tag{2.17}$$

, where C_{fuel} is the fuel costs in €, η_{Tr} is the efficiency of the truck in $\frac{L}{km}$, P_{fuel} is the fuel price in $\frac{€}{L}$, and $\bar{d}$ is the average distance from charging location to LV-grid and back in km.

The wage costs are calculated according to Equation 2.18.

$$C_{wage} = (\frac{\bar{d}}{\bar{v}} + (2 \cdot \bar{t}_{bs}) \cdot C_{wtr} + C_{woe} \tag{2.18}$$

, where C_{wage} is the wage costs in €, $\bar{d}$ is the average distance from charging location to LV-grid and back in km, $\bar{v}$ is the average speed of the truck $\frac{km}{h}$, $\bar{t}_{bs}$ is the average time to switch batteries in hour, C_{wtr} is the wage of the truck driver in $\frac{€}{h}$, and C_{woe} is the wage for operational employers in $\frac{€}{relocation}$.

The total costs per relocation can be calculated by summing the three parts, leading to Equation 2.19.

$$C_{rel} = C_{truck} + C_{fuel} + C_{wage} \tag{2.19}$$

, where C_{rel} is the total relocation costs in €, C_{truck} is the truck costs in €, C_{fuel} is the fuel costs in €, and C_{wage} is the wage costs in €.

2.6.3. Other costs

Next to the CAPEX and transportation costs, other costs are involved. These are connection costs to the grid and electricity costs. These costs will not be considered in this research. The reason is that the total costs are used for comparison between Lithium-ion battery and Iron Air battery, whilst the grid connection costs and electricity costs are indifferent for the battery technologies. Therefore, including the grid connection costs and electricity costs will not affect the results. However, by excluding these costs for mobile battery deployment, it is not possible to compare the costs with the costs of alternative solutions.

The grid connections have fixed costs and variable costs. These costs will be the same for the Lithium-ion battery and the Iron Air battery, as the charging profiles [in kW] are the same. Therefore, the grid connection should have the same size for both battery technologies.

Furthermore, the electricity costs will also be equal for both battery technologies, as the charging profile [in kW] will be the same for both battery technologies.

3

Design choices and input data

3.1. Low-voltage grid

As discussed in Section 2, a LV-grid will be chosen from the low-voltage grids provided by Phase to Phase. In the download portal of Phase to Phase can be chosen between multiple different types of neighbourhoods, called archetypes. These archetypes, shown in Appendix A, will be referenced throughout this section. To choose one archetype for analysis, criteria were established. Here, a distinction was made between hard criteria and soft criteria that the archetype should comply to. The hard criteria must be met to make battery deployment feasible in the archetype of choice. Soft criteria may be met, but only indicate the relevance of researching deployment strategies for mobile batteries in particular archetypes. The following hard and soft criteria were established.

Hard criteria:

1. **Space**
   The type of neighbourhood should provide enough space to accommodate the battery. The physical size of the batteries is expected to be around container-sized. This depends on the battery type, as short-duration batteries have smaller capacities than long-duration batteries for the same power. To enable the accommodation of container-sized batteries, neighbourhoods with a high density of addresses are expected to be unfeasible for battery deployment to resolve congestion. This excludes archetypes 1 and 2, 'Pre-woningwet' and 'Pre-war residences', from the analysis.

2. **Residential area**
   The focus of this study is on the residential area, where the proportion of households is high relative to the overall built environment. Therefore, industrial areas will not be considered in this study. This criterion excludes archetype 8, 'Limited Population & Industry', from the analysis.

Soft criteria:

1. **Modularity**
   The type of LV grid studied should occur frequently in the Netherlands to enhance the modularity and generalizability of this research. As shown in Appendix A, archetypes have been precisely defined based on several neighbourhood characteristics, resulting in a fragmented set of archetypes. As a result, the share of each LV-grid archetype in the Netherlands is relatively low. However, some archytpes might have overlap with other archeypes, so it would be unfair to solely select the archetypes with the highest share. Nevertheless, a threshold of 10% has been set. This leads to less preference for archetypes 4 and 5, 'Post-war Tenements' and 'Corporation Residents', for analysis.

After excluding archetypes 1, 2, and 8 based on the hard criteria, and deprioritizing archetypes 4 and 5 based on the soft criteria, archetypes 3, 6, and 7 were identified as suitable for further analysis. These archetypes represent approximately 72% of Dutch neighbourhoods. Their high prevalence makes them both relevant for research and promising candidates for battery deployment.

To choose a single LV-grid, the remaining LV-grids were analysed in GAIA based on peak load. Peak load was chosen as the key criterion, as it directly relates to grid congestion and the potential need for battery deployment. The peak load in the LV-grid is highly dependent on installed capacities of PV, EV charging

points and HPs. Therefore, high installed capacities of electrical equipment implies a potential for battery deployment to alleviate congestion.

The remaining LV-grids were analysed on installed capacities, and a preliminary peak load analysis was performed in GAIA to obtain an indication of maximum congestion across the LV-grids. Based on the analysis, the LV-grid shown in Figure 3.1 was chosen. It should be noted, however, that while this specific LV-grid was chosen, the findings from the analysis are expected to be applicable to the other remaining LV-grids that were not excluded by the hard criteria.

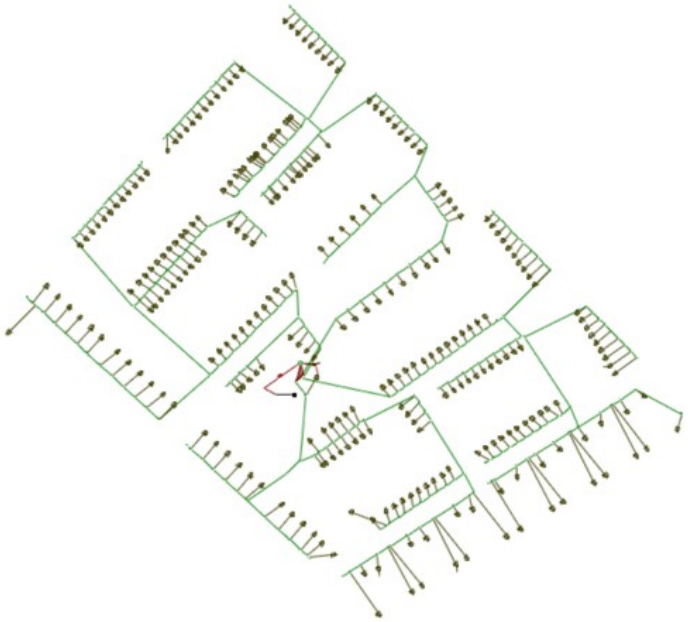

Figure 3.1: Chosen neighbourhood for studying the deployment strategy for mobile batteries.

The chosen LV-grid shows a neighbourhood with a MV-station and four LV-grids. These four LV-grids are only connected via the MV-station and can be seen as independently operating grids when the MV-station is considered the system boundary. Therefore, one of the LV-grids will be chosen for further analysis.

The four LV-grids have a comparable number of residents, have comparable installed capacities of electrical equipment, and comparable peak load. Therefore, one of the LV-grids is selected at random for further analysis. The chosen LV-grid is shown in Figure 3.2.

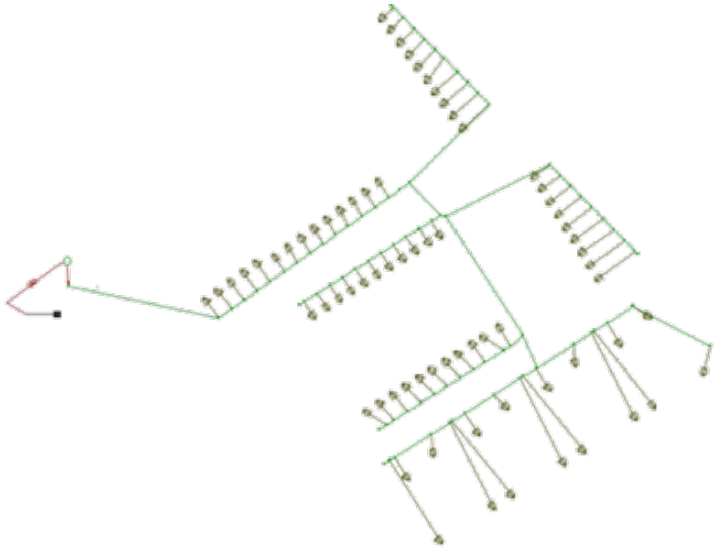

Figure 3.2: Chosen LV-grid for studying the deployment strategy for mobile batteries.

3.2. Potentially suitable battery locations

This section presents a congestion analysis to support further design decisions. An analysis to setup potentially suitable battery locations will be presented. This includes the three criteria as defined in Section 2.4.3: closeness centrality, congested cables, and cable capacities.

The first criteria is the centrality of the battery location, which is determined by using the closeness centrality. Figure 3.3 shows the top 10 scoring nodes for the closeness centrality. When electricity demand and supply would be equal for all nodes in the LV-grid, locating the battery at the best scoring node (indicated with a 1 in the figure) will minimize flow of electricity.

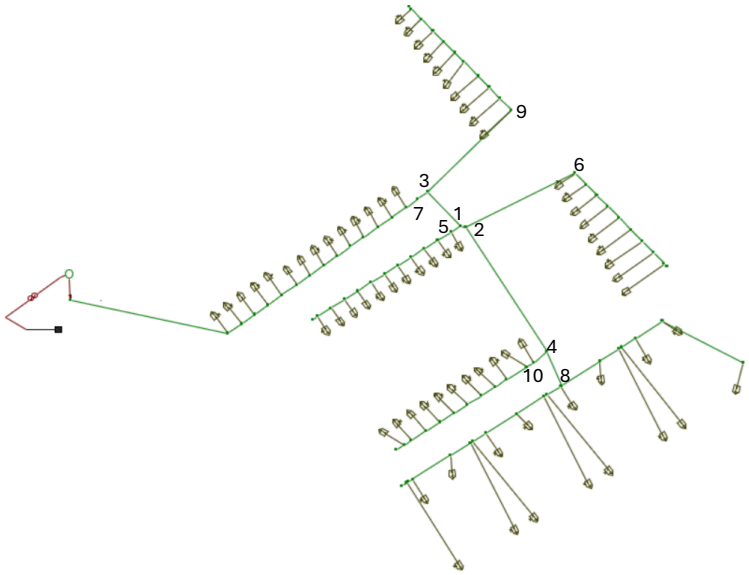

Figure 3.3: Top 10 scoring nodes for closeness centrality in LV-grid.

The second criteria is the congestion occurring in the cables. The result is shown in Figure 3.4. The figure shows the cables that are congested somewhere throughout the year in red.

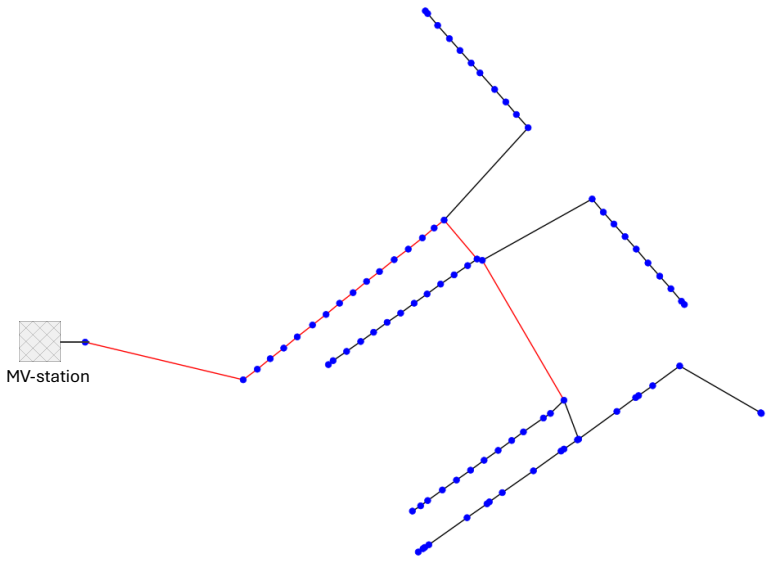

Figure 3.4: The expected congested cables are shown in red.

In addition, Figure 3.5 shows the thickness on the lines based on the cable capacity. The figure shows a sequence of cables with higher capacity (I_{nom} = 185A) as well as multiple shorter sequences cable segments with smaller capacities (I_{nom} = 120A).

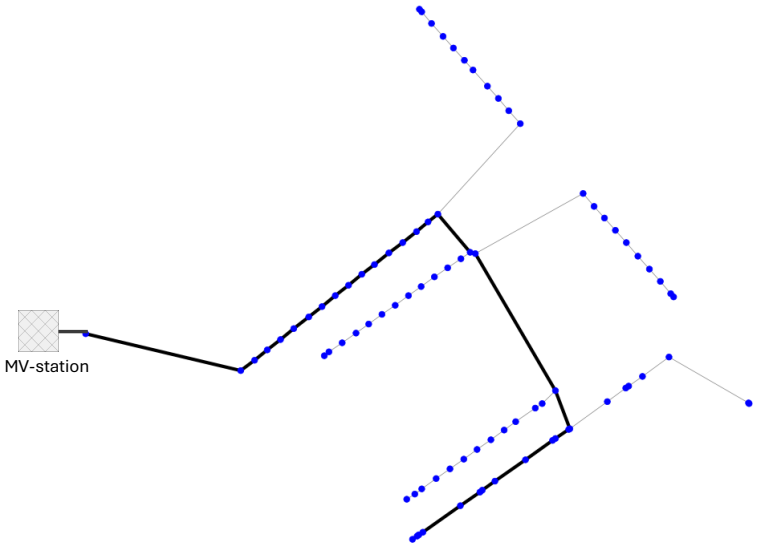

Figure 3.5: The cables shown in black have a capacity of 185A and the cables in grey have a capacity of 120A.

The observations based on the criteria, along with Figure 3.3, Figure 3.4 and Figure 3.5, led to the proposed locations shown in Figure 3.6. Six battery positions are chosen, which are indicated with the L of location and the location-specific number. The locations chosen are, except for L6 chosen from the top 10 most central nodes of the LV-grid to minimize the flow of electricity. In addition, all locations chosen are along the cable with the higher capacity, as this will minimize the probability that the battery will introduce additional congestion. Furthermore, potentially suitable battery locations were selected both inside and outside the congested area to enable comparison of battery deployment in different congestion contexts. Specifically, the locations L1, L2, L3 are in the congested area, the location L4 at the end of the last congested cable, and L5 and L6 are chosen outside the congested area. The optimal battery location will be determined by deploying the battery with the charging profile at the six locations and comparing the resulting congestion.

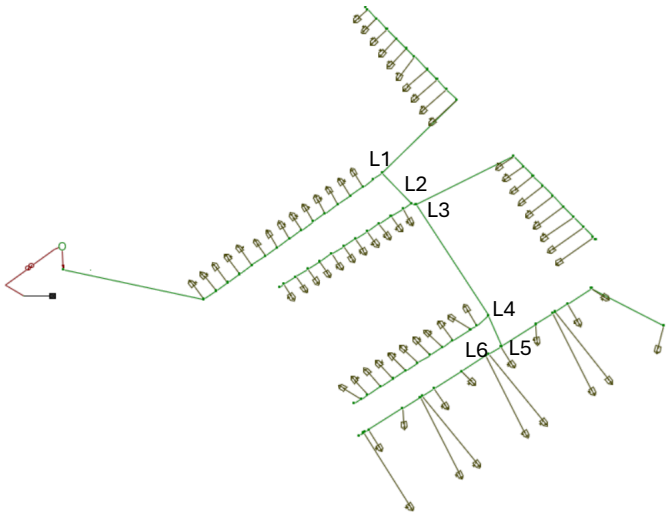

Figure 3.6: LV-grids including the six positions for which the battery deployment is assessed.

3.3. Congestion trend analysis

An annual congestion analysis will be examined in the chosen LV-grid to obtain trends in congestion. The trends will provide information on the optimal battery duration as explained in Section 2.2.4.

The result of the Fourier transform applied to the congestion during the year in the LV-grid is shown in Figure 3.7. The figure shows three main peaks of which one correspond to 12 hours ($\frac{1}{0.0833} = 12$) and two peaks correspond to 24 hours ($\frac{1}{0.0397} \approx 25$ & $\frac{1}{0.0437} \approx 23$). The peak corresponding to 12 hours is probably due to the higher demand during the morning and beginning of the evening. In addition, the peaks around 24 hours are due to daily fluctuations, such as congestion due to high PV generation around noon and congestion due to the two reoccurring demand peaks in the morning and beginning of the evening. One of the peaks around 24 hours has a frequency of a little higher than 24 hours, and one peak has a frequency of a little lower than 24 hours, as congestion shifts slightly over time due to the changing seasons.

From the figure can be concluded that a cycle time of 12 or 24 hours would be a fitting battery cycle time. Recall from Section 2.2.4 that this indicates a fitting duration of 6 or 12 hours. A duration of 6 hours is chosen, as lower capacity decreases the CAPEX. However, it is expected that the battery should be transported twice as much as a battery with a discharge time of 12 hours. Therefore, transportation costs will be twice as high.

Furthermore, from the figure can be obtained that in the range of the long-duration batteries, no significant peaks arise. This does not indicate that long-duration batteries are not suitable for congestion management in this LV-grid, as the result focuses on trends and neglects other battery specifications, such as costs. However, it does indicate that there is no significant preference for a particular long-term duration.

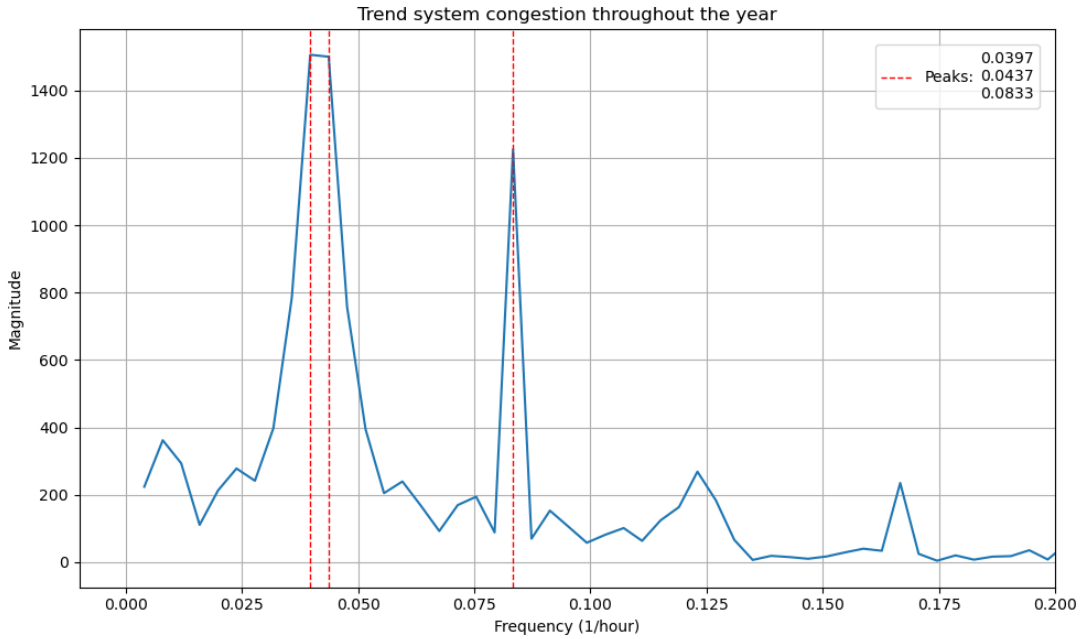

Figure 3.7: Congestion trend analysis to determine optimal battery duration for congestion management purposes.

3.4. Battery technologies

This research focuses on short-duration and long-duration batteries. The boundaries of short- and long-duration batteries are not fixed and vary per research. According to Smdani, Islam, Yahaya *et al.* [67], short-duration batteries range from a few hours to a few days, and long-duration batteries can store energy for a few months. Luo, Wang, Dooner *et al.* [68] distinguish between short-term, medium-term and long-term durations that are up to a few hours, a few days, and a few months, respectively. In addition, Hunter, Penev, Reznicek *et al.* [69] states that long-duration storage is days to weeks to months. The classification uncertainty was acknowledged in Twitchell, DeSomber and Bhatnagar [70] who reviewed

how generation industry and academia classified long duration. The study concluded that a duration of at least 10 hours is usually classified as long duration.

As no standard threshold is available, this research considers a duration of 12 hours or shorter short-duration and long-duration when it has a duration of more than 12 hours. This section will explain the choice made for the short-duration and long-duration battery technology in this research. In addition, specifications of the chosen batteries, such as charging and discharging efficiency, will be presented.

3.4.1. Short-duration battery technology

The most widely deployed short-duration battery is the Lithium-ion battery, which represented 89% of the electrochemical battery generating capacity (so, including long-duration) in 2020 world-wide [29]. Lithium-ion batteries are suitable for applications that require short response time, as Lithium-ion batteries have a response time of milliseconds [68]. This is highly important, as the battery should be capable of reacting to load predictions of fractions in the future. In addition, Lithium-ion batteries are suitable for applications where weight is important [68]. This is due to the high energy density of the battery. This is an advantage of the battery technology over other technologies, as less weight will ease transportation of the battery. Furthermore, Chen, Jin, Lv *et al.* [71] states that Lithium-ion batteries are considered key battery technologies for grid balancing activities due their high energy efficiency. To this end, Lithium-ion battery is chosen as short-duration battery, as it contains the required characteristics to be suitable for congestion management, it has high energy density which simplifies transportation, and it is already widely available on the market which enhances quick deployment.

3.4.2. Long-duration battery technology

For the choice for the long-duration battery technology, energy capital costs [in €/kWh] are crucial [72]. Costs for long-duration batteries are crucial, as the technologies have significantly less daily cycles compared to short-duration batteries. This is due to the higher capacity for the same power. If energy capital costs would be the same for short- and long-duration batteries, long-duration would be much more expensive as their capacity is larger. Furthermore, energy density is important for mobile batteries for the same reason as for short-duration technologies: it will eas transportation. According to Olabi, Sayed, Wilberforce *et al.* [73], Iron Air batteries are suitable as for long-duration storage, as the technology is cheap due to the abundance of raw materials, and environmentally friendly. Therefore, the Iron Air battery is chosen as long-duration battery technology.

3.5. Input data

This section will provide the battery input parameters that are required to calculate the number of batteries required and the number of relocations. In addition, this section will examine the costs associated with battery relocation and the costs per relocation will be calculated.

3.5.1. Battery input parameters

The battery technology-specific parameters for the Iron Air battery and Lithium-ion battery are shown in Table 3.1.

Table 3.1: Battery-specific duration and efficiencies.

Battery type	Duration [h]	Charging efficiency [%]	Discharging efficiency [%]
Iron Air	100[74]	71[74]	60[74]
Lithium-ion	6	95[75]	95[75]

Furthermore, the battery technology-specific energy density and power density are visualized in Figure 3.8. The figure shows the power and capacity of a 20ft container of both battery technologies. The capacity of the 20ft containers will be taken into account for the number of required battery relocations. Recall from Section 2.5 that the capacity of the 20ft container is the maximum allowed capacity per relocation.

(a) Power and capacity for a 20ft Lithium-ion container [76].

(b) Power and capacity for a 20ft Iron Air container.

Figure 3.8: Maximum power and capacity per 20ft container for both Lithium-ion and Iron Air.

Equation 2.15 and the cost values shown in Table 3.2 are used to calculate the CAPEX.

Table 3.2: Total instalment cost and lifetime for both the Lithium-ion battery and Iron Air battery.

Battery type	Total instalment costs [€/kWh]	Lifetime [years]
Iron Air	17.5 [74]	17.5 [74]
Lithium-ion	277 [77]	16 [78]

3.5.2. Relocation costs

In Section 2.5 is discussed that the relocation costs consist of three parts: truck costs, fuel costs, and wages. These can be calculated according to Equation 2.16, Equation 2.17, and Equation 2.18, respectively. To enable these calculations input data is required. This section will outline the input data and calculate the costs per battery relocation.

Truck costs

The depreciation costs for the truck are calculated by dividing the costs of a truck (i.e. €150.00 [79]) by the expected lifetime [in km] (i.e. 1,500,000 km [80]). This results in truck depreciation costs of 0.10 $\frac{€}{km}$.

In addition, the average distance from the LV-grid to the charging location cannot be known exactly because the LV-grid is anonymized. Therefore, an estimation is made. To do this, a map for the existing windfarms in 2020 and a map with the expected windfarms in 2030 is used. The maps can be found in Appendix D in Figure D.1. The maps show that the number of windfarms is expected to increase in the upcoming years and will be wide spread throughout the Netherlands. The estimation is that the average distance from LV-grid to a windfarm is 30km. This distance should be doubled, as the truck needs to drive back and forth.

Fuel costs

To calculate the fuel costs, the efficiency of the truck is required. The efficiency is highly related on the weight and route of the truck [81]. However, according to Scania, which is one of the world largest truck building companies, the average efficiency is about 3.5 $\frac{km}{L}$ [81].

In addition, the costs per litre fuel is important. The fuel used in most trucks is diesel and this price fluctuates daily. At the moment of writing, the diesel price is 1.667 $\frac{€}{L}$ [82].

Furthermore, the average distance is the same as for the truck costs.

Wages

An important cost for battery transport is the wage expenses of the truck driver. According to the CAO (collectieve arbeidsovereenkomst, or collective bargaining agreement), the hourly wage of a truck driver is about €20 [83]. This wage is taken from a range of wages, that depend on the scale of employment. However, €20 is higher than the wage in most scales. Therefore, this number is assumed to be reliable for costs calculation and does not underestimate the costs of truck driver employment. Nevertheless, the

costs of employment are higher than the gross wage. According to [84]–[86], the additional employment cost, such as insurance, are about 25%. As a result, the hourly costs of a truck driver is found to be €25.

The total wage of the truck driver is dependent on the average distance of transportation, the average speed of transportation and the average time of switching the battery. The average distance is the same as for the truck. In addition the average speed of the truck is estimated at 50km/h. This is chosen as it middles the maximum speed of a truck at the highway (i.e. 80km/h) and the maximum speed in most neighbourhoods (i.e. 30km/h). The average of both speeds is rounded from 55km/h down to 50km/h, as it is expected that the truck will drive longer in 30km/h area than on highway. In addition, the average time to switch the battery is estimated to be 15 minutes.

Furthermore, the costs of logistics, such as logistic-related personnel, should be considered. The costs for logistic-related personnel is highly dependent on factors, such as use of route planning software and economies of scale. Therefore, a rough estimation is done for €10 per battery relocation.

Total relocation costs

Table 3.3 summarized the values found in the previous paragraphs and will be used to calculate the total costs for one battery relocation.

Table 3.3: Parameters for transportation costs per 20ft container relocation.

Truck depreciation [€/km]	Average transportation distance [km]	Average transportation speed [km/h]	Fuel use [km/L]	Fuel price [€/L]	Average time of switching the battery [h]	Wage truck driver [€/h]	Wage operational employee [€/relocation]
0.10	60	50	3.5 [81]	1.667 [82]	0.25	25	10

As a result of the values shown in Table 3.3, the cost for one battery relocation could be calculated. These costs will be considered for every battery relocation equal or smaller than the maximum capacity of one 20ft container. The costs increase step wise, as the costs for a battery relocation with the capacity of a half container is equal to the costs for a battery relocation of a whole container.

The truck costs, fuel costs, wage costs are shown in Table 3.4. In addition total costs per battery relocation are calculated in Equation 2.19, resulting in the total costs of €87.08 per relocation.

Table 3.4: Costs for the truck, fuel and wages, resulting in the total costs per battery relocation

Cost type	Costs [€]
Truck	6
Fuel	28.58
Wage	52.50
Total relocation	87.08

4

Results

This chapter will discuss the results of the deployment strategy for mobile batteries to alleviate congestion in LV-grids. The following aspects of the deployment strategy will be discussed. First, the proposed real time planning approach, as discussed in Section 2.4.2, to determine the charging profile will be validated for a workday in January, a weekend day in January, a workday in July, and a weekend day in July. Second, the charging profile is tested at various locations in the LV-grid for a workday in January and a workday in July. As a result, the most suitable battery location in the LV-grid will be determined. Third, a congestion analysis is with the designed deployment strategy (consisting of the charging profile and battery location) to obtain the congestion reduction compared to the congestion without battery deployment. Fourth, battery technology specific parameters are considered to calculate the number of required battery relocations for every month of the year. Fifth, a cost comparison between the Lithium-ion and the Iron Air battery will be performed.

4.1. Charging profile

To test the real time planning approach proposed in the Section 2.4.2, a battery is used without limitations. This means that it is assumed that the battery is able to (dis)charge the electricity needed to alleviate congestion, without being constrained by its capacity. By using an unconstrained battery, the success of the real time planning approach cannot be affected by battery limitations. This allows for an unconditional assessment of the approach. Consequently, the difference in results of the comparison between Lithium-ion and Iron Air will be caused by limitations for that specific battery type, such as capacity.

Furthermore, the real time planning approach to obtain the charging profile for the battery is tested for one workday and one weekend day in both January and in July, to see if the method is valid under different conditions. In addition, the approach is tested at L4, which indicates a location in the LV-grid as shown in Figure 3.6. Although it was not known in advance whether L4 was the optimal location or not, L4 was chosen, as this location was expected to be close to the optimal location. The actual optimal location could not be known in advance to this validation, as the charging profile and location depend on each other. Therefore, either the charging profile or the location should be assessed first.

4.1.1. System congestion

The results of the validation of the charging profile are shown in Figure 4.1. The figure shows the four scenarios as explained in the introduction of the validation section. The blue curves indicate the congestion before battery deployment. In January, one congestion peak occurs. This peak is due to high demand in the beginning of the evening. In July, a second congestion peak occurs around noon. This peak is caused by high PV generation. Note that the figures show the level of congestion and do not indicate its direction. The direction of congestion is opposite during the afternoon and evening for the scenarios in July.

The figures also show that more congestion in the evening occurred during a workday than on a weekend day for both January and July. This is mainly caused by EV charging, that is performed more often during working days. The curves also show that the system congestion in the evening is higher in January than in July. This seasonal difference is mainly caused by HPs, as more activity is required during colder days.

The seasonal patterns for congestion arising from PV generation around noon are much larger, as no congestion occurred during winter and much congestion in summer. The daily differences are almost absent, as insolation is indifferent for the type of day.

The figure also shows yellow curves, which indicate congestion after battery deployment. The figures show that congestion is significantly reduced for all four scenarios. This is especially the case for the congestion at the beginning of the evening, when the battery discharges. The congestion occurring around noon is also significantly alleviated, but some congestion remains. The remaining congestion is stable over time, independently of the amount of congestion without battery deployment. This indicates a fixed value contributing to the load required to be charged during PV generation. The only value in the equation to calculate the charging profile (i.e. Equation 2.9) is the capacity of the main cable. However, the used capacity of the main cable is undeniable. Therefore, the exact reason for the remaining stable congestion around noon is unclear.

Another observation from the figures is that congestion is equal for the scenarios with and without battery (except for a weekend day in January shown in Figure 4.1b) during the first 30 minutes of congestion. This indicates that the charging profile might inhibit a delay. To further improve the charging profile, it could be considered to start (dis)charging before congestion is expected.

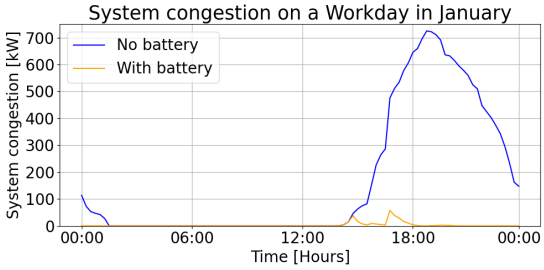

(a) System congestion was reduced by 98.3%, using the real time planning approach to determine the charging profile for a workday in January.

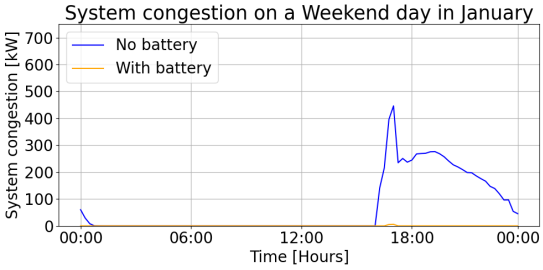

(b) System congestion was reduced by 99.8%, using the real time planning approach to determine the charging profile for a weekend day in January.

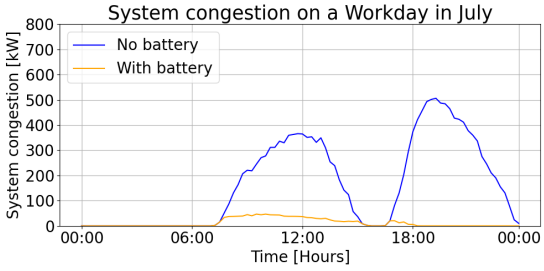

(c) System congestion was reduced by 92.3%, using the real time planning approach to determine the charging profile for a workday in July.

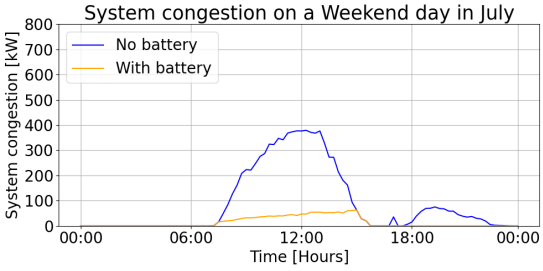

(d) System congestion was reduced by 84.6%, using the real time planning approach to determine the charging profile for a weekend day in July.

Figure 4.1: Charging validation for system congestion.

4.1.2. Maximum congestion

Next to system congestion, the real time planning approach is assessed to determine the charging profile based on its reduction of maximum congestion. Reducing maximum congestion is important as high congestion peaks might damage the LV-grid. The exact allowed overcurrent depends on factors as time of the overcurrent, ambient temperature, and cable type. These specifications are outside the scope of this research. However, the hard limit of overcurrent is 45% in LV-grids for very short periods of time [87], [88]. This hard limit will be used to assess the overcurrent without and with battery deployment, although the limit will be set lower in most cases in practise. The same scenarios: a workday and a weekend day in January, and a workday and a weekend day in July, that were used to assess the system congestion are

considered. The results are shown in Figure 4.2.

The results of the maximum congestion analysis are shown in Figure 4.2. The figure shows that maximum congestion is significantly reduced in all four days with battery deployment compared to the same days without battery deployment. The maximum congestion reductions are 78.7%, 88.1%, 80.0%, and 69.9% for the days as shown in the figure, respectively. In addition, the figure shows a red dotted horizontal line indicating the hard limit for overcurrent over a short period. This actual limit varies for each case, depending on the cable and the situation. Nevertheless, the hard limit provides an indication of the amount of congestion and the effectiveness of the charging profile.

Furthermore, the figures show comparable curves to the curves shown in Figure 4.1. This is reasonable, as when no system congestion is present, there cannot be a maximum congestion higher than zero. On the other hand, when there is high amount of system congestion, the probability that there will be a high maximum congestion is also high.

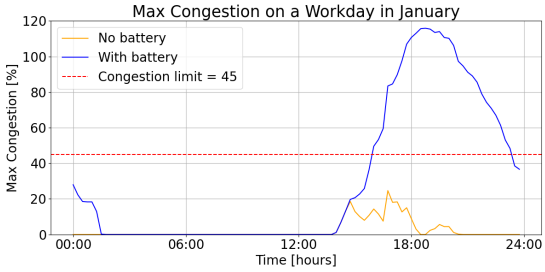

(a) Maximum congestion was reduced by 78.7%, using the real time planning approach to determine the charging profile for a workday in January.

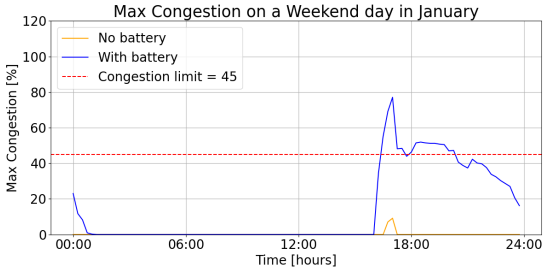

(b) Maximum congestion was reduced by 88.1%, using the real time planning approach to determine the charging profile for a weekend day in January.

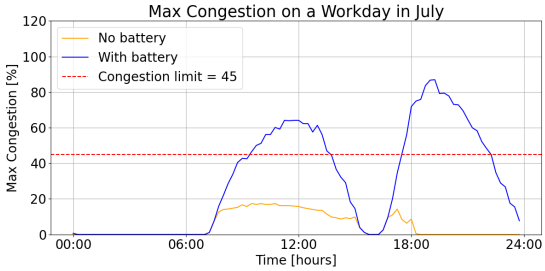

(c) Maximum congestion was reduced by 80.0%, using the real time planning approach to determine the charging profile for a workday in July.

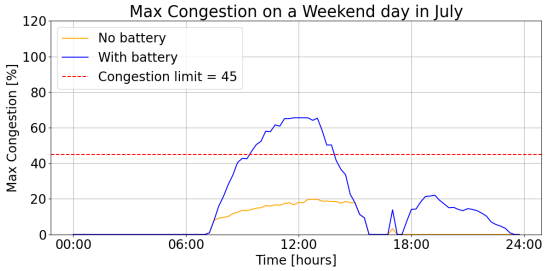

(d) Maximum congestion was reduced by 69.9%, using the real time planning approach to determine the charging profile for a weekend day in July.

Figure 4.2: Charging validation for maximum congestion.

Validation resistance half way

The real time planning approach assumes that the MV-station is the source and sink for half of the load and the battery is the source and sink of half of the load. Making an assumption based on the load division is necessary to calculate the power loss, as the power loss is dependent on distance. The actual distance covered by the load cannot be known exactly, as the PV generated electricity might travel to electricity demanding neighbours, and does not go to either MV-station or battery.

Table 4.1 shows the energy that used the MV-station as source or sink and the energy that used the battery as source or sink for both a workday in January and a workday in July. From the table can be concluded that electricity flow is comparable for the MV-station and the battery for both months. Although the energy is not exactly equally distributed (i.e. 50%), the assumption of using the average load distance to the MV station and LV grid is considered valid, as it is of the same order of magnitude, which results in only minor errors.

Table 4.1: Validation of using the distance for half of the load from the source to the MV-station and half of the load to the battery.

Day	Electricity flow [kW]	
	MV-station	Battery
Workday January	3701	4900
Workday July	3182	4259

Although this assumption holds for this LV-grid during this year, it does not indicate that this will be the case for another year or at other LV-grids. The assumption is highly dependable on the level of congestion. This can be explained by the situation of no congestion. When no congestion is occurring, the battery will not be active. This leads to all energy flowing from and towards the MV-station. Therefore, a situation with less congestion will shift the share of source and sink use from the battery towards the MV-station. To make this assumption applicable to other LV-grids, an estimation must be made of the energy share flowing to the MV-station and to the battery.

4.2. Battery location

The location of the battery in the LV-grid is important to minimize congestion. For instance, the location influences the power losses due to the variable distance, as explained in Section 2.4.1. Therefore, minimum distance from the battery to the nodes is favourable. On the other hand, Section 3.2 explained that deploying the battery in congested area will hinder alleviation in the cables at the opposite site of the MV-station, from the battery perspective. This section will provide the results of the deployment of a battery at the six potentially suitable battery locations using the charging profile. The various locations will be tested for a workday in January and a workday in July. These two days are chosen because they represent the extremes of congestion throughout the year. This means that the congestion during these two days differ the most from each other compared to all other days of the year. Using them to determine the optimal battery location is valid, as all other days will have less congestion differences. Consequently, the selected locations will also differ less. Besides, Figure 4.3 is shown below again, to make the results easier to interpret.

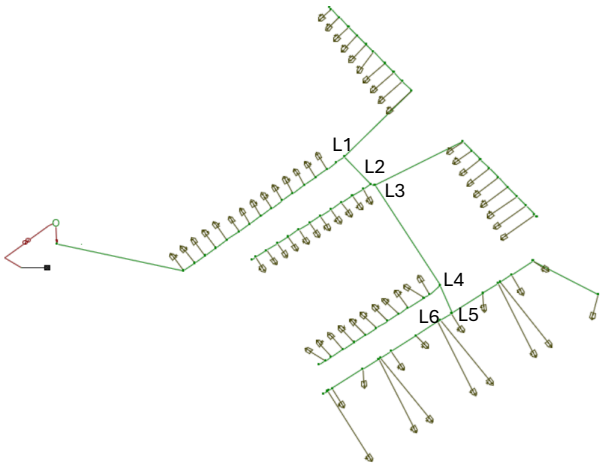

Figure 4.3: The figure showing the six potentially suitable battery locations is copied from Section 3.2 to make the results for the optimal battery location easier to interpret.

Figure 4.4 shows the results for the battery deployment at the six locations. Figure 4.4a shows that L4 is the optimum location for battery deployment in January, as both system congestion and maximum congestion are the lowest. Figure 4.4b shows that there is a trade-off for battery deployment in July, as L5 has the lowest system congestion, and L6 has the lowest maximum congestion, implying that congestion was more evenly distributed over the cables when the battery was deployed at L6. However, differences are minimal and might be negligible in reality. In addition, the difference between system congestion for the locations is bigger in July than in January. This is due to the charging profile that alleviates

congestion better in January than in July, as was found in Section 2.4.1. This indicates that choosing the optimum location during July is more important than choosing the optimum location in January, since overall system congestion will be reduced more. Therefore, L5 is chosen as most suitable battery location, according to the numerical results.

Furthermore, although that the system congestion and maximum congestion differs for the locations, the differences between the level of congestion between the locations is relatively small compared to the level of congestion without battery deployment, as can be obtained from Figure 4.4a and Figure 4.4b and their captions. This is an important observation, as it tells that the ability of the battery to alleviate congestion is not highly dependent on the location. As the studied LV-grid is anonymized, and the design of the neighbourhood is unknown, this finding allows for battery deployment at a location close to the optimal location rather than only at the optimal location. To this end, the deployment of the battery at different locations also functions as a sensitivity analysis from which can be concluded that it is possible to deploy the battery close to the optimum location and still being able to alleviate congestion significantly.

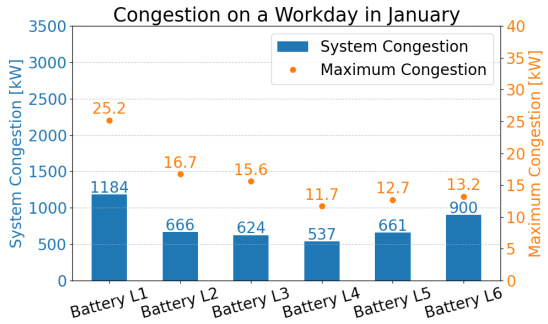

(a) The system congestion and maximum congestion without battery deployment are 16603 kW and 49.3 kW, respectively.

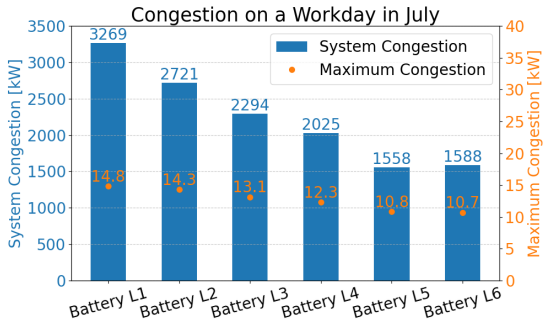

(b) The system congestion and maximum congestion without battery deployment are 15946 kW and 37.0 kW, respectively.

Figure 4.4: Results battery deployment at various locations for a workday in January and a workday in July.

Furthermore, recall that the data used for this analysis is data for 2030. In addition, it is important to consider that congestion is increasing in general. From this reasoning, it is expected that the congestion is currently less prominent than found in the results, and that congestion might become worse after 2030. The level of system congestion will affect the number of congested cables and the location of the end of the congested area. This implies that the optimum battery location may shift over time, further into the Lv-grid. As a grid connection should be created at the battery location, which is costly and time consuming, an estimation should be made for the future expected congestion. The expected congestion might influence the optimal location. When no significant congestion increase is expected in the LV-grid after 2030, the location should remain at L5. If there is expected rise of congestion, deploying the battery at L6 could be a better option.

Note that the optimal battery location is independent of battery technology and for stationary and mobile batteries, as the charging profile is also independent for these factors.

4.3. Congestion

The congestion in the LV-grid is analysed for the LV-grid without battery deployment and with battery deployment. For the analysis with battery deployment, the battery is deployed at location L5, as concluded to be the optimal location in Section 4.2, and with the charging profile determined according to the methodology described in Section 2.4.1. The charging profile was developed to allow any battery technology to alleviate all congestion, as the battery size will be adjusted to the required power. Recall that the battery capacity is adjusted based on the required power and the battery specific duration. It could be the case that capacity is the limiting factor to alleviate congestion, then, battery transportation will take place. This will increase costs which will be analysed in Section 4.5. To this end, the congestion analysis can be done without taking battery specifications into account, as all battery technologies will alleviate the same amount of congestion. This approach will allow for a quick scan of the potential of

alleviating congestion with batteries in LV-grids. Thereafter, a cost analysis can be done to obtain the cheapest battery technology to achieve that particular amount of congestion alleviation.

The monthly results of the system congestion analysis with and without battery deployment are shown in Figure 4.5. The results of the analysis without battery deployment show two peaks: one in winter and one in summer. The figure also shows that the system congestion in winter and in summer is similar. However, the system congestion in winter consists of congestion due to high demand, and the system congestion in summer consists of both congestion due to both high demand and high PV generation, as could be obtained from Section 2.4.1.

The results of the analysis with battery deployment show that more congestion remains in summer than in winter. This suggests that the charging profile is more effective in reducing congestion caused by demand than by PV generation. Overall, the combination of the charging profile and the optimal location was able to reduce congestion in a range of 91% to 99%, except for June when congestion was reduced with 84%.

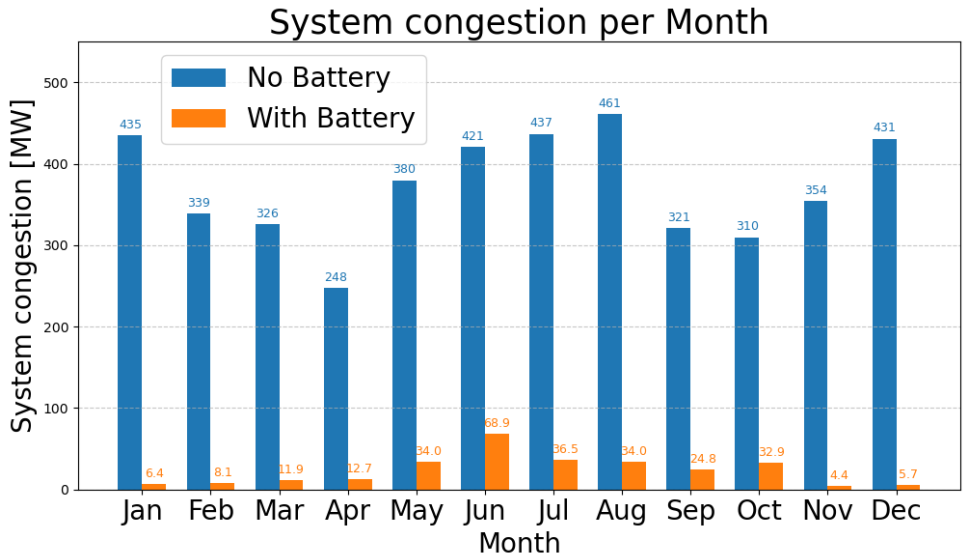

Figure 4.5: System congestion for every month of the year for a scenario without battery deployment, and a scenario with battery deployment.

As shown in Figure 4.5, the system congestion in winter is similar to the system congestion in summer, although the congestion time in summer is higher than in winter. Therefore, it can be expected that the maximum congestion in summer is lower than in winter. The results of the maximum congestion per month are shown in Figure 4.6. The figure shows the maximum congestion for the months of the year without and with battery deployment. The figure confirms that the maximum congestion in summer is lower than in winter. However, the difference in maximum congestion is smaller than the difference in system congestion. In addition, the maximum congestion shows a different curve than system congestion, as the maximum congestion only peaks during winter.

Furthermore, the figure shows the distribution of the maximum congestion in the congested cables. Every point represents the maximum congestion in one cable. This results in a distribution of the maximum congestion for all congested cables during that month. For the results without battery deployment, the figure illustrates that the maximum congestion in the congested cables do not vary significantly. The clustered maximum congestions are the cables located between the MV-station and L1. The, cables with significantly lower maximum congestions are located between L1 and L4. In addition, no significant differences in the distribution can be found for the different seasons, showing that the maximum congestion is similar for all months.

The maximum congestion distributions shown for the scenario with battery deployment does not show clear seasonal patterns and seem rather random. This might be caused by the mismatch between the charging profile and the actual load.

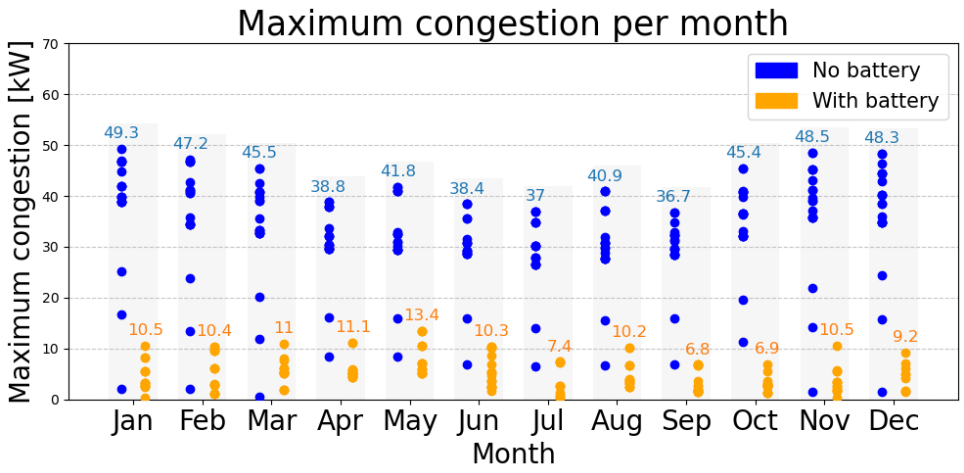

Figure 4.6: Distribution of maximum congestion in cables with and without battery deployment.

In addition, Figure 4.7 shows the number of congested cables per month without and with battery deployment. The figure shows that, except for June, the number of congested cables is reduced. However, only in a small share of the congested cables is congestion completely resolved. This illustrates the deployment strategy is primarily suitable to alleviate congestion equally over the entire system rather than solving congestion at one particularly location. Again, the results of the number of cables in which congestion is completely resolved do not show clear seasonal pattern.

The number of cables congested in June increased with battery deployment. The additional congested cable is the cable connected to the battery. The cable was congested during the discharging of the battery. At this moment, congestion could be alleviated almost exactly within the boundaries in the entire LV-grid. Nevertheless, the congested cable indicates that the battery might have been discharging slightly too hard.

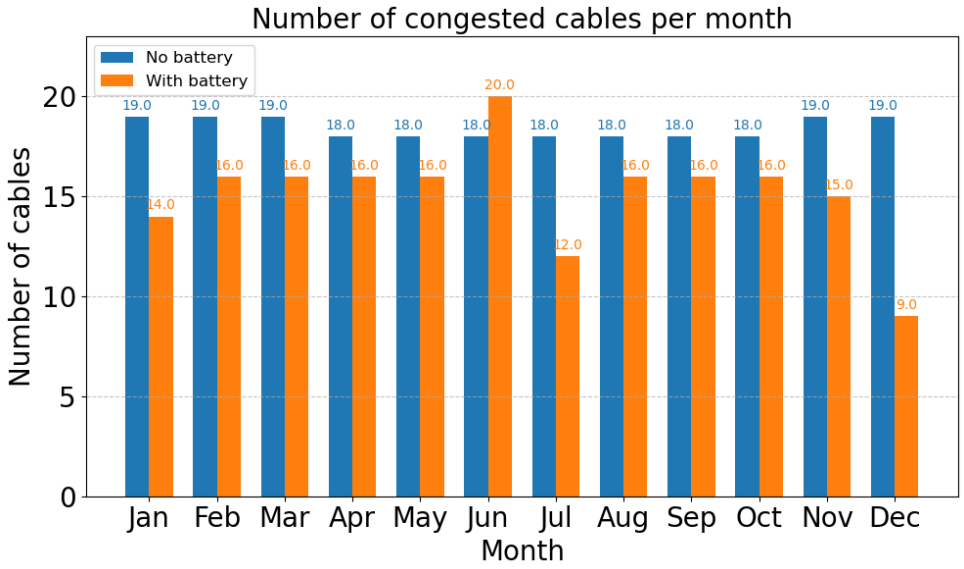

Figure 4.7: Number of congested cables per month with and without battery deployment.

4.4. Battery relocations

This section will discuss the number of required relocations. The number of relocations will be shown per month in order to capture the seasonal variations. In addition, this section will propose a suitable charging location based on the seasonal variations found in Section 4.4.1.

4.4.1. Number of relocations

Figure 4.8 presents the monthly number of battery relocations for both the Lithium-ion battery and Iron–Air battery. The figure shows that the Lithium-ion battery requires more frequent relocations overall. This is primarily due to its lower capacity, which causes it to deplete more quickly. Although the Lithium-ion battery has a higher discharge efficiency compared to the Iron Air battery, which results in a slower decline in SoC at a given output power, its limited capacity still requires more frequent replacements. With the same reasoning, the SoC of the Lithium-ion battery also rises more quickly when charging is possible during idle time. As a result of the higher charging efficiency, it can be seen that in April, only the Iron Air battery requires transfer.

Furthermore, Figure 4.8 shows a relation between required battery relocations and seasons. Most relocations are required in winter, as the charging profile in winter mainly prescribes the battery to discharge. In addition, demand in the LV-grids remains high during idle, which limits the possibility to charge. In summer, no battery relocations are required for either Lithium-ion battery or Iron Air battery, as PV-congestion arises around noon, prescribing the battery to charge. During these months, sufficient grid capacity is available to enable charging or discharging according to the charging profile and respecting the boundaries of the batteries' SoC.

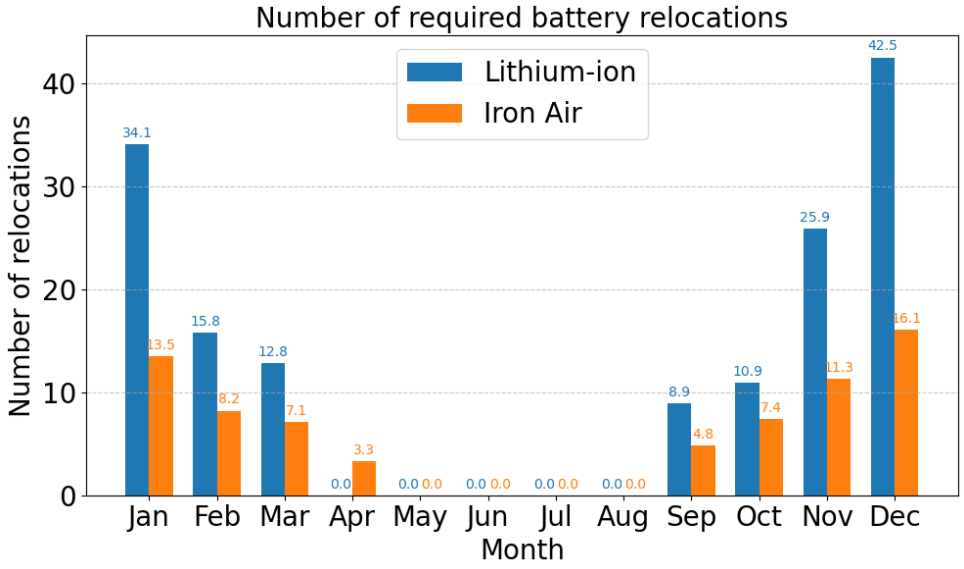

Figure 4.8: Number of required relocations for Lithium-ion batteries and Iron Air batteries per month.

4.4.2. Charging location

The seasonal dependence, found in Section 4.4, for battery relocations introduces information to determine a suitable charging location. A charging location is argued to be suitable, when there is potential to add value by charging electricity. Adding value by charging can be done by congestion management. However, it can not be chosen when the battery needs to charge, as it should be full when a new battery transfer is required. Another possibility to add value by charging is curtailment prevention. This can be realized at solar and wind farms.

In the Netherlands, insolation is six times smaller in winter than in summer [89]. This means that the surplus of energy at a solar facility is highly likely much smaller in winter than in summer. Therefore, the potential to prevent curtailment at solar facilities in winter is insignificant. On the other hand, wind power generation is about two times bigger in winter than in summer [89]. This indicates a higher chance of energy surplus and a higher probability of curtailment prevention in winter than in summer. By this means, wind facilities seem the most suitable charging locations for the mobile battery deployed in this LV-grid.

4.5. Cost comparison

The costs considered in this research are the CAPEX and transportation costs of the battery technologies. The CAPEX is derived from the size of the batteries required to support the charging profile and the expected battery lifetime. The transportation costs are also based on the required battery size and the capacity per relocation (i.e. capacity per 20ft container).

Before the CAPEX for both battery technologies can be determined, the number of batteries required must be calculated. This is done by using Equation 1.1 to calculate the battery capacity and by using the maximum capacity per 20ft container as defined in Section 3.5.1.

For Lithium-ion this indicates that a battery capacity of 965.4 kWh is required. This is below the maximum container capacity of 6.25 MWh, indicating that only one battery is required in the LV-grid to alleviate congestion. As mentioned in Section 2.5, this also implies that one additional Lithium-ion battery is required to charge at the wind park.

For the Iron Air battery, a capacity of 16.09 MWh is required. Given the maximum container capacity of 4.2 MWh, 4 ($\frac{16.09 \cdot 0.95}{4.2} = 3.8$) batteries are required. To determine the number of additional batteries required at the wind farm, the month with the largest mismatch between charged and discharged energy is considered. In December, the average daily shortage is 2069 kWh, meaning that the Iron Air battery is unable to charge this additional amount per day to match the charged and discharged energy.

To calculate the required number of batteries that charge at the wind park, the potential daily charged capacity of one Iron Air container is calculated. This is done by multiplying the power per battery container by the hours per day and the Iron Air battery efficiency. Accordingly, one Iron Air container can charge 746 kWh ($42kW \cdot 24hours \cdot 0.74$) per day. Therefore, the total number of additional batteries required at the wind park is three ($\frac{2069}{746} = 2.8$). For this calculation, it is assumed that the battery is always able to charge at full power.

The results for the annual CAPEX for Lithium-ion and the annual CAPEX for the Iron Air are shown in Equation 4.1 and Equation 4.2, respectively

$$CAPEX_{an,Li}[€] = \frac{277 \cdot 2 \cdot 965.4}{16} = €33,426.98 \tag{4.1}$$

$$CAPEX_{an,IA}[€] = \frac{17.5 \cdot 7 \cdot 4200}{17.5} = €29,400 \tag{4.2}$$

In addition, the relocation costs are calculated by multiplying the number of relocations, calculated according to the approach given in Section 2.5, and the costs per relocation as calculated in in Section 3.5.2.

The results of the cost analysis to compare the Lithium-ion battery and the Iron Air battery are shown in Figure 4.9. The figure shows the fixed costs and the transportation costs for both battery technologies stacked to obtain the total costs. The Figure shows that the fixed costs of both battery technologies is similar. This is due to the much lower installed costs for the Iron Air battery [in €/kWh] and the higher installed capacity compensating for this. Furthermore, the figure shows that the transportation costs have the same shape as the number of required battery relocations explained in Section 4.4, as these are proportional. Therefore, the costs of the battery relocations for Lithium-ion are higher than for the Iron Air battery. As a result, the total costs for deployment of the Lithium-ion battery is more expensive than deployment of the Iron Air battery. More specifically, the yearly costs for Iron Air deployment is €35,634, and deployment of the Lithium-ion battery is €46,575.

For both battery technologies, the ratio of the total costs differ. For the Iron Air battery, the largest share of the costs is due to the CAPEX, which is responsible for 82% of the total costs. For the Lithium-ion battery, the share of CAPEX is 72%. The difference in ratio for the battery technologies is due to the different capacities. The Lithium-ion battery has a smaller capacity, resulting in the need to be transferred more often during winter. However, the CAPEX is also reduced due to the smaller required capacity. On the other hand, the Iron Air battery has a larger capacity, which limits the number of battery relocations required.

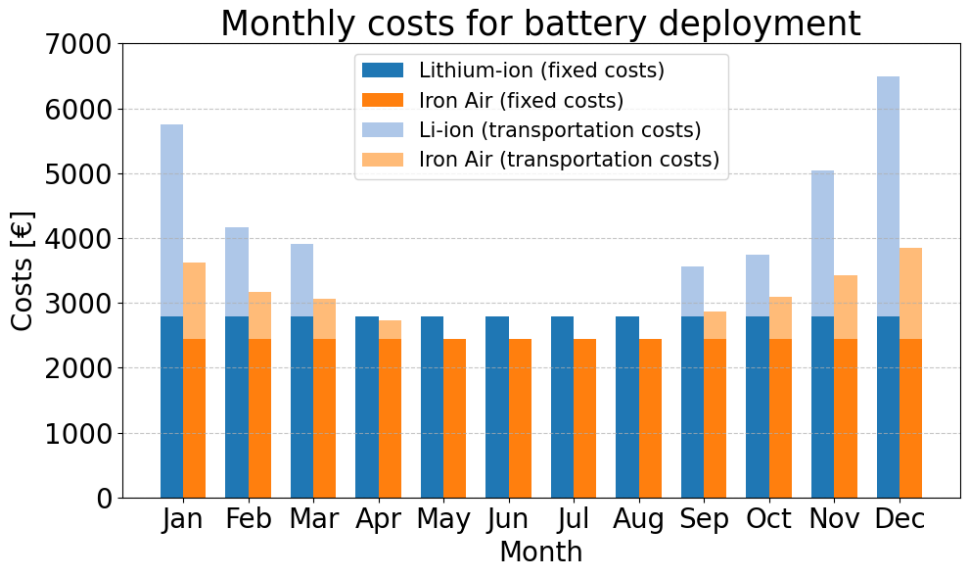

Figure 4.9: The total costs, consisting of the CAPEX and transportation costs, of the Lithium-ion battery and Iron Air battery. Over the whole year, the total costs for Lithium-ion are €46,575, and for the Iron Air €35,634.

It is not possible to directly compare the calculated costs to those of alternative solutions for LV-grid congestion, as not all costs, such as electricity costs and grid connection fees are considered. These costs are not taken into account, as they are indifferent for the battery technologies. Therefore, the neglected costs are not required to obtain the most cost-effective battery technology. In addition, additional benefits, such as curtailment prevention at the wind park and in the LV-grid, prevention of unmet load due to high demand in the LV-grid, and value stacking (e.g. also trading on the imbalance market), of mobile batteries have not be taken into account. Both additional advantages and disadvantages should be considered before conclusions can be drawn upon the costs of deploying mobile batteries in this LV-grid compared to an alternative solution. Therefore, the results presented in Figure 4.9 should be interpreted solely in the context of comparing battery technologies.

Nevertheless, some household energy system costs are included to give a ballpark estimate of mobile battery costs. These figures should be interpreted with caution, and no definitive conclusions should be drawn from them. The number of households in the studied LV-grid is 71. Therefore, to deploy the Lithium-ion battery, the annual costs per household to alleviate congestion in their LV-grid is €656, and for the Iron Air battery €502. For comparison, the expected grid costs per household in 2030 will be €70 per month, resulting in €840 per year [90]. In addition, according to *Ontwikkeling netkosten tot 2050 en de kostenverdeling over groepen gebruikers* [91], the expected grid costs per household will increase with €350 to €550 by 2050. These costs do not only consists of balancing costs, but also operational and maintenance costs, for instance.

Besides, it is not attempted to conduct a sensitivity analysis on the costs, as the results of such analysis can be well reasoned. For instance, the outcomes for scenarios involving increased relocation costs can already be anticipated. This is because an increase in relocation costs will cause the Lithium-ion battery costs to rise more than those of the Iron Air battery. As a result, the total costs difference between the two battery technologies will increase. In addition, tweaking the total instalment costs will result in a proportional change in the fixed costs. Therefore, it is concluded that the Lithium-ion battery will become more cost attractive than the Iron Air battery when the CAPEX will decrease.

5

Discussions

This chapter discusses the findings of this research. First, the relevance of the results related to mobile batteries is addressed. Second, the applicability of these results is examined. Third, the feasibility of the proposed deployment strategy is evaluated. Fourth, practical considerations necessary for implementing the strategy are outlined. Finally, the limitations of this research are discussed.

5.1. Relevance

The relevance of this research depends on context. For instance, mobile batteries are more expensive than stationary batteries. Therefore, this research adds value when mobile batteries outperform stationary batteries. In the LV-grid studied, it was found that stationary batteries will not be able to alleviate congestion continuously due to the boundaries of the battery capacity and the available capacity in the grid during battery idle time. Therefore, mobile batteries are required. In LV-grids with a lower amount of congestion, there might be no need to transfer the battery. In addition, lower installed capacities of electrical equipment than is forecasted by the DSOs might decrease the need for battery transfers. However, considering the LV-grid and associated data provided, mobile batteries outperform stationary batteries and could be considered for actual deployment in this LV-grid.

In addition, as deploying a stationary battery is not able to alleviate all congestion, home batteries will also not be able to do it. This is for exactly the same reason as one centralized battery: there is not sufficient available capacity during idle time to charge enough to enable the required discharging.

On the other hand, smart EV charging might allow congestion alleviation in this LV-grid. However, this depends on many different aspects, such as people behaviour and market incentives. It would also require that EVs are discharged during peak demand hours which are currently partly caused by EV charging. This implies a required drastic change in EV charging behaviour, and a complicated logistical challenge for EV charging and discharging which is both time and spatially dependent. Although, the grid would be balanced with existing materials and no additional materials are required. However, the EV battery will deteriorate due to charging and discharging for grid balancing purposes. Therefore, it can be expected that people would want a significant remuneration for their rapidly deteriorating EV.

Arguably the most important competitive solution to mobile batteries in the LV-grid studied is grid expansion. As explained in Section 1.2.3, grid expansion is particularly effective when load is structurally above the grids capacity. From the analysis in Section 2.4.1 became clear that, especially in summer, congestion is expected for several hours a day. This indicates that grid expansion might be a suitable solution. Nevertheless, this does not take away that resources, such as time and personnel, required for grid expansion are scarce. The exact time it takes to create a grid connection for the battery is context dependent, such as the weighting list for the specific DSO, and the availability of personnel. However, what can be argued is that it will take less time to create a grid connection and a short cable to the battery, than it would take to replace an entire cable for which trenching throughout a whole neighbourhood is required. In addition, for grid balancing purposes, priority might be provided for grid connections [92]. This will reduce time. With respect to personnel, the people required for mobile batteries have different capabilities than the people required for grid expansion. For mobile batteries, logistic personnel and truck drivers are necessary. Therefore, mobile battery deployment would have limited effect on

decelerating grid expansion speed.

In short, for the LV-grid studied, stationary batteries are not a solution, as they are not able to alleviate all congestion. In addition, smart EV charging might be a competitive solution to mobile batteries. However, this requires more complex and social aspects than centrally operated mobile batteries. It would also impose significant remuneration for EV owners to incentivize smart EV charging. At last, grid expansion is a potentially good solution for the LV-grid studied due to the structural congestion. However, the main advantage of mobile batteries is that it is easier and quicker to deploy than grid expansion. This could lead to continued gird expansion at certain LV-grids, and using mobile batteries as a short-term solution to reduce the pressure of grid expansion.

5.2. Applicability

This research studied a deployment strategy for mobile batteries for a specific LV-grid. The method for determining the charging profile was validated and the optimal location was found. From this case alone, it is difficult to conclude that the method for determining the charging profile is also valid in other LV-grids. To be able to prove this, additional LV-grids with different topologies and characteristics should be tested. These LV-grids should represent the existing LV-grids in the Netherlands. The same applies to the batter deployment location in the LV-grid. Additional tests in LV-grids with varying topologies and characteristics should be conducted to determine whether the battery should always be deployed at the end of the congested area. In addition, the results should indicate that the difference in congestion reduction between locations at the end of the congested area is not significant, suggesting that the deployment location is flexible with respect to physical or regulatory constraints This will enable conclusion of applicability in all LV-grids.

5.3. Feasibility

The deployment of mobile batteries in the studied LV-grid has been shown to effectively alleviate congestion. Therefore, it is expected that deploying a mobile battery in this real-world LV-grid will yield similar results.

To apply the proposed deployment strategy in real-world LV-grids, data on the installed capacities of electrical equipment and the base load of all households is required to determine the appropriate charging profile. Additionally, the grid topology must be known, as the distance between the energy source and sink is necessary for calculating power losses. For successful deployment according to the proposed strategy, access to these data is essential.

In the Netherlands, it is legally obligatory to register installed PV capacity [93]. Furthermore, registration of a HP is mandatory when its power exceeds 5 kW [94]. In the LV-grid studied, all HPs have a power rating above 5 kW. In contrast, there is currently no legal obligation to register private EV chargers in the Netherlands. However, installing a public EV charger requires a permit from the municipality [95]. In Belgium, however, registration of EV chargers is mandatory [96].

To this end, obtaining a complete overview of installed capacities in the Netherlands may be challenging, as EV chargers are not required to be registered. However, installation must be carried out by a licensed company. This opens the possibility of data sharing between installation companies and the DSO. However, such data may include personal information, which could limit its availability due to privacy regulations. However, the legal framework surrounding data sharing falls outside the scope of this research and will therefore not be discussed further.

Another option for obtaining the installed capacities of EV chargers is to directly ask neighbourhood residents by means of a survey. This process could be more straightforward if residents have partial ownership of the battery, as they may be more willing to share information. The effort involved is expected to be limited, requiring only the preparation of a letter and a simple registration process, which is unlikely to present a significant barrier.

5.4. Qualitative stakeholder values

The deployment strategy found for the LV-grid includes determining the optimal location for the battery. While this location is theoretically optimal, practical factors must be considered for real-world deployment. An important factor are the qualitative stakeholders values. Ignoring these values might cause resistance against battery deployment. This section will discuss the qualitative stakeholder values: liveability and spatial integrity.

5.4.1. Liveability

An important value is liveability, including aesthetics and nuisance, of the neighbourhood. Optimal battery deployment in the LV-grid will be near demand and supply. This means that the battery will be deployed near households. To reduce social resistance, the location of the battery must be placed at the side of the LV-grid, as long as the optimal location allows. This will reduce the visual impact on the neighbourhood. In addition, efforts can be made to reduce visual impact, by providing green walls or place a hedge around the deployment location, for instance.

In addition, noise pollution should be avoided. Batteries can generate noise through their cooling systems, particularly due to the airflow from ventilation fans. To minimize this, liquid-cooled batteries can be used. For lithium-ion batteries, liquid cooled batteries are already available. However, for Iron-Air batteries, liquid cooling is not yet in development, but it may become necessary for deployment in densely populated neighbourhoods, such as LV-grids. In areas with lower housing density, air-cooled systems may still be suitable.

5.4.2. Spatial integrity

Spatial integrity is valued by the municipality. Deploying a battery in neighbourhoods with high household density might be difficult. This is especially the case in the Netherlands, as space is valuable and scarce. The hard criteria for the LV-grids chosen was focused on space. As a result, no LV-grid was chosen in a city centre for analysis. However, even in neighbourhoods with a lower density of households, it might be a challenge to accommodate the battery. Therefore, the physical size of the battery should be considered and can even be a limiting factor.

Furthermore, the results were generated for 20ft containers. Larger containers allow for more capacity and a potential decrease in transportation costs. However, deploying a battery container larger than 20ft might be too heavy for transportation in neighbourhoods, as the roads are not designed to withstand these pressures. This will depend on the roads in the neighbourhood, but should be considered when the batteries are deployed. In general, the allowed road weight, without restrictions, of trucks in the Netherlands is 44tons [97]. A 20ft Lithium-ion battery weights about 16tons [98], so including the truck it will still be within the margins. This will also be the case for the Iron Air battery, as the volumetric energy density is comparable to the volumetric energy density of the Lithium-ion battery.

The values discussed above must be taken into account before mobile battery deployment is applied. The weight of the values is context specific and must be considered by the municipality and DSO, as the municipality must provide a permit for battery deployment whilst considering public interest, and the DSO must weight the added value of battery deployment.

5.4.3. Efficiency

The results showed that batteries are required to be mobile during winter. As explained, the batteries will be switched with batteries charged at the wind farm when they are empty. In summer, switching batteries is not required, as stationary batteries are able to alleviate congestion. As the batteries on the LV-grid will be stationary in summer, the batteries at the wind farm will also be stationary. Therefore, in summer, the batteries at the wind farm should be used for a different purpose. This purpose can be to alleviate congestion at the wind farm itself, by storing surplus of generated wind energy. This would prevent curtailment and allow for a smaller grid connection, which would reduce costs.

However, an alternative strategy would be to transfer the batteries to a solar farm during the summer months, where their deployment would be more beneficial. As explained in Section 4.4, wind power generation in the Netherlands are typically twice as big in winter compared to summer, making battery deployment at wind farms more effective for curtailment prevention during winter. Conversely, solar insolation in summer is approximately six times higher than in winter, suggesting that deploying batteries at solar farms during this period would more effectively reduce curtailment of solar energy.

Furthermore, mobile batteries can be deployed as short-term solution to alleviate congestion and reduce pressure on grid expansion until grid expansion or a more cost effective alternative is feasible. This means that batteries might not be needed for their entire lifetime. That will result in a surplus of batteries. Various solutions can be found to deal with these batteries, such as managing energy profiles for companies behind the meter. The purpose of batteries after deployment should be considered when a large number of batteries will be deployed to alleviate congestion for the short term.

5.5. Limitations

A limitation of this research is that the optimal charging was not found, as no optimization model was used. However, the real time planning approach as proposed in this research is an easier and quicker method than development of an optimization model to determine the charging profile. Moreover, the deployment strategy has been validated and showed a significant reduction in system congestion. In addition, maximum congestion was significantly reduced to meet the European Standard. Since no optimization model was applied, this research differs considerably from existing studies. As a result, a direct comparison with the literature was not feasible. Previous studies typically pursued multiple objectives, including cost minimization. Consequently, while they reported lower costs, the achieved congestion reduction was also significantly less. The methodological differences are therefore too fundamental to allow a fair comparison.

Another limitation of this research is that some costs were not taken into account. Potentially considerable costs excluded are electricity costs and grid connection costs. These costs were excluded as they are indifferent for the battery technologies. Therefore, the costs will not influence the most cost effective battery technology for this LV-grid. However, to enable comparison with alternative solutions, these costs should be considered. On the other hand, some additional benefits of mobile batteries were also not included. These are the added value of curtailment prevention, prevention of unmet load during high demand in the LV-grid, and value stacking opportunities during idle time. These effects should also be taken into account to allow for comparison with alternative solutions.

Another limitation concerns the availability of data. The data used was available for one workday and one weekday for every month of the year. To obtain results for the entire year, data had to be interpolated. This results in the lack of finer variations within weeks or months. However, a benefit is that the 24 days of data (two per month) allows for the simulation of one year. If all 365 days had to be modelled separately, the computational time would exceed a feasible range.

Furthermore, this research did not propose an agreement between battery owner and DSO. However, a few possibilities were provided no clear conclusion could be drawn. This lack of clarity regarding ownership and collaboration mechanisms might limit the broader deployment of mobile batteries, despite their proved potential to alleviate congestion in the studied LV-grid.

The last limitation discussed is the generalizability of this research. The real time planning approach to determine the charging profile was validated for the LV-grid studied. However, this does not necessarily imply that the approach will also be valid in other LV-grids. The real time planning approach should be tested in additional LV-grids representing the LV-grids in the Netherlands to be able to validate its general applicability in the Netherlands. Nevertheless, it is expected that the method can be validated in other LV-grids, as the congestion reduction was significantly within the European standards. In addition, for both the location and the cost effectiveness of the battery technologies applies the same logic: generalizing the conclusion is only possible after validation in additional LV-grids.

6

Conclusions and recommendations

6.1. Addressing the research questions

This researched aimed to answer the following research question:

How can mobile batteries be deployed to alleviate low-voltage grid congestion, based on a case study comparing short- and long-duration batteries?

The research question is answered by answering the five sub-questions. These will discussed one by one.

1. **How can the optimal charging profile for mobile batteries be designed to address low-voltage grid congestion while reflecting the specific characteristics of an LV-grid?**

   This research found that the proposed real time planning approach is a suitable approach to determine the charging profile to alleviate congestion in the LV-grid studied. The method estimates the total load and total power losses in the LV-grid and subtracts the capacity of the main cable (the cable connecting the MV-station with the LV-grid) to capture the demand or supply that cannot be satisfied by the cables. This was expected to be a proper strategy, as the battery will only charge or discharge when the cable capacities were expected to be exceeded. The validation showed that system congestion was reduced between 84.6% and 99.8% for a workday and a weekend day in both January and July. In addition, the maximum congestion was reduced between 69.9% and 88.1%. To this end, the maximum congestion was kept within the hard limit of 45% congestion set in the European Standard IEC 60364-4-43.

2. **What is the optimal location to deploy mobile batteries to alleviate congestion in a low-voltage grid?**

   This research found that the optimum battery location is in the area at the end of the congested sequence of cables. In addition, it was found that the congestion reduction for the battery locations near the optimal location were similar. This implies that deploying the battery close to the optimal location would not influence the result significantly. This conclusion might be useful when real-world constraints, such as the reluctance of space, or stakeholder values might limit battery deployment at the optimum location.

3. **What trends in required battery relocations arise when following the designed deployment strategy to minimize congestion in low-voltage grids?**

   This research found that stationary batteries are able to alleviate congestion from April to Augustus. During these months, the battery is able to use its idle time to balance daily charged and discharged energy to follow the charging profile while respecting the SoC boundaries. From September until March, battery relocations are required, as the battery is not able to charge enough to balance the daily charged and discharged energy. This leads to a fully discharged battery at a certain moment in time, unable to alleviate congestion according to the charging profile. Furthermore, the Lithium-ion battery requires more battery relocations than the Iron air battery, as it has a lower energy capacity.

4. **How do short-duration and long-duration mobile batteries compare in terms of cost effectiveness for alleviating congestion in low-voltage grids?**

   This research found that the annual CAPEX of Lithium-ion is slightly higher, though comparable, to that of the Iron Air battery for alleviating congestion in the studied LV-grid. Despite the smaller capacity, the Lithium-ion battery has higher total instalment costs [in €/kWh] compared to the Iron Air battery's total instalment costs, causing the higher CAPEX. In addition, the higher number of required battery relocations for the Lithium-ion battery leads to higher transportation costs. As a result, the total costs for the Lithium-ion battery exceeds the total costs for the Iron Air battery.

5. **Which real-world factors must be considered to support effective deployment of mobile batteries?**

   This research found that spatial constraints might limit battery deployment, as some LV-grids might accommodate little space for batteries. In addition, stakeholder values, such as neighbourhood liveability, should be considered, as neglecting these values might poses social resistance. Enhancing neighbourhood liveability can be achieved by deploying liquid cooled batteries to reduce noise, or choosing the battery deployment location at the side of the LV-grid to minimize its impact. The real-world factors and their relevance are dependent on neighbourhood. One factor might be more relevant than the other in one neighbourhood, and the other way around in the other neighbourhood. Therefore, different trade-offs must be made for every neighbourhood.

Thus, to answer the research question: **"How can mobile batteries be deployed to alleviate low-voltage grid congestion, based on a case study comparing short- and long-duration batteries?"**, mobile batteries can effectively be deployed by determining the LV-grid-specific charging profile by means of the real time planning approach. In addition, the theoretically optimal battery location is around the end of the sequence of congested cables. Furthermore, battery relocations are required from September to March, whilst stationary batteries satisfy in the remaining months. Furthermore, the Iron Air battery is more cost effective than the Lithium-ion battery. However, trade-offs must be made between battery location, battery technology and real-world factors, such as space and nuisance, for every neighbourhood, as their relevance is neighbourhood dependent.

By this means, the research contributed to existing literature to include practical considerations to the deployment strategy of mobile batteries. This yields more feasible results for real-world deployment than was previously available. In addition, this research included seasonal variance to provide a more complete overview. Furthermore, this research distinguished between battery durations, providing additional insights into the possibilities to alleviate LV-grid congestion with mobile batteries.

6.2. Policy recommendations

From this research conclusion, the following policy recommendations have been derived. First, the real-time planning approach is a promising method to alleviate LV-grid congestion and can be implemented for effective congestion alleviation. The real time planning approach provides a quick-to-deploy though tailor-made charging profile capable of alleviation significant amount of congestion. By this means, using this approach will allow for congestion alleviation on short-term, reducing pressure on grid expansion.

Second, the most promising battery location to alleviate LV-grid congestion is at the end of the congested area. The deployment location should be chosen by firstly determining the most suitable locations based on the location centrality, the congested cables, and the cable capacities. Thereafter, the battery should be simulated for the network at those locations to determine the most promising location. It is also possible to locate the battery at on of the other potentially suitable locations when factors, such as space or nuisance, limit deployment at the optimal location. Although not ideal, this would have limited effect on congestion reduction.

Third, the Iron Air battery must be considered for congestion alleviation in LV-grids, as it is a more cost effective solution compared to the widely deployed Lithium-ion battery. To make the neighbourhood-dependent trade-off between battery technologies, liveability of the neighbourhood, spatial integrity, and efficient battery use should be considered to capture stakeholder values and improve practical feasibility.

Fourth, a plan must be made for mobile battery logistics for September until March. This is required to enable continuous congestion alleviation by means of batteries. In addition, the plan must be co-created with wind farms, as these are the most suitable charging locations.

Fifth, additional validation of the promising deployment strategy must be supported. This will provide the opportunity the deploy mobile batteries across LV-grids in the Netherlands to reduce pressure on grid expansion. LV-grid validation must be prioritized on the urgency of congestion alleviation and be performed in cooperation with DSO grid expansion planning department.

6.3. Future research

Future research could focus on validating the proposed deployment strategy for mobile batteries to alleviate LV-grid congestion, using LV-grids that represent the LV-grids in the Netherlands. This would yield a generic deployment strategy for mobile batteries to alleviate LV-grid congestion that can be used throughout the Netherlands.

In addition, expanding the cost analysis performed in this research would enable comparison between mobile battery deployment to alleviate LV-grid congestion and alternative solutions, such as grid expansion, on cost effectiveness. This would yield additional insights in the competitiveness of mobile batteries.

References

[1] *Netcapaciteitskaart*. [Online]. Available: https://www.tennet.eu/nl/de-elektriciteitsmarkt/congestiemanagement/netcapaciteitskaart.

[2] M. S. Alam, F. S. Al-Ismail, A. Salem and M. A. Abido, "High-Level Penetration of Renewable Energy Sources Into Grid Utility: Challenges and Solutions", *IEEE Access*, vol. 8, pp. 190 277–190 299, Jan. 2020. DOI: 10.1109/access.2020.3031481. [Online]. Available: https://doi.org/10.1109/access.2020.3031481.

[3] *Uitbreidingen van het net worden goed zichtbaar, wachtrijen blijven bestaan*. [Online]. Available: https://www.netbeheernederland.nl/artikelen/nieuws/uitbreidingen-van-het-net-worden-goed-zichtbaar-wachtrijen-blijven-bestaan.

[4] *Tennet's position on battery energy storage systems (bess)*, Accessed: Oct 2024, 2024. [Online]. Available: https://tennet-drupal.s3.eu-central-1.amazonaws.com/default/2024-08/TenneT%27s%20position%20large%20BESS%20-%20Public%20Info%20-%20update_3.pdf.

[5] J. Van De Worp, "Netcongestie remt nu ook transitie en economie in Rijnmond", Nov. 2024. [Online]. Available: https://www.vemw.nl/nieuwsbericht/2024/11/06/netcongestie-remt-nu-ook-transitie-en-economie-in-rijnmond.

[6] Fstoutjesdijk, *Netcongestie amp; logistiek laden - NKL Nederland*, Dec. 2024. [Online]. Available: https://nklnederland.nl/netcongestie-logistiek-laden/.

[7] T. N. Pham, R. Shah, M. N. Dao, N. Sultanova and S. Islam, "Low and medium voltage distribution network planning with distributed energy resources: a survey", *Electrical Engineering*, Jul. 2024. DOI: 10.1007/s00202-024-02535-0. [Online]. Available: https://doi.org/10.1007/s00202-024-02535-0.

[8] D. Kiedanski, D. Kofman, P. Maille and J. Horta, "Misalignments of objectives in demand response programs: a look at local energy markets", *2020 IEEE International Conference on Communications, Control, and Computing Technologies for Smart Grids (SmartGridComm)*, pp. 1–7, Nov. 2020. DOI: 10.1109/smartgridcomm47815.2020.9302939. [Online]. Available: https://doi.org/10.1109/smartgridcomm47815.2020.9302939.

[9] H. Saboori, "Enhancing resilience and sustainability of distribution networks by emergency operation of a truck-mounted mobile battery energy storage fleet", *Sustainable Energy Grids and Networks*, vol. 34, p. 101 037, Mar. 2023. DOI: 10.1016/j.segan.2023.101037. [Online]. Available: https://doi.org/10.1016/j.segan.2023.101037.

[10] *Netcongestie*. [Online]. Available: https://www.tennet.eu/nl/netcongestie.

[11] A. A. Sallam and O. P. Malik, *Electric distribution systems*. John Wiley Sons, Nov. 2018.

[12] *Wat doet een netbeheerder? | Stedin*. [Online]. Available: https://www.stedin.net/klantenservice/veelgestelde-vragen/wat-doet-een-netbeheerder.

[13] *Wie is Enexis Netbeheer | Enexis Netbeheer*. [Online]. Available: https://www.enexis.nl/over-ons/wie-is-enexis-netbeheer.

[14] E. David and K. Jon, *Networks, Crowds, and Markets: Reasoning about a Highly Connected World*. Jul. 2010. [Online]. Available: http://dx.doi.org/10.1017/cbo9780511761942.

[15] *Dutch market*. [Online]. Available: https://www.tennet.eu/node/111.

[16] HoogspanningsNet, *Laagspanning - HoogspanningsNet*, Oct. 2024. [Online]. Available: https://www.hoogspanningsnet.com/hetnet/laagspanning/.

[17] HoogspanningsNet, *Het landelijk koppelnet: 380 kV en 220 kV - HoogspanningsNet*, Apr. 2025. [Online]. Available: https://www.hoogspanningsnet.com/hetnet/koppelnet/.

[18] *Een vol elektriciteitnet | Stedin*. [Online]. Available: https://www.stedin.net/energietransitie/congestie.

[19] *Congestie Drechtsteden en Centraal Molenlanden | Stedin*. [Online]. Available: https://www.stedin.net/zakelijk/energietransitie/beschikbare-netcapaciteit/congestie-en-congestiemanagement/drechtsteden-en-centraal-molenlanden#:~:text=De%20vraag%20naar%20transport%20van,Daarom%20kondigen%20we%20congestie%20aan..

[20] S. Brandligt, "Probleemanalyse congestie in het laagspanningsnet", Tech. Rep., Jan. 2024. [Online]. Available: https://www.rijksoverheid.nl/documenten/rapporten/2024/01/22/bijlage-1-actieagenda-netcongestie-laagspanningsnetten.

[21] P. Huang and Z. Ma, "Unveiling electric vehicle (EV) charging patterns and their transformative role in electricity balancing and delivery: insights from real-world data in Sweden", *Renewable Energy*, p. 121 511, Oct. 2024. DOI: 10.1016/j.renene.2024.121511. [Online]. Available: https://doi.org/10.1016/j.renene.2024.121511.

[22] M. van Algemene Zaken, *Kabinet neemt maatregelen tegen vol elektriciteitsnet*, Apr. 2025. [Online]. Available: https://www.rijksoverheid.nl/onderwerpen/duurzame-energie/kabinet-neemt-maatregelen-tegen-vol-elektriciteitsnet-netcongestie.

[23] A. Navon, R. Nitskansky, E. Lipman *et al.*, "Energy storage for mitigating grid congestion caused by electric vehicles: A techno-economic analysis using a computationally efficient graph-based methodology", *Journal of Energy Storage*, vol. 58, p. 106 324, Dec. 2022. DOI: 10.1016/j.est.2022.106324. [Online]. Available: https://doi.org/10.1016/j.est.2022.106324.

[24] "ELEKTRICITEITSNET IN UW GEMEENTE KLAAR MAKEN VOOR DE ENERGIETRANSITIE", Tech. Rep., 2019.

[25] M. Rohden, D. Jung, S. Tamrakar and S. Kettemann, "Cascading failures in ac electricity grids", *Physical review. E*, vol. 94, no. 3, Sep. 2016. DOI: 10.1103/physreve.94.032209. [Online]. Available: https://doi.org/10.1103/physreve.94.032209.

[26] *DPG Media Privacy Gate*. [Online]. Available: https://www.volkskrant.nl/politiek/verzwaring-stroomnet-kost-ruim-10-000-euro-per-nederlander~b62b5c8e/?referrer=https%3A%2F%2Fstatics.teams.cdn.office.net%2F.

[27] *Waarom duurt het zo lang om het elektriciteitsnet uit te breiden? | Stedin*. [Online]. Available: https://www.stedin.net/klantenservice/veelgestelde-vragen/zelf-energie-opwekken/spanningsproblemen/ik-heb-een-brief-ontvangen-waarin-staat-dat-de-netten-uitgebreid-moeten-worden#:~:text=Hoe%20komt%20het%20dat%20het,maken%20van%20een%20elektrische%20warmtepomp..

[28] *Curtailment*. [Online]. Available: https://www.tennet.eu/nl/curtailment.

[29] G. Smdani, M. R. Islam, A. N. A. Yahaya and S. I. B. Safie, "PERFORMANCE EVALUATION OF ADVANCED ENERGY STORAGE SYSTEMS: a REVIEW", *Energy Environment*, vol. 34, no. 4, pp. 1094–1141, Jan. 2022. DOI: 10.1177/0958305x221074729. [Online]. Available: https://doi.org/10.1177/0958305x221074729.

[30] H. M. Ahmed, H. F. Sindi, M. A. Azzouz and A. S. Awad, "Stochastic multi-benefit planning of mobile energy storage in reconfigurable active distribution systems", *Sustainable Energy Grids and Networks*, vol. 36, p. 101 190, Oct. 2023. DOI: 10.1016/j.segan.2023.101190. [Online]. Available: https://doi.org/10.1016/j.segan.2023.101190.

[31] *Codewijzigingsvoorstel overspanningsbeveiliging*, Geraadpleegd op 7 juni 2025, 2025. [Online]. Available: https://www.acm.nl/system/files/documents/codewijzigingsvoorstel-overspanningsbeveiliging.pdf.

[32] L. van Cappellen, H. Groenewegen, M. Bongaerts *et al.*, "Thuis- en buurtbatterijen", Tech. Rep. 23.230315.183, Dec. 2023. [Online]. Available: https://cedelft.eu/wp-content/uploads/sites/2/2024/02/CE_Delft_WitteveenBos_230315_Thuis-_en_buurtbatterijen_Def.pdf.

[33] *Access and Affordability*. [Online]. Available: https://www.iea.org/topics/access-and-affordability.

[34] J. Mandemakers, K. Leidelmeijer, F. Burema *et al.*, "Instrumentontwikkeling Leefbaarometer 3.0", Tech. Rep., 2021. [Online]. Available: https://www.leefbaarometer.nl/resources/LBM3Instrumentontwikkeling.pdf.

[35] *Subsidie Ruimte voor duurzaam initiatief - Duurzame projecten en Programma's*. [Online]. Available: https://www.amsterdam.nl/subsidies/subsidieregelingen/subsidie-ruimte-duurzaam-initiatief/#hbe184435-378e-4cea-8c95-6ee9616b808a.

[36] *Subsidie smart energy systems aanvragen*. [Online]. Available: https://www.rotterdam.nl/subsidie-smart-energy-systems-aanvragen.

[37] *Taken van een gemeente*. [Online]. Available: https://www.rijksoverheid.nl/onderwerpen/gemeenten/taken-gemeente#:~:text=Over%20veel%20zaken%20mag%20de,ook%20veel%20landelijke%20wetten%20uit..

[38] "Beleid voor grootschalige batterijsystemen en afnamenetcongestie", Tech. Rep., Mar. 2023. [Online]. Available: https://ce.nl/wp-content/uploads/2023/04/CE_Delft_220376_Achtergrondrapport_Beleid_voor_grootschalige_batterijsystemen_en_afnamenetcongestie_DEF.pdf.

[39] L. van Cappellen, H. Groenewegen, F. Rooijers and T. Scholten, "Beleid voor grootschalige batterijen en opweknetcongestie", Tech. Rep., Oct. 2023.

[40] International Renewable Energy Agency (IRENA), *Renewable energy in cities*, Accessed 2025-06-09, 2016. [Online]. Available: https://www.irena.org/publications/2016/Oct/Renewable-Energy-in-Cities.

[41] Y. Wang, A. O. Rousis and G. Strbac, "Resilience-driven optimal sizing and pre-positioning of mobile energy storage systems in decentralized networked microgrids", *Applied Energy*, vol. 305, p. 117 921, Oct. 2021. DOI: 10.1016/j.apenergy.2021.117921. [Online]. Available: https://doi.org/10.1016/j.apenergy.2021.117921.

[42] M. Martínez, C. Mateo, T. Gómez, B. Alonso and P. Frías, "Distributed battery energy storage systems for deferring distribution network reinforcements under sustained load growth scenarios", *Journal of Energy Storage*, vol. 100, p. 113 404, Aug. 2024. DOI: 10.1016/j.est.2024.113404. [Online]. Available: https://doi.org/10.1016/j.est.2024.113404.

[43] H. Saboori and S. Jadid, "Optimal scheduling of mobile utility-scale battery energy storage systems in electric power distribution networks", *Journal of Energy Storage*, vol. 31, p. 101 615, Jun. 2020. DOI: 10.1016/j.est.2020.101615. [Online]. Available: https://doi.org/10.1016/j.est.2020.101615.

[44] J. Hu, S. You, M. Lind and J. Ostergaard, "Coordinated Charging of Electric Vehicles for Congestion Prevention in the Distribution Grid", *IEEE Transactions on Smart Grid*, vol. 5, no. 2, pp. 703–711, Nov. 2013. DOI: 10.1109/tsg.2013.2279007. [Online]. Available: https://doi.org/10.1109/tsg.2013.2279007.

[45] *Ancillary Services - EASE storage*, Dec. 2021. [Online]. Available: https://ease-storage.eu/publication/ancillary-services/.

[46] L. Aspitarte and C. R. Woodside, "A techno-economic survey of energy storage media for long-duration energy storage applications", *Cell Reports Sustainability*, vol. 1, no. 1, p. 100 007, Jan. 2024. DOI: 10.1016/j.crsus.2023.100007. [Online]. Available: https://doi.org/10.1016/j.crsus.2023.100007.

[47] A. K. Chu, E. Baik and S. M. Benson, "Long-duration energy storage in transmission-constrained variable renewable energy systems", *Cell Reports Sustainability*, p. 100 285, Dec. 2024. DOI: 10.1016/j.crsus.2024.100285. [Online]. Available: https://doi.org/10.1016/j.crsus.2024.100285.

[48] G. Mantegna, W. Ricks, A. Manocha, N. Patankar, D. S. Mallapragada and J. Jenkins, "Establishing best practices for modeling multi-day energy storage in deeply decarbonized energy systems", *Environmental Research Energy*, Nov. 2024. DOI: 10.1088/2753-3751/ad96bd. [Online]. Available: https://doi.org/10.1088/2753-3751/ad96bd.

[49] J. A. Dowling, K. Z. Rinaldi, T. H. Ruggles *et al.*, "Role of Long-Duration Energy Storage in Variable Renewable Electricity Systems", *Joule*, vol. 4, no. 9, pp. 1907–1928, Aug. 2020. DOI: 10.1016/j.joule.2020.07.007. [Online]. Available: https://doi.org/10.1016/j.joule.2020.07.007.

[50] J. Qiao, Y. Mi, J. Shen, D. Xia, D. Li and P. Wang, "Active and reactive power coordination optimization for active distribution network considering mobile energy storage system and dynamic network reconfiguration", *Electric Power Systems Research*, vol. 238, p. 111 080, Sep. 2024. DOI: 10.1016/j.epsr.2024.111080. [Online]. Available: https://doi.org/10.1016/j.epsr.2024.111080.

[51] K. Wang, Y. Ma, F. Wei, X. Lin, Z. Li and S. M. Dawoud, "Resilient market bidding strategy for Mobile energy storage system considering transfer uncertainty", *Applied Energy*, vol. 377, p. 124 498, Oct. 2024. DOI: 10.1016/j.apenergy.2024.124498. [Online]. Available: https://doi.org/10.1016/j.apenergy.2024.124498.

[52] J. W. Moraski, N. D. Popovich and A. A. Phadke, "Leveraging rail-based mobile energy storage to increase grid reliability in the face of climate uncertainty", *Nature Energy*, vol. 8, no. 7, pp. 736–746, Jun. 2023. DOI: 10.1038/s41560-023-01276-x. [Online]. Available: https://doi.org/10.1038/s41560-023-01276-x.

[53] G. He, J. Michalek, S. Kar, Q. Chen, D. Zhang and J. F. Whitacre, "Utility-Scale portable energy storage systems", *Joule*, vol. 5, no. 2, pp. 379–392, Dec. 2020. DOI: 10.1016/j.joule.2020.12.005. [Online]. Available: https://doi.org/10.1016/j.joule.2020.12.005.

[54] M. J. Ghadi, D. K. Mishra, A. Azizivahed, L. Li and J. Zhang, "Mobile compressed air energy storage for active distribution systems", *International Journal of Electrical Power Energy Systems*, vol. 154, p. 109 434, Aug. 2023. DOI: 10.1016/j.ijepes.2023.109434. [Online]. Available: https://doi.org/10.1016/j.ijepes.2023.109434.

[55] A. Arabkoohsar, *Compressed air energy storage system*. Elsevier, 2021. DOI: 10.1016/b978-0-12-820023-0.00003-1. [Online]. Available: https://doi.org/10.1016/b978-0-12-820023-0.00003-1.

[56] G. Alva, Y. Lin and G. Fang, "An overview of thermal energy storage systems", *Energy*, vol. 144, pp. 341–378, Dec. 2017. DOI: 10.1016/j.energy.2017.12.037. [Online]. Available: https://doi.org/10.1016/j.energy.2017.12.037.

[57] Z. Qu, J. Chen, K. Peng, Y. Zhao, Z. Rong and M. Zhang, "Enhancing stochastic multi-microgrid operational flexibility with mobile energy storage system and power transaction", *Sustainable Cities and Society*, vol. 71, p. 102 962, Apr. 2021. DOI: 10.1016/j.scs.2021.102962. [Online]. Available: https://doi.org/10.1016/j.scs.2021.102962.

[58] I. Nikolic, Z. Lukszo, E. Chappin *et al.*, "Guide for Good Modelling Practice in Policy Support", *TU Delft*, Jan. 2019. DOI: 10.4233/uuid:cbe7a9cb-6585-4dd5-a34b-0d3507d4f188. [Online]. Available: https://repository.tudelft.nl/islandora/object/uuid%3Acbe7a9cb-6585-4dd5-a34b-0d3507d4f188.

[59] *Phase to phase*, Jan. 2025. [Online]. Available: https://www.phasetophase.nl/.

[60] "Beter benutten van het net", Tech. Rep., Apr. 2025. [Online]. Available: https://www.rvo.nl/sites/default/files/2025-04/20241118_NBNL_Overzicht-Flexproducten_Productcatalogus.pdf.

[61] "Stochastische Load Flow in Gaia met het Gaussian-Mixture belastingmodel", Tech. Rep., 2022.

[62] M. Mallik, A. K. Panja and C. Chowdhury, "Paving the way with machine learning for seamless indoor–outdoor positioning: A survey", *Information Fusion*, vol. 94, pp. 126–151, Jan. 2023. DOI: 10.1016/j.inffus.2023.01.023. [Online]. Available: https://doi.org/10.1016/j.inffus.2023.01.023.

[63] *Triple Power Solar Batterij | Solax Power*. [Online]. Available: https://nl.solaxpower.com/triple-power-battery/.

[64] W. Van Drongelen, *Continuous, Discrete, and Fast Fourier Transform*. Jan. 2007, pp. 91–105. DOI: 10.1016/b978-012370867-0/50006-1. [Online]. Available: https://doi.org/10.1016/b978-012370867-0/50006-1.

[65] S. Secure, *The Importance of Depth of Discharge (DoD) in Battery Performance*. [Online]. Available: https://www.solar-secure.com.au/blog/the-importance-of-depth-of-discharge-in-battery-performance/#:~:text=Depth%20of%20Discharge%20of%20Lithium%2DIon%20Batteries%20(Li%2Dion)&text=Their%20popularity%20stems%20from%20their,between%2020%25%20and%2080%25..

[66] W. Cole, A. W. Frazier and C. Augustine, "Cost projections for utility-scale battery storage: 2021 update", Jun. 2021. DOI: 10.2172/1786976. [Online]. Available: https://www.osti.gov/biblio/1786976.

[67] G. Smdani, M. R. Islam, A. N. A. Yahaya and S. I. B. Safie, "PERFORMANCE EVALUATION OF ADVANCED ENERGY STORAGE SYSTEMS: a REVIEW", *Energy Environment*, vol. 34, no. 4, pp. 1094–1141, Jan. 2022. DOI: 10.1177/0958305x221074729. [Online]. Available: https://doi.org/10.1177/0958305x221074729.

[68] X. Luo, J. Wang, M. Dooner and J. Clarke, "Overview of current development in electrical energy storage technologies and the application potential in power system operation", *Applied Energy*, vol. 137, pp. 511–536, Oct. 2014. DOI: 10.1016/j.apenergy.2014.09.081. [Online]. Available: https://doi.org/10.1016/j.apenergy.2014.09.081.

[69] C. A. Hunter, M. M. Penev, E. P. Reznicek, J. Eichman, N. Rustagi and S. F. Baldwin, "Techno-economic analysis of long-duration energy storage and flexible power generation technologies to support high-variable renewable energy grids", *Joule*, vol. 5, no. 8, pp. 2077–2101, Jul. 2021. DOI: 10.1016/j.joule.2021.06.018. [Online]. Available: https://doi.org/10.1016/j.joule.2021.06.018.

[70] J. Twitchell, K. DeSomber and D. Bhatnagar, "Defining long duration energy storage", *Journal of Energy Storage*, vol. 60, p. 105 787, Jan. 2023. DOI: 10.1016/j.est.2022.105787. [Online]. Available: https://doi.org/10.1016/j.est.2022.105787.

[71] T. Chen, Y. Jin, H. Lv *et al.*, "Applications of Lithium-Ion Batteries in Grid-Scale Energy Storage Systems", *Transactions of Tianjin University*, vol. 26, no. 3, pp. 208–217, Feb. 2020. DOI: 10.1007/s12209-020-00236-w. [Online]. Available: https://doi.org/10.1007/s12209-020-00236-w.

[72] G. Mantegna, W. Ricks, A. Manocha, N. Patankar, D. S. Mallapragada and J. Jenkins, "Establishing best practices for modeling multi-day energy storage in deeply decarbonized energy systems", *Environmental Research Energy*, Nov. 2024. DOI: 10.1088/2753-3751/ad96bd. [Online]. Available: https://doi.org/10.1088/2753-3751/ad96bd.

[73] A. G. Olabi, E. T. Sayed, T. Wilberforce *et al.*, "Metal-Air Batteries—A review", *Energies*, vol. 14, no. 21, p. 7373, Nov. 2021. DOI: 10.3390/en14217373. [Online]. Available: https://doi.org/10.3390/en14217373.

[74] "Recommended Approaches for Modeling Utility Electric Grids with Multi-Day Energy Storage", Tech. Rep., Mar. 2023.

[75] X. Su, B. Sun, J. Wang, H. Ruan, W. Zhang and Y. Bao, "Experimental study on charging energy efficiency of lithium-ion battery under different charging stress", *Journal of Energy Storage*, vol. 68, p. 107 793, Jun. 2023. DOI: 10.1016/j.est.2023.107793. [Online]. Available: https://doi.org/10.1016/j.est.2023.107793.

[76] h., *CATL Unveils TENER, the World's First Five-Year Zero Degradation Energy Storage System with 6.25MWh Capacity*. [Online]. Available: https://www.catl.com/en/news/6232.html.

[77] M. A. Giovanniello and X.-Y. Wu, "Hybrid lithium-ion battery and hydrogen energy storage systems for a wind-supplied microgrid", *Applied Energy*, vol. 345, p. 121 311, Jun. 2023. DOI: 10.1016/j.apenergy.2023.121311. [Online]. Available: https://doi.org/10.1016/j.apenergy.2023.121311.

[78] V. Viswanathan, K. Mongird, R. Franks, X. Li and V. Sprenkle, *2022 grid energy storage technology cost and performance assessment*, Accessed: Oct 2024, 2022. [Online]. Available: https://www.pnnl.gov/sites/default/files/media/file/ESGC%20Cost%20Performance%20Report%202022%20PNNL-33283.pdf.

[79] *Nieuwe MAN vrachtwagens te koop, nieuw MAN vrachtwagen kopen | Autoline België*, Oct. 2024. [Online]. Available: https://autoline.be/nl/-/vrachtwagens/MAN/nieuw--c2tm2665st13177.

[80] V. van den Heuvel, *How many kilometers can a truck drive?*, Mar. 2025. [Online]. Available: https://www.basworld.com/content/how-many-kilometers-can-a-truck-drive.

[81] *Verbruik vrachtwagen | Scania Nederland*. [Online]. Available: https://www.scania.com/nl/nl/home/info/verbruik-vrachtwagen.html#:~:text=Het%20gemiddelde%20verbruik%20van%20een,het%20verbruik%20van%20uw%20vrachtwagen..

[82] *Brandstofprijzen | Shell België*. [Online]. Available: https://www.shell.be/nl_be/motorists/fuel-pricing.html.

[83] "Collectieve Arbeidsovereenkomst voor het Beroepsgoederenvervoer over de weg en de verhuur van mobiele kranen", Tech. Rep.

[84] HetSalarisKantoor.nl, *Welke loonkosten heeft een werkgever? Het Salariskantoor*, Jun. 2024. [Online]. Available: https://hetsalariskantoor.nl/nieuws/welke-loonkosten-werkgever/.

[85] O. M. Personeel, *Dit zijn de kosten van personeel*, Apr. 2025. [Online]. Available: https://www.ondernemenmetpersoneel.nl/orienteren/personeelskosten/dit-zijn-de-kosten-van-personeel.

[86] Dion, *Wat kost een werknemer? + rekenvoorbeelden - Werktijden.nl*, Jan. 2025. [Online]. Available: https://werktijden.nl/blog/wat-kost-een-werknemer.

[87] I. E. Commission, *Low-voltage electrical installations – Part 4-43: Protection for safety – Protection against overcurrent*. IEC, Jul. 2023. [Online]. Available: https://cdn.standards.iteh.ai/samples/23683/86789a8844914f84861c12928d57bdc3/IEC-60364-4-43-2023.pdf?utm_source=chatgpt.com.

[88] *TiSoft - Engineering software*. [Online]. Available: https://www.ti-soft.com/en/support/help/electricaldesign/project/distribution/circuits/circuit-protection-checks/protection-against-overload?utm_source=chatgpt.com.

[89] F. M. Mulder, "Implications of diurnal and seasonal variations in renewable energy generation for large scale energy storage", *Journal of Renewable and Sustainable Energy*, vol. 6, no. 3, May 2014. DOI: 10.1063/1.4874845. [Online]. Available: https://doi.org/10.1063/1.4874845.

[90] K. Kuijper, *Energietransitie kost jaarlijks 400 euro per Nederlander*, Aug. 2024. [Online]. Available: https://www.energievergelijk.nl/nieuws/energietransitie-kost-jaarlijks-400-euro-per-nederlander.

[91] "Ontwikkeling netkosten tot 2050 en de kostenverdeling over groepen gebruikers", Tech. Rep., Sep. 2024. [Online]. Available: https://www.acm.nl/system/files/documents/ontwikkeling-netkosten-tot-en-met-2050-en-de-kostenverdeling-via-nettarieven.pdf.

[92] Acm, *Codebesluit prioriteringsruimte bij transportverzoeken*, Apr. 2024. [Online]. Available: https://www.acm.nl/nl/publicaties/codebesluit-prioriteringsruimte-bij-transportverzoeken.

[93] *Aanmelden zonnepanelen | stedin*, https://www.stedin.net/aanmelden-zonnepanelen, Accessed: 2025-06-08.

[94] Maarten, *Warmtepomp vergunning – warmtepomp-info.nl*, https://www.warmtepomp-info.nl/vergunning/, Accessed: 2025-06-08, Nov. 2021.

[95] *Ik wil een laadpaal | stedin*, https://www.stedin.net/aansluiting/ik-wil-een-laadpaal, Accessed: 2025-06-08.

[96] *Obligation to register charging stations with grid operator*, https://www.pluginvest.eu/blog/pluginsights-1/meldingsplicht-voor-laadpalen-aan-netbeheerder-68, Accessed: 2025-06-08, May 2025.

[97] *UCT - United Container Transport 088-828-0000*. [Online]. Available: https://uctransport.nl/diensten/maximum-gewichten-en-afmetingen/.

[98] Bredenoord, *Battery Box: De mobiele energieopslag voor grotere vermogens*. [Online]. Available: https://www.bredenoord.com/media/default/Infographic-Battery-Box.pdf.

[99] *TNO Windmolen kaart Nederland*. [Online]. Available: https://windmolens.tno.nl/.

A

Types LV-grids

Figure A.1 shows the eight different archetypes available in the Phase to Phase download portal. Multiple LV-grids corresponding to these neighbourhood types can be uploaded into GAIA for simulation.

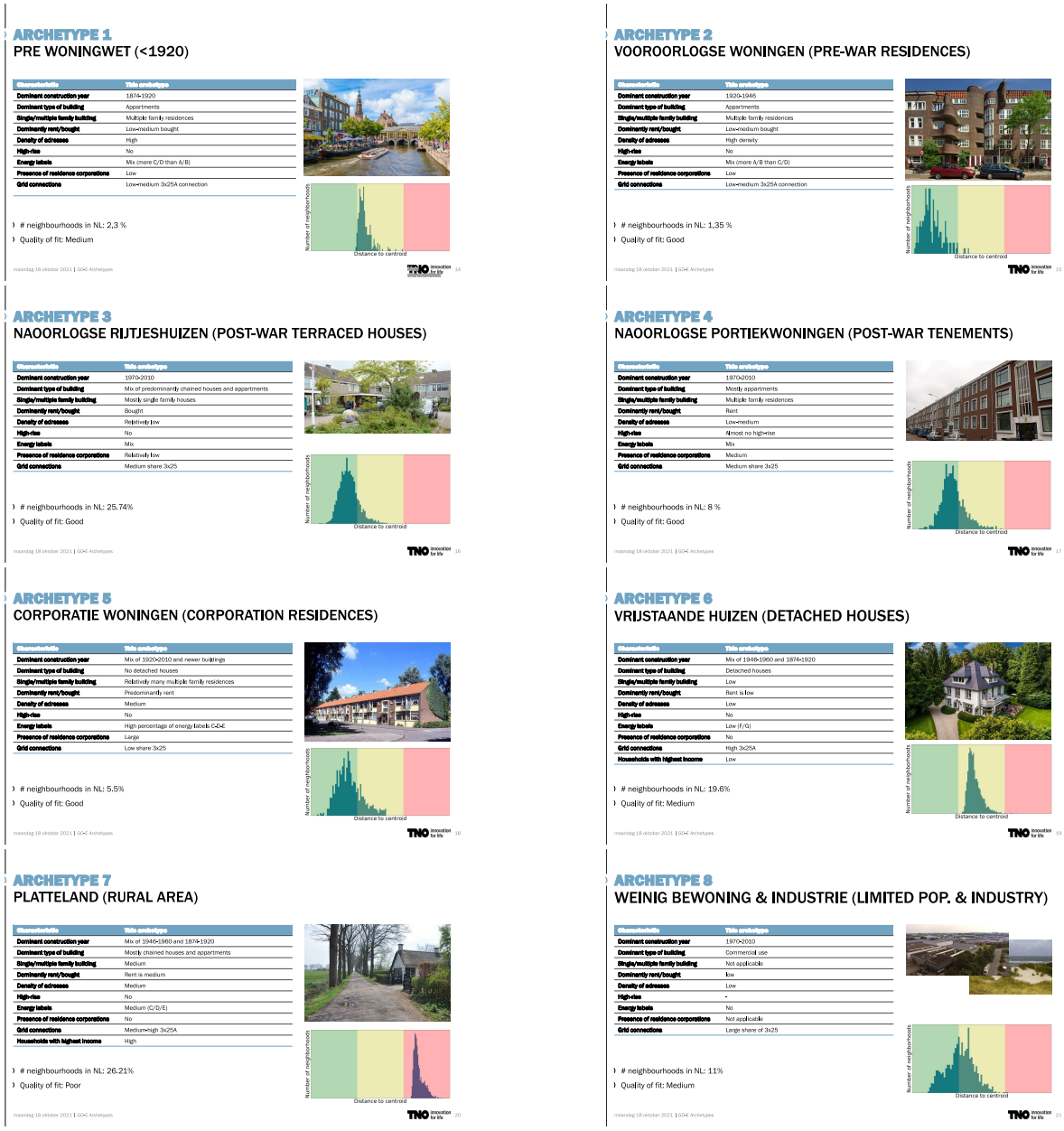

Figure A.1: Available archetypes in the download portal of Phase to Phase. These can be used for simulation in GAIA.

B

GAIA output example

Figure B.1 shows a part of the output from a simulation in GAIA. The figure shows the date and time, the current [A], the direction of flow (depending on positive to negative or negative to positive current), and the maximum load in the cable (which is the 95th percentile value from MCS as explained in Section 2.2.2.

Name	Branch 100		
Type	cable		
Date & time	**I_van,max**	**I_naar,max**	**Load,max**
	A	*A*	%
11-1-2025 00:00	227.8	-227.8	126

Figure B.1: Example of GAIA output after simulation of a weekend day in January (January 11th).

C

Parameters simplified network

Table C.1: Parameters to calculate power losses with battery deployed at location L. Lengths shown are from location L to middle of the node group.

Node group	Resistivity $[\Omega \cdot m]$	cross-sectional area $[mm^2]$	Length [m]						
			L1	L2	L3	L4	L5	L6	MV-station
Red	$2.82 \cdot 10^{-8}$	95	46.9	66.0	68.7	119.7	134.2	143.5	100.4
Yellow	$2.82 \cdot 10^{-8}$	50	70.3	89.4	92.1	143.1	157.5	166.8	217.7
Orange	$2.82 \cdot 10^{-8}$	50	50.2	31.1	33.8	84.7	99.2	108.5	197.6
Green	$2.82 \cdot 10^{-8}$	50	90.8	71.7	69.0	120.0	134.4	143.7	238.2
Blue	$2.82 \cdot 10^{-8}$	50	106.1	87.0	84.3	33.3	47.7	57	253.5
Dark blue	$2.82 \cdot 10^{-8}$	95	120.3	101.2	98.5	47.5	33.1	23.8	267.7
Purple	$2.82 \cdot 10^{-8}$	50	134.1	115.0	112.3	61.3	46.9	56.2	281.5

D

Windfarms

Figure D.1 show the map of the Netherlands with the existing windfarms in 2020 and the projected windfarms in 2030.

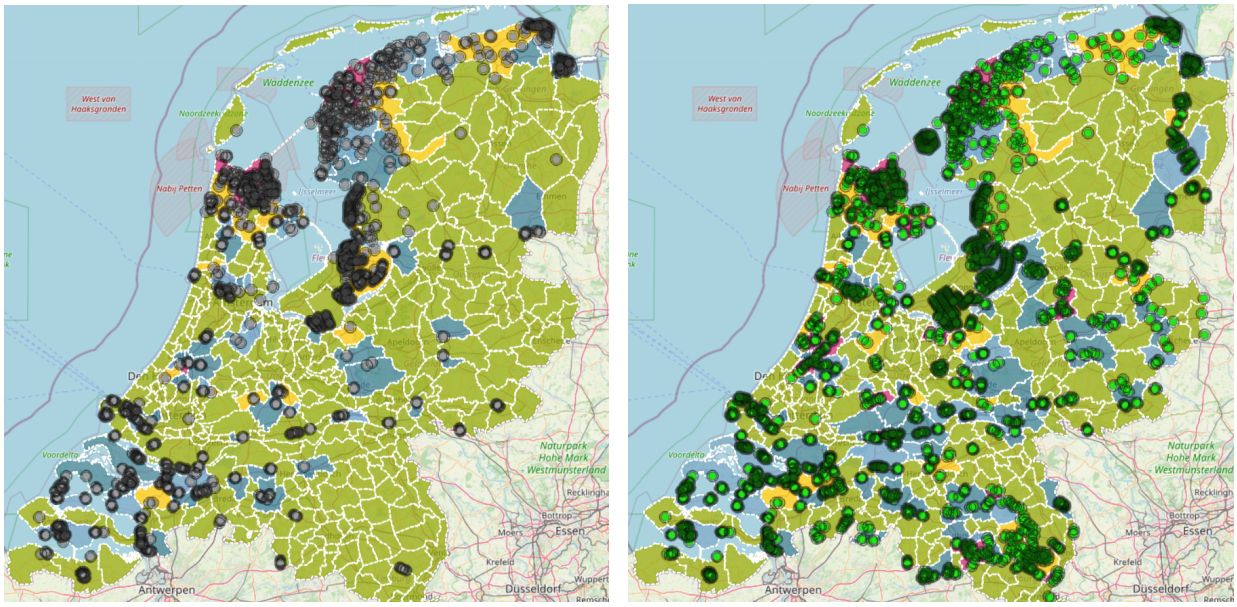

(a) Actual windfarms in 2020.

(b) Expected windfarms in 2030.

Figure D.1: Windfarms in the Netherlands for 2020 and 2030. Source: [99]

E

Python code

E.1. 15 minutes values for base load and demand for whole year

The code calculates the expected average value [in % for electrical equipment and in kW for base load] for every 15 minutes of the year

In [ ]:
```
pip install pandas openpyxl
```

In [ ]:
```
#### update with trends for PV
#### find quarterly values for sjv [kW], PV, EV and HP [%] for workdays weekenddays for all months
import openpyxl
from openpyxl import Workbook, load_workbook

# Load source workbook and required sheets
source_wb = load_workbook('Types Scraped.xlsx', data_only=True)
source_ws = source_wb.active
gm_ws = source_wb['GM']

# Create new workbook and sheet
new_wb = Workbook()
new_ws = new_wb.active
new_ws.title = 'Complete data'

# Step 1: Copy first column from source sheet
for row in range(1, source_ws.max_row + 1):
    new_ws.cell(row=row, column=1, value=source_ws.cell(row=row, column=1).value)

# Step 2: Write headers
column_index = 2  # Start from column 2

# Month 1 Workday
for i in range(1, 97):
    new_ws.cell(row=1, column=column_index, value=f'Month 1 Workday [1,{i}]')
    new_ws.column_dimensions[openpyxl.utils.get_column_letter(column_index)].width = 18
    column_index += 1

# Month 1 Weekendday
for i in range(1, 97):
    new_ws.cell(row=1, column=column_index, value=f'Month 1 Weekendday [1,{i}]')
    new_ws.column_dimensions[openpyxl.utils.get_column_letter(column_index)].width = 18
    column_index += 1

# Month 2 to 12 Workday and Weekendday
for month in range(2, 13):
    for day_type in ['Workday', 'Weekendday']:
        for i in range(1, 97):
            new_ws.cell(row=1, column=column_index, value=f'Month {month} {day_type} [1,{i}]')
            new_ws.column_dimensions[openpyxl.utils.get_column_letter(column_index)].width = 18
            column_index += 1

# Also widen first column
new_ws.column_dimensions['A'].width = 25

# Step 3: Rows 3 to 5 - fill PV, EV, HP properly
for row in range(3, 6):  # Rows for HP, PV, EV
    for month in range(1, 13):  # Months 1–12
        for day_type_index, day_type in enumerate(["Workday", "Weekendday"]):
            block_index = (month - 1) * 2 + day_type_index
            target_col_start = 2 + block_index * 96

            base_value = gm_ws.cell(row=row, column=3).value or 0 #average value in %

            for i in range(96):  # i = 0 to 95
                gm_col = (6 if day_type == "Workday" else 390) + i + 1
                gm_value = gm_ws.cell(row=row, column=gm_col).value or 0 # quaterly probabiltiy value to have a

                ref_col = 774 + month
                ref_value = gm_ws.cell(row=row, column=ref_col).value or 0 # montly probabiltiy value to have a

                weight = gm_value * ref_value # probability at time is t to have active equipment

                if row == 4:  # PV
                    if day_type == "Workday":
                        trend_daytype_col_start = 823 # daily PV trend for workday
                    else:
                        trend_daytype_col_start = 919 # daily PV trend for Weekendday

                    trend_daytype_value = gm_ws.cell(row=row, column=trend_daytype_col_start + i).value or 0
                    trend_month_value = gm_ws.cell(row=row, column=1014 + month).value or 0

                    updated_base_value = trend_daytype_value * trend_month_value + base_value

                    result = round(weight * updated_base_value, 3)

                else:
                    # Original HP and EV logic
                    result = round(weight * base_value, 3)

                new_ws.cell(row=row, column=target_col_start + i, value=result)
```

E.2. Calculating 15 minutes load values for whole LV-grid

The code multiplies the installed capacity of electrical equipment at the all node separately with the expected percentage, and adds this to the expected base load for the corresponding nodes. For every time step, the code calculates the total load in the LV-grid.

In [ ]:
```
pip install pandas networkx matplotlib openpyxl
```

In [ ]:
```
import pandas as pd
import re

# Load the Excel file
file_path = 'Exporteren.xlsx'
sheet_name = 'Aansluitingen'
df = pd.read_excel(file_path, sheet_name=sheet_name)

# Define the column index (36 because pandas uses 0-based index)
col_index = 36

# Create 4 empty columns to the right of column 37
df.insert(col_index + 1, 'sjv', '')
df.insert(col_index + 2, 'PV', '')
df.insert(col_index + 3, 'EV', '')
df.insert(col_index + 4, 'HP', '')  # Replaces 'extra'

# Function to extract numbers based on keywords and round them
def extract_values(text):
    sjv_match = re.search(r'sjv(\d+)', text)

    # Updated regex to handle both integer and decimal numbers
    pv_match = re.search(r'(\d+,\d+|\d+)\s*kW\s*PV', text)
    ev_match = re.search(r'(\d+,\d+|\d+)\s*kW\s*EV', text)
    private_ev_match = re.search(r'(\d+,\d+|\d+)\s*kW\s*Private EV', text)
    hp_match = re.search(r'(\d+,\d+|\d+)\s*kW\s*HP', text)

    # Extract values
    sjv_value = sjv_match.group(1) if sjv_match else ''
    pv_value = pv_match.group(1) if pv_match else ''
    ev_value = private_ev_match.group(1) if private_ev_match else (ev_match.group(1) if ev_match else '')
    hp_value = hp_match.group(1) if hp_match else ''

    # Round decimal values
    if pv_value:
        pv_value = round(float(pv_value.replace(',', '.')))
    if ev_value:
        ev_value = round(float(ev_value.replace(',', '.')))
    if hp_value:
        hp_value = round(float(hp_value.replace(',', '.')))

    return sjv_value, pv_value, ev_value, hp_value

# Apply the function to extract values and round them
df[['sjv', 'PV', 'EV', 'HP']] = df.iloc[:, col_index].astype(str).apply(extract_values).apply(pd.Series)

# Save the modified file
output_file_path = 'Bewerkt_Exporteren.xlsx'
df.to_excel(output_file_path, sheet_name=sheet_name, index=False)

print(f'Modified file saved as {output_file_path}')
```

In [ ]:
```
import pandas as pd

# Load GUIDs from 'Excel tak 100.xlsx'
knooppunten_file = 'Excel tak 100.xlsx'
knooppunten_sheet = 'Knooppunten (schema)'
knooppunten_df = pd.read_excel(knooppunten_file, sheet_name=knooppunten_sheet)

# Extract unique GUIDs from column 1
guids_to_keep = knooppunten_df.iloc[:, 0].astype(str).str.strip().unique()

# Load main Excel file
bewerkt_file = 'Bewerkt_Exporteren.xlsx'
bewerkt_sheet = 'Aansluitingen'
df = pd.read_excel(bewerkt_file, sheet_name=bewerkt_sheet)

# Extract and filter rows with matching GUIDs (from column 4)
df['GUID_check'] = df.iloc[:, 3].astype(str).str.strip()
filtered_df = df[df['GUID_check'].isin(guids_to_keep)].copy()
filtered_df.drop(columns=['GUID_check'], inplace=True)

# Find unmatched GUIDs
matched_guids = filtered_df.iloc[:, 3].astype(str).str.strip().unique()
unmatched_guids = [guid for guid in guids_to_keep if guid not in matched_guids]

# Prepare rows for unmatched GUIDs with zero values in 'sjv', 'PV', 'EV', 'HP'
# Determine column names for safe creation
columns = df.columns.tolist()

# Create a DataFrame with zeros in relevant columns
missing_data = pd.DataFrame(columns=columns)

for guid in unmatched_guids:
```

```
    new_row = {columns[3]: guid, 'sjv': 0, 'PV': 0, 'EV': 0, 'HP': 0}
    missing_data = pd.concat([missing_data, pd.DataFrame([new_row])], ignore_index=True)

# Concatenate filtered data with missing rows
final_df = pd.concat([filtered_df, missing_data], ignore_index=True)

# Add sjv1 column
sjv_index = final_df.columns.get_loc('sjv')
previous_col = final_df.columns[sjv_index - 1]
final_df.insert(sjv_index, 'sjv1', final_df[previous_col].astype(str).str.split(';').str[0])

# Save to new file
output_file = 'Bewerkt_Exporteren tak 100.xlsx'
final_df.to_excel(output_file, sheet_name=bewerkt_sheet, index=False)

print(f'Filtered and extended data saved to {output_file}')
```

In [ ]:

```
import pandas as pd

# Load the Excel file
file_path = 'Bewerkt_Exporteren tak 100.xlsx'
sheet_name = 'Aansluitingen'
df = pd.read_excel(file_path, sheet_name=sheet_name)

# --- Remove columns 43 to 58 (index 42 to 57) ---
cols_to_drop = df.columns[42:58]
df.drop(columns=cols_to_drop, inplace=True)

# Configuration
types = ['sjv', 'PV', 'EV', 'HP']
num_columns = 96
months = 12
day_types = ['Workday', 'Weekendday']

# Generate all new columns in a dictionary
new_data = {}

for month in range(1, months + 1):
    for day_type in day_types:
        for t in types:
            for i in range(1, num_columns + 1):
                col_name = f'Month {month} {day_type} {t} [{i}]'
                new_data[col_name] = [0] * len(df)  # Fill with zeros

# Create a new DataFrame with these columns
new_columns_df = pd.DataFrame(new_data)

# Concatenate with the original DataFrame
df_extended = pd.concat([df, new_columns_df], axis=1)

# Save to a new Excel file
output_file = 'Ready to fill in load tak 100.xlsx'
df_extended.to_excel(output_file, sheet_name=sheet_name, index=False)

print(f'Successfully saved extended file to {output_file}')
```

In [ ]:

```
import pandas as pd
from openpyxl import load_workbook

# Load files
file_main = 'Ready to fill in load tak 100.xlsx' #previously new_update Types
file_update = 'Base and equipment load from Types whole year.xlsx'

# Load workbooks and sheets
wb_main = load_workbook(filename=file_main)
ws_main = wb_main.active

wb_update = load_workbook(filename=file_update, data_only=True)
ws_update = wb_update.active

# Constants
daytypes = ['Workday', 'Weekendday']
loadtypes = {
    'sjv': {'base_col': 38, 'divisor': 0.98},
    'PV':  {'base_col': 40, 'divisor': 100},
    'EV':  {'base_col': 41, 'divisor': 100},
    'HP':  {'base_col': 42, 'divisor': 100 * 0.95},
}

# Start processing rows from row 3
row = 3
while True:
    if ws_main.cell(row=row, column=38).value is None:
        break  # No more rows

    # === PART 1: SJV (same as before) ===
    node_value = ws_main.cell(row=row, column=38).value
```

```
    # Find matching row in update sheet
    matching_row = None
    for r in range(2, ws_update.max_row + 1):
        if ws_update.cell(row=r, column=1).value == node_value:
            matching_row = r
            break

    if not matching_row:
        print(f"❌ No match in update sheet for node: {node_value}")
        row += 1
        continue

    for month in range(1, 13):
        for daytype_index, daytype in enumerate(daytypes):
            for i in range(1, 97):
                # Construct update header for sjv
                header = f"Month {month} {daytype} [1,{i}]"

                # Find update column
                update_col = None
                for c in range(2, ws_update.max_column + 1):
                    if ws_update.cell(row=1, column=c).value == header:
                        update_col = c
                        break

                if not update_col:
                    print(f"⚠️ Header not found: {header}")
                    continue

                value = ws_update.cell(row=matching_row, column=update_col).value
                if value is not None:
                    # Target column for sjv
                    target_col = 43 + ((month - 1) * 768) + (daytype_index * 384) + (0 * 96) + (i - 1)
                    ws_main.cell(row=row, column=target_col, value=value / 0.98)

    # === PART 2: PV, EV, HP ===
    for load_index, (loadtype, settings) in enumerate(list(loadtypes.items())[1:], start=1):  # skip sjv
        base_val = ws_main.cell(row=row, column=settings['base_col']).value
        if base_val is None:
            continue

        for month in range(1, 13):
            for daytype_index, daytype in enumerate(daytypes):
                for i in range(1, 97):
                    header = f"Month {month} {daytype} [1,{i}]"

                    # Find update column
                    update_col = None
                    for c in range(2, ws_update.max_column + 1):
                        if ws_update.cell(row=1, column=c).value == header:
                            update_col = c
                            break

                    if not update_col:
                        print(f"⚠️ Header not found for {loadtype}: {header}")
                        continue

                    if loadtype == 'PV':
                        update_row = 4
                    elif loadtype == 'EV':
                        update_row = 5
                    else:
                        update_row = 3

                    update_val = ws_update.cell(row=update_row, column=update_col).value
                    if update_val is None:
                        continue

                    result = (base_val * update_val) / settings['divisor']

                    # Target column for this loadtype
                    target_col = 43 + ((month - 1) * 768) + (daytype_index * 384) + (load_index * 96) + (i - 1)
                    ws_main.cell(row=row, column=target_col, value=result)

    row += 1

# Save file
wb_main.save('Enexis load for 1 year.xlsx')
print("✅ File updated with sjv, PV, EV, and HP.")
```

In [ ]:

```
import openpyxl

# Load the workbook and the 'Aansluitingen' sheet
wb = openpyxl.load_workbook('Enexis load for 1 year.xlsx')
sheet_aansluitingen = wb['Aansluitingen']

# Create or reset the 'Summed load' sheet
if 'Summed load' in wb.sheetnames:
```

```
    del wb['Summed load']
sheet_summed_load = wb.create_sheet('Summed load')

# Step 1: Copy column 4 from 'Aansluitingen' to column 1 of 'Summed load'
for row in range(3, sheet_aansluitingen.max_row + 1):  # Start from row 3
    sheet_summed_load.cell(row=row, column=1).value = sheet_aansluitingen.cell(row=row, column=4).value

# Step 2: Create headers and track where each combination starts
column_index = 2  # Start at column 2 (column 1 is for IDs)

for month in range(1, 13):  # Months 1 to 12
    for daytype in ['Workday', 'Weekendday']:  # Day types
        for quarter in range(1, 97):  # Quarters 1 to 96
            header = f'Summed load Month {month} {daytype} [1,{quarter}]'
            sheet_summed_load.cell(row=1, column=column_index).value = header
            column_index += 1

# Step 3: Fill in the sums starting from row 3
for row in range(3, sheet_aansluitingen.max_row + 1):
    write_col = 2  # Reset to column 2 for each row in 'Summed load'

    for month in range(1, 13):  # Months 1 to 12
        month_offset = (month - 1) * 768  # 768 = 384 (Workday) + 384 (Weekendday)

        for daytype in ['Workday', 'Weekendday']:
            daytype_offset = 0 if daytype == 'Workday' else 384  # 384 columns per daytype

            for quarter in range(96):  # 96 quarters
                # Base column = 43 + month_offset + daytype_offset
                base_col = 43 + month_offset + daytype_offset

                sjv_col = base_col + quarter                    # sjv
                pv_col  = base_col + 96 + quarter               # PV
                ev_col  = base_col + 192 + quarter              # EV
                hp_col  = base_col + 288 + quarter              # HP

                values_to_sum = [
                    sheet_aansluitingen.cell(row=row, column=sjv_col).value,
                    sheet_aansluitingen.cell(row=row, column=pv_col).value,
                    sheet_aansluitingen.cell(row=row, column=ev_col).value,
                    sheet_aansluitingen.cell(row=row, column=hp_col).value,
                ]

                summed_value = sum(val for val in values_to_sum if val is not None)
                sheet_summed_load.cell(row=row, column=write_col).value = summed_value
                write_col += 1


# Save the workbook after making changes
wb.save('Enexis summed load for 1 year.xlsx')
```

E.3. Scraping data and calculating congestion

In [ ]:
```python
#########
# This scripts scrapes the Excel data from one LV-grid from the multiple LV-grids that are connected with the M
##########

import pandas as pd

def extract_branch_data(file1, file2, output_file):
    # Load Excel files with specified sheets
    df1 = pd.read_excel(file1, sheet_name='Takken', header=None)
    df2 = pd.read_excel(file2, sheet_name='Takken (schema)', usecols=[1], header=None)

    # Get the list of branches from LV-grid 1
    branches_to_keep = df2.iloc[:, 0].dropna().astype(str).tolist()

    # Ensure the first column is also a branch to keep
    if str(df1.iloc[0, 0]).strip() in branches_to_keep:
        selected_columns = [0]  # Include the first column
    else:
        selected_columns = []

    # Iterate over Excel file 1, starting from the second column
    i = 1
    empty_count = 0

    while i < len(df1.columns):
        branch_name = str(df1.iloc[0, i]).strip()

        if branch_name:
            empty_count = 0
            if branch_name in branches_to_keep:
                selected_columns.extend(range(i, min(i + 6, len(df1.columns))))  # Keep the column and next 6 c
        else:
            empty_count += 1  # Increment empty cell count
            if empty_count >= 7:
                break  # Stop if we encounter 7 consecutive empty cells

        i += 1

    # Extract relevant data
    df_filtered = df1.iloc[:, selected_columns]

    # Save to new Excel file
    df_filtered.to_excel(output_file, index=False, header=False)
    print(f"Filtered data saved to {output_file}")

# Example usage
extract_branch_data('File 1.xlsx', 'LV-grid 1.xlsx', 'File 1 LV-grid 1.xlsx')
```

```
Filtered data saved to Month 8 Weekend L5 tak 100.xlsx
```

In [ ]:
```python
### This script calculates system and maximum congestion for all branches and each time step
import openpyxl
import pandas as pd

# Bestanden
bestand = 'File 1 LV-grid 1.xlsx'
referentie_excel = 'LV-grid 1.xlsx'

# # Load Excel files with specified sheets and start from column 13 row 3
df_modifiers = pd.read_excel(referentie_excel, sheet_name='Takken (schema)', header=None)
modifier_values = df_modifiers.iloc[2:, 12].tolist()  # Start bij rij 3

# Load file
wb = openpyxl.load_workbook(bestand)
sheet = wb.active

rij_5 = 5
laatste_kolom_5 = sheet.max_column
kolom = 1
modifier_index = 0

total_sum_congested = 0
overall_max_congested = 0
rij_max = sheet.max_row + 1
rij_sum = rij_max + 1
congested_columns = []

while kolom <= laatste_kolom_5:
    cel_5 = sheet.cell(row=rij_5, column=kolom)

    if cel_5.value == 'Belastinggraad,max':
        # Check when belastinggraad,max is stated in the cell and start counting from there
        if modifier_index < len(modifier_values):
            modifier_value = modifier_values[modifier_index]
        else:
            modifier_value = 1
```

```
        if not isinstance(modifier_value, (int, float)):
            modifier_value = 1

        sheet.insert_cols(kolom + 1)
        sheet.cell(row=rij_5, column=kolom + 1, value='Congested amount [kW]')
        sheet.cell(row=rij_5 - 1, column=kolom + 1, value=modifier_value)

        congested_values = []
        for rij in range(6, rij_max):
            waarde = sheet.cell(row=rij, column=kolom - 2).value
            nieuwe_cel = sheet.cell(row=rij, column=kolom + 1)

            if isinstance(waarde, (int, float)):
                waarde = abs(waarde)
                nieuwe_cel.value = round(max(waarde - modifier_value, 0) * 230 / 1000, 1)
                congested_values.append(nieuwe_cel.value)
            else:
                nieuwe_cel.value = None

        if congested_values:
            max_value = max(congested_values)
            sum_value = sum(congested_values)
            total_sum_congested += sum_value
            overall_max_congested = max(overall_max_congested, max_value)
            sheet.cell(row=rij_max, column=kolom + 1, value=max_value)
            sheet.cell(row=rij_sum, column=kolom + 1, value=sum_value)

        congested_columns.append(kolom + 1)
        modifier_index += 1
        kolom += 2
        laatste_kolom_5 += 1
    else:
        kolom += 1

    if cel_5.value is None:
        break

# Create additional column for congestion
congestion_sum_col = sheet.max_column + 1
sheet.cell(row=rij_5, column=congestion_sum_col, value='Congestion time series')

# Calculate sum congestion for every row
time_series_values = []
for rij in range(6, rij_max):
    rij_som = 0
    for c in congested_columns:
        waarde = sheet.cell(row=rij, column=c).value
        if isinstance(waarde, (int, float)):
            rij_som += waarde
    sheet.cell(row=rij, column=congestion_sum_col, value=round(rij_som, 1))
    time_series_values.append(rij_som)

# Add maximum and system congestion beneath the last row
if time_series_values:
    sheet.cell(row=rij_max, column=congestion_sum_col, value=max(time_series_values))
    sheet.cell(row=rij_sum, column=congestion_sum_col, value=sum(time_series_values))

# Add aditional column for maximum congestion for every time step
congestion_max_col = sheet.max_column + 1
sheet.cell(row=rij_5, column=congestion_max_col, value='Max congested value [kW]')

# Obtain maximum congestion for every branch
row_max_values = []
for rij in range(6, rij_max):
    waarden = []
    for c in congested_columns:
        waarde = sheet.cell(row=rij, column=c).value
        if isinstance(waarde, (int, float)):
            waarden.append(waarde)
    max_waarde = max(waarden) if waarden else None
    sheet.cell(row=rij, column=congestion_max_col, value=max_waarde)
    if isinstance(max_waarde, (int, float)):
        row_max_values.append(max_waarde)

# Add system congestion and maximum congestion for all time steps and branches
if row_max_values:
    sheet.cell(row=rij_max, column=congestion_max_col, value=max(row_max_values))
    sheet.cell(row=rij_sum, column=congestion_max_col, value=sum(row_max_values))

# Add total
sheet.cell(row=rij_max, column=congestion_max_col + 1, value=overall_max_congested)
sheet.cell(row=rij_sum, column=congestion_max_col + 1, value=total_sum_congested)

wb.save('Congestion File 1 LV-grid 1.xlsx')
```

E.4. Data interpolation

Data of the 24 different day types (i.e. a workday and a weekend day for every month of the year) is extended to a whole year of data.

In [8]:
```python
import pandas as pd
from datetime import datetime, timedelta

# File and sheet setup
input_file = 'Hourly_1weekendday_1weekday_per_month tak 100.xlsx'
output_file = 'Hourly_year tak 100.xlsx'
sheet_name = 'Sheet1'

# Step 1: Load the full sheet, then separate the first 6 rows
full_sheet = pd.read_excel(input_file, sheet_name=sheet_name, header=None)

# First 6 rows (rows 0–5) to preserve
header_rows = full_sheet.iloc[:6].copy()

# Step 2: Load the data starting from row 6 with real headers
df = pd.read_excel(input_file, sheet_name=sheet_name, skiprows=5)

# Make sure the first column is datetime
df.iloc[:, 0] = pd.to_datetime(df.iloc[:, 0])

# Extract useful info
df['date'] = df.iloc[:, 0].dt.date
df['month'] = df.iloc[:, 0].dt.month
df['weekday'] = df.iloc[:, 0].dt.weekday  # Monday=0, Sunday=6

# Step 3: Get weekday/weekend samples per month
month_data = {}
for month in range(1, 13):
    month_df = df[df['month'] == month]
    weekday_sample = month_df[month_df['weekday'] < 5].iloc[:24].copy()
    weekend_sample = month_df[month_df['weekday'] >= 5].iloc[:24].copy()
    month_data[month] = {'weekday': weekday_sample, 'weekend': weekend_sample}

# Step 4: Expand full-year data based on weekday/weekend
year = datetime.now().year  # Or set to a specific year
start_date = datetime(year, 1, 1)
end_date = datetime(year, 12, 31)
current = start_date

expanded_blocks = []

while current <= end_date:
    is_weekend = current.weekday() >= 5
    sample_type = 'weekend' if is_weekend else 'weekday'
    day_template = month_data[current.month][sample_type].copy()

    # Adjust timestamps for this day
    base_time = datetime.combine(current.date(), datetime.min.time())
    day_template.iloc[:, 0] = [base_time + timedelta(hours=i) for i in range(24)]

    expanded_blocks.append(day_template)
    current += timedelta(days=1)

# Step 5: Combine all data rows
expanded_data = pd.concat(expanded_blocks, ignore_index=True)

# Step 6: Concatenate with the original top 6 rows (preserve layout)
# We'll write the final result row-by-row using openpyxl to preserve the formatting
from openpyxl import load_workbook
from openpyxl.utils.dataframe import dataframe_to_rows
from openpyxl import Workbook

# Create a new workbook and get active sheet
wb = Workbook()
ws = wb.active
ws.title = sheet_name

# Write the preserved top 6 rows manually
for row in header_rows.itertuples(index=False):
    ws.append(list(row))

# Write the expanded data
for row in dataframe_to_rows(expanded_data, index=False, header=False):
    ws.append(row)

# Save the result
wb.save(output_file)
print(f"✅ Data expanded and saved to: {output_file}")
```

```
✅ Data expanded and saved to: Hourly_year tak 100.xlsx
```

E.5. Fourier transform

In [ ]:
```python
import pandas as pd
import numpy as np
import matplotlib.pyplot as plt

# === Configuration ===
excel_file = 'Data Fourier transform.xlsx'
sheet_name = 'Blad2'
column_time = 'Datum & tijd'
column_value = 'Congestion'

# === Read and Clean Data ===
df = pd.read_excel(excel_file, sheet_name=sheet_name, parse_dates=[column_time])
df.columns = df.columns.str.strip()
df = df.dropna(subset=[column_time, column_value])
df[column_value] = pd.to_numeric(df[column_value], errors='coerce')
df = df.dropna(subset=[column_value])
df = df.sort_values(by=column_time)

# === Calculate time step (in hours) ===
time = df[column_time]
data = df[column_value].values
time_deltas = time.diff().dropna().dt.total_seconds() / 3600
dt = time_deltas.mode()[0]

# === FFT ===
n = len(data)
fft_result = np.fft.fft(data)
freq = np.fft.fftfreq(n, d=dt)

# === Keep positive frequencies only
positive_mask = freq > 0
positive_freq = freq[positive_mask]
magnitude = np.abs(fft_result)[positive_mask]

# === Find the top 3 highest peaks
top_indices = np.argpartition(magnitude, -3)[-3:]
top_indices = top_indices[np.argsort(magnitude[top_indices])[::-1]]  # Sort descending

peak_frequencies = [positive_freq[idx] for idx in top_indices]
peak_labels = "\n".join([f"{f:.4f}" for f in peak_frequencies])

print(" Top 3 frequency peaks:")
for i, (f, idx) in enumerate(zip(peak_frequencies, top_indices), start=1):
    m = magnitude[idx]
    period = 1 / f
    print(f"{i}. Frequency: {f:.5f} 1/hour | Period: {period:.2f} hours | Magnitude: {m:.2f}")

# === Plot ===
plt.figure(figsize=(10, 6))
plt.plot(positive_freq, magnitude, label='FFT Magnitude')
plt.title('Trend system congestion throughout the year')
plt.xlabel('Frequency (1/hour)')
plt.ylabel('Magnitude')
plt.xlim([-0.01, 0.2])
plt.grid(True)

# Highlight top 3 peaks
for idx in top_indices:
    f = positive_freq[idx]
    plt.axvline(x=f, color='red', linestyle='--', linewidth=1)

# Custom legend parts:
custom_line = plt.Line2D([0], [0], color='red', linestyle='--', linewidth=1)
label_peaks = "Peaks:"
label_values = peak_labels  # This is multi-line string

# Create a combined legend with 3 "columns"
# Trick: use 3 handles and labels; empty handles for text-only entries
empty_handle = plt.Line2D([], [], color='none')

plt.legend(
    handles=[custom_line, empty_handle, empty_handle],
    labels=["", label_peaks, label_values],
    handlelength=2,  # length of line handle
    handletextpad=0.4,
    borderaxespad=1,
    loc='upper right',
    fontsize=10,
    frameon=True,
    labelspacing=0.1,
    columnspacing=-2,
    ncol=3
)

plt.tight_layout()
plt.show()
```